博　士　論　文

Development of biomarkers for delayed wound healing caused by pressure

（圧力起因性創傷治癒遅延バイオマーカーの開発）

金澤　寿樹

CONTENTS

LIST of TABLES and FIGURES

ABSTRACT

Pressure ulcers are characterized by chronicity, which results in delayed wound healing because of pressure. An early intervention into delayed healing caused by pressure requires a detection method. There are no reports on detection of delayed healing caused by pressure. Therefore, this study was focused on biological-response-based markers, namely, development of an assay for detection of delayed healing caused by pressure. I tested the hypothesis that pressure loading applied to a full-thickness wound in an animal model leads to upregulation of prostaglandin E_2 (PGE_2), hyaluronan (HA), and Heat shock protein 90α (HSP90α) along with delayed healing based on our previous *in vitro* study. First, I developed animal models for delayed wound healing caused by pressure. Then, I detected HSP90α secretion into wound exudates that is induced by pressure loading in the animal models along with delayed healing. Based on the results of the animal experiments, I verified the usefulness of HSP90α as the marker for delayed wound healing caused by pressure in clinical setting. In case series study, HSP90α could explain the cases of delayed wound healing caused by pressure with its positive signal and the cases of PU improved from exposure to pressure with its negative signal. In a quantitative analysis of the repeated examinations, HSP90α was significantly associated with delayed healing in a model adjusted for covariates. These findings indicate that HSP90α is a promising marker of delayed healing caused by pressure.

INTRODUCTION

Epidemiology of pressure ulcers

Pressure ulcers (PUs), have been the subject of extensive research for more than 3 decades but remain a frequent problem in health care (Parish et al., 2007; Vanderwee et al., 2007). PUs are pathomechanically and pathophysiologically induced by ischemia-reperfusion injuries that primarily result from unrelieved pressure (Salcido et al., 2007). Severity of PUs was defined by the international classification system as follows: category I, nonblanchable erythema; category II, partial-thickness tissue loss; category III, full-thickness tissue loss; and category IV, full-thickness tissue loss with exposed muscle, tendon or bone, and unstageable: the base of the ulcer is covered with necrotic tissue in the wound bed (NPUAP/EPUAP/PPPIA, 2014).

A recent report indicated that the international prevalence of PUs is 15–20% in acute care settings including various types of intensive care units, 8–14% in general acute care settings including various acute care medical and surgical units, and 8–12% in nursing homes (Berlowitz, 2014). By region, the prevalence of PUs is 13.5% in the USA; 18.1% in the EU including Belgium, Italy, Portugal, UK, and Sweden; 17.6% in Australia; and 25.0% in UAE (Victorian Quality Council, 2006; Vanderwee et al., 2007; VanGilder et al., 2009; Tariq, 2014). On the other hand, in Japan, the prevalence of PUs had decreased to 3.64% (Sanada et al., 2008). Although this figure is relatively lower than that of other countries or regions, PUs remain a serious problem in Japan. In a large-scale study in all care settings, the proportion of severe PUs that are defined as category III, IV, or unstageable PUs (VanGilder et al., 2010), was found to be 34.8% among all PUs (Sanada et al., 2008). Another prevalence study involving general hospitals in Japan estimated the proportion of severe PUs at 43.9% (Japanese Society of Pressure Ulcers, 2015). This proportion is higher than that in the USA, where the proportion is 29% (VanGilder et al., 2010). Other studies outside Japan also

showed that the majority of PUs belong to category I or II in severity (Gallagher et al., 2008; Moore et al., 2011). PUs, once developed, represent a significant financial burden (which is mainly attributable to nursing time); the cost of treating a PU increases according to its severity from £1,214 (category I) to £14,108 (category IV) (Bennett et al., 2004; Dealey et al., 2012). In addition, along with the cost, the mean time to heal increases with severity from 28.4 days (category I) to 154.7 days (category IV) (Bennett et al., 2004). Changing demographics and the increase in the number of the elderly in the future mean that the number of PUs is likely to increase in the years ahead (Moore and Cowman, 2012). These data on prevalence, severity, costs, healing time, and changing demographics illustrate the importance of early and appropriate treatment of PUs, not to mention prevention.

Fundamental factor of delayed healing according to the etiology of PUs

These unacceptably high prevalence and severity may be related to PU chronicity, representing delayed wound healing caused by pressure; the latter mainly inhibits tissue granulation in the wound healing process. PUs are continuously exposed to pressure as noted in the definition: a PU is localized damage to the skin and the underlying tissue, mainly as a result of continuous exposure to pressure (NPUAP/EPUAP/PPPIA, 2014). The etiology is linked to sustained localized pressure, which plays a significant role (Parish et al., 2007). I hypothesized that the significant role of pressure could also result in delayed healing. Berlowitz et al. (2007) stated in their review that the 4 most commonly considered pathophysiological explanations related to pressure in terms of the development of PUs include (1) ischemia caused by capillary occlusion (Kosiak, 1961); (2) reperfusion injury, i.e., injury resulting from accumulation of substances associated with the inflammatory response to ischemia as blood is reintroduced into an ischemic region (Salcido et al., 1994; Houwing et al., 2000); (3) impaired lymphatic function that causes metabolic waste products, proteins,

and enzymes to accumulate (Krouskop et al., 1978; Krouskop, 1983); and (4) prolonged mechanical deformation of tissue resulting in apoptosis of cells (Stekelenburg et al., 2006; Siu et al., 2009). Wound healing is a normal response to injury. Nonetheless, sustained unrelieved pressure in PUs is also a factor of delayed healing. Failure to redistribute pressure around the wound area results in ongoing oxygen deprivation, poor wound healing, and further tissue damage (Defloor et al., 2005). Thus, sustained unrelieved pressure is one of the fundamental reasons why PUs are considered chronic wounds characterized by delayed healing. This is particularly common among patients who are bedridden or wheelchair bound or have a spinal cord injury, because in these cases, it is quite difficult to completely eliminate pressure.

Of course, besides pressure, there are some other factors of delayed healing such as wound infection after fecal pollution, malnutrition, and poor general state of health due to an underlying disease, e.g., arteriosclerosis, diabetes, or cancer (Alvarez, 1991; Koivukangas et al., 1999; Thomas, 2006; Hendrichova et al., 2010; Wild et al., 2010). It is necessary to detect the factor of delayed healing for the appropriate treatment and care. Some researchers reported (as a detection method) infrared thermography (Nakagami et al., 2010) and wound fluid RT-PCR (Asada et al., 2012) in relation to infection and nutritional markers (Iizaka et al., 2010) and nutritional status assessment by the color of granulation (Iizaka et al., 2011), but there are no studies on pressure in this regard.

Necessity of a marker of delayed healing caused by pressure

Early intervention to PUs requires a timely method for detection of delayed healing caused by pressure within a short time frame such as 1 week. The TIME concept systematically assists clinicians in the assessment and management of chronic wound, including PUs (Dowsett and Newton, 2005). TIME is an acronym that summarizes the 4 main components of wound bed preparation: Tissue nonviable or deficient, Infection or inflammation, Moisture imbalance,

and Edge of wound–nonadvancing or undermining. This concept does not imply detection of delayed healing caused by pressure in granulation tissue. Although a clinical manifestation such as “thickened edges” (Okuwa et al., 2005) has been reported, it only indicates the chronic situation that pressure has already affected the PU healing process, thus, this indicator does not contribute to the timely detective strategy within a short period such as 1 week. To my knowledge, no study has reported timely detection of delayed healing caused by pressure.

On the other hand, as for pressure redistribution care such as repositioning and using special support surfaces including beds, mattresses, and cushions, international best practice advocates the use of repositioning and support surfaces as integral components of a PU management strategy. Although many studies on pressure redistribution have been carried out, the appropriate and easy-to-use criteria have not been elucidated in systematic reviews (Moore and Cowman 2012; McInnes et al., 2011). The guideline on prevention and treatment of PUs according to NPUAP/EPUAP/PPPIA (2014) suggests determining repositioning frequency depending on individual cases, such as tissue tolerance, the level of activity and mobility, general medical condition, overall treatment objectives, skin condition, and comfort. These guideline also recommends considering, when selecting a support surface, the individual’s need for pressure redistribution based on the following factors: the level of immobility and inactivity; need for microclimate control and shear reduction; size and weight of the individual; risk of development of new PUs; and the number, severity, and location of existing PU(s). However, these complicated criteria require an experienced clinician, and uncertainty will undoubtedly affect such a subjective assessment. Therefore, an objective and timely method for detection of delayed healing caused by pressure is needed to improve the procedure of pressure redistribution.

A strategy for identifying candidate markers

Why is there no method to detect delayed healing caused by pressure? There are 2 possible reasons. First, it is quite difficult to estimate pressure-induced mechanical stress within the tissue, which directly causes cell damage, by measuring the pressure with a pressure sensor such as a multi-pad type device that is widely used in clinical practice (Sugama et al., 2002). Second, we cannot estimate the magnitude of mechanical stress responsible for cell damage. Even if mechanical stress can be measured, the cellular response that leads to tissue damage is not uniform because of interpatient variability related to comorbidity, wound location, nutrition, tissue tolerance, and age (Verzijl et al., 2000; Moseley et al., 2004; Sae-Sia et al., 2007; Wild et al., 2010). I therefore considered that analysis of cellular response to mechanical stress is the best scheme for the detection of delayed wound healing caused by pressure and focused on the secreted substance along with the gene expression as a biomarker that could be collected noninvasively from the wound exudates in a clinical setting. Moseley et al. (2004) reports that analysis of wound exudates has a scientific and objective rationale of assessing the wound condition.

We have previously reported the candidate markers for delayed healing caused by pressure in *in vitro* study (Kanazawa et al., 2014). In that study, we applied sustained compressive loading to *in vitro* granulation model, which was three-dimensional cultured fibroblasts using collagen sponges as scaffolds, and developed experimental system in which apoptosis increased and cell proliferation did not occur. Secreted substances associated with increased gene expression significantly were quantified. Our results revealed that *Heat shock protein* (*Hsp*) *90aa1*, *Cd44*, *Hyaluronan synthase* (*Has*) *2*, and *Cyclooxygenase* (*Cox*) *2* were upregulated, and along with these upregulated genes, HSP90α, hyaluronan (HA), and Prostaglandin E_2 (PGE_2) were also increased by sustained compressive loading in three-dimensional cultured fibroblasts. From the insight regarding our previous study (Kanazawa et al., 2014) and other previous studies related to the compressive or shear stress

applied to hypertrophic scars, endothelial cells, or periodontal ligament cells (Renò et al., 2001; Maroski et al., 2011; Mitsuhashi et al., 2011), these three substances are seen to be associated with mechanical stress.

An overview of these secreted substances induced by compressive loading

Sreedhar and Csermely (2004) summarize in their review that HSP90 acts as molecular chaperones of numerous client proteins involving in the refolding of misfolded proteins and assisting in their elimination if they become irreversibly damaged (Buchner, 1999; Pearl and Prodromou, 2000; Young et al., 2001; Pratt and Toft, 2003). Inhibition of HSP90 resulted in apoptosis, contributing to the recruitment of death domain (Vanden Berghe et al., 2003). On the other hand, HSP90 is an important factor involving in the propagation of the apoptotic signal from the plasma membrane (Galea-Lauri et al., 1996). HSP90 is required to activate the death domain kinase and the receptor interacting protein, which sensitize cells to TNF-induced cell death (Chen et al., 2002). Thus, in some cases, wherein it is better if the cell dies, there is no reason to defend any further (Sreedhar and Csermely, 2004). While there are two isoforms with 85% identity (HSP90α and HSP90β) in higher eukaryotes and the functional difference between the isoforms remains less understood, it is reported that HSP90α is an inducible protein but HSP90β is a constitutive protein (Terasawa et al., 2005; Toivola et al., 2010).

HA is a ubiquitous component of the extracellular matrix, and high molecular weight (HMW) form serves as structural scaffolding in tissue (Mascarenhas et al., 2004). Synthesis of HA is accomplished by three HA synthases (HAS1, HAS 2, and HAS 3) (Itano et al., 1996; Spicer et al., 1996, 1997). The full-length polymer has a very high molecular mass, ranging from 10^5 to 10^7 Da; HAS1 and HAS2 produce HMW HA, whereas HAS3 produces relative low molecular weight forms of HA (Itano et al., 1999). The interaction of HA with CD44,

which is a well-characterized receptor, activates a signaling cascade, whereas increased HA production and matrix formation influence proliferation and protein synthesis of human dermal fibroblasts; these processes are crucial for the role of fibroblasts in wound healing (Croce et al., 2001; David-Raoudi et al., 2008).

PGE_2, which is synthesized from arachidonic acid by COXs and specific prostaglandin syntheses, acts as both an inflammatory mediator and fibroblast modulator (Sandulache et al., 2007). PGE_2 secretion from skin tissue after abnormal stimuli involves local edema formation and hyperalgesia (Sehgal et al., 2005). PGE_2 is one of the major lipid mediators of inflammation in diseases, such as rheumatoid arthritis and osteoarthritis, and is also involved in skin inflammation (Narumiya et al., 1999; Fiorucci et al., 2001; Su et al., 2010). Multiple studies have demonstrated that COX2 expression and PGE_2 secretion increase subsequent to tissue damage (Sandulache et al., 2007). In addition, PGE_2 has an important role in tissue ischemia from the report of a neuroprotective function in PGE_2 in cerebral ischemia through its receptor (Park et al., 2006).

Research problems

There are persistent issues with the use of these candidate markers for clinical applications as a method for detection of delayed healing caused by pressure. First, the candidate markers were identified in an in vitro study in rat fibroblasts and have not been proven to work in the granulation tissue of a real wound in an *in vivo* study. Second, the candidate markers were quantified in a supernatant of the culture medium and have not been analyzed in wound exudates in an *in vivo* study and in clinical PUs in cases of delayed healing caused by pressure.

The purpose of this study, therefore, was to verify the candidate markers by means of an *in vivo* study in clinical settings. To test the markers, the following strategy was pursued: first,

animal models of delayed wound healing caused by pressure were developed, and the list of candidate markers was narrowed down in these models (Chapter 1). Second, I verified the validity of the candidate markers using samples of clinical PUs to detect delayed healing caused by pressure, and I tested whether the cases in clinical PUs with delayed healing were caused by pressure or not using the validated marker compared with the other factors affecting delayed healing (Chapter 2).

CHAPTER 1.

Establishment of an animal model for delayed wound healing caused by pressure and validation of candidate markers for detection of delayed wound healing caused by pressure in these models

BACKGROUND

The purpose of this chapter was to narrow down *in vivo* the list of candidate markers, namely, PGE2, HA, and HSP90α, reported in our previous in vitro study (Kanazawa et al., 2014). The reason why the *in vivo* study was needed is as follows. Wound healing is a complicated phenomenon caused not only by activation of dermal fibroblasts but also by activation of epidermal keratinocytes, inflammatory responses, angiogenesis, nerve regeneration, and activation of somatic stem cells. In this complicated situation, it is necessary to confirm whether the increases of expression and secretion in granulation tissue, occurs in response to pressure loading. To perform the experiments that meet these requirements, I needed to obtain (1) animal models of delayed wound healing caused by pressure and (2) a biochemical method for analysis of wound exudates.

As for the former aspect, there has been no animal model according to delayed wound healing caused by pressure until now. Regarding delayed wound healing as chronic wound or PU model, there are large multiple studies available (Sugama et al., 2005; Tsuji et al., 2005; Salcido et al., 2007; Inoue et al., 2008; Tong et al., 2011; Demiot et al., 2011; O'Loughlin et al., 2013; Huang et al., 2013; Tsumano et al., 2013); however, most of the delayed wound healing was induced by hyperglycemia assumed as a diabetic wound model, by bacterial inoculation as a infected wound model, or by irradiation for a treatment of cancer therapy, but not by pressure loading. Among the PU models, most are ulceration models based on external clamping of a pair of magnet disks or some fixed materials with pulling of the skin. Although in a clinical situation, pressure that is applied to a wound reaches muscle tissue on a bony prominence from granulation tissue, with the above method, epidermis, dermis, and subcutaneous tissue layer are pinched, but not muscles. In this respect, the device used by Sugama et al., (2005) was able to apply pressure loading to a muscle layer from granulation tissue by pinching with an indenter applied to the skin and a metal plate inserted into the

intraperitoneal cavity through skin incisions; this approach meets my requirements as well. Nonetheless, it was necessary to verify the effects of Sugama's device on wound healing besides pressure because the skin incision and the plate insertion might adversely affect the wound healing due to the invasiveness. Definitions of models of delayed wound healing caused by pressure are as follows: first, delayed healing resulting from application of pressure loading to granulation tissue in the wound, and second, delayed healing is dependent on the magnitude of pressure loading. Accordingly, in this chapter, I developed animal models of delayed wound healing by applying pressure loading to the granulation tissue of a wound directly after verifying the effects of the skin incision and plate insertion.

As for the latter aspect, we have previously reported a convenient biochemical assessment tool, termed "wound blotting", for components in exudates of chronic wounds (Minematsu et al., 2013). Wound blotting allows us to easily collect fresh exudates by attaching a nitrocellulose membrane onto the wound surface and to quantitatively visualize the target component of exudates with a chemiluminescent reagent by an immunostaining method. In this chapter, I quantitatively assayed the candidate marker using the wound blotting method as a biochemical method for assessment of wound exudates.

Taken together, to achieve the purpose of this chapter, I developed animal models for delayed wound healing caused by pressure, and then narrowed down the candidate markers from our previous *in vitro* study in the analyses of mRNA expression, substance quantification related to the mRNA expression in granulation tissue and wound exudates from these rat models.

MATERIALS AND METHODS

Animals

Ninety-seven healthy male Wistar rats (age: approximately 6 months; weight: 480–580g)

were used in total; they were purchased from Japan SLC Inc. (Shizuoka, Japan). All animals were confirmed to be specific-pathogen-free for various microorganisms. They were administered pelleted food and water *ad libitum* and were maintained under a 12 h/12 h light/dark cycle starting at 8:00 am, with the ambient temperature maintained at 23 ± 2°C and humidity at 55 ± 10%. Animals were allowed at least five-day acclimatization prior to the experiments. Experimental protocol was approved by the Animal Research Committee of The University of Tokyo. All animals were treated according to the Guide for the Care and Use of Laboratory of the National Institute of Health (NIH).

Experimental design

In this chapter, first to establish animal models for delayed wound healing caused by pressure, I (1) verified delayed healing effect by the skin incisions and the plate insertion in pressure applying system and (2) elucidated the phenomenon of delayed wound healing caused by pressure. As the former aspect, I prepared 3 groups, which consisted of skin incisions with wound group (the incision group; n = 4), plate insertion through the incisions with wound group (the insertion group; n = 4), and only wound group (the control group; n = 6) to verify delayed healing by these effects. As the latter aspect, I prepared animal models that pressure loadings of 0-, 1-, 5-, and 10-kg/3 cm^2 were applied to the wounds to confirm delayed healing based on the wound area, wound period, macroscopic and histological findings in loadings groups compared with control group (n = 5 in each group). Next, to narrow down the candidate markers, I revealed the dynamics of exudates concentration and synthesis in the candidate markers using these animal models that pressure loadings of 0-, 1-, 5-, and 10-kg/3 cm^2 were applied to the wounds (n = 5 in each group).

Pressure loading procedures

One day after shaving the trunk hair of rats, a full-thickness round wound, a diameter of 1.5 cm, was created in the lateral region of each rat using sterile scissors, under sedation with an intraperitoneal injection of pentobarbital sodium (30 mg/kg body weight) (Somnopentyl; Kyoritsu Seiyaku Corporation, Tokyo, Japan). Each wound was covered with hydrocellular form dressing (ALLEVYN; Smith & Nephew Medical Ltd., Hull, UK) with film dressing (Tegaderm™ HP transparent dressing; 3M Health Care, St. Paul, MN) as a secondary dressing to keep the form dressing attached to the wound. In the verification of wound healing period by the effect of the skin incision and plate insertion into the intraperitoneal (without loading) and by the effect of pressure loading to the wound, the wound area was measured every day until wound healing date, which means the date of the epithelialization completion, after wounding using image analysis soft wear (ImageJ version 1.42; NIH, Bethesda, MD) from the photographed data, and the results were expressed relative to the wound area on post-wounding day-wounding day (PWD) 0 or 7.

On PWD 7, pressure loading was applied to each wound using pressure loading device for PU model developed by Sugama et al., 2005 (Figure 1-1 A). Briefly, skin incisions were created in lateroabdominal and dorsal region using sterile scissors then a metal plate was inserted under the wound. In this study, the indenter was modified by attaching rounded prominence to the tip to press the center of the wound. In reference to the previous studies in which pressure was loaded onto the skin not the wound (Sugama et al., 2005; Nakagami et al., 2008; Sari et al., 2015a), pressure was applied to the wounds at 0-, 1-, 5-, and 10-kg/3 cm^2 for 2 h. The 0-kg loading group means the negative control group, namely a plate was inserted but pressure was not loaded to animals in this group. During pressure loading, wounds were covered with the film dressing. During pressure loading, all wounds were covered with the film dressing. After pressure relief, the metal plate was removed and skin incisions were sutured. The form dressing was applied to the compressed wound and hydrocolloid dressing

(DuoDERM® Signal™ Dressing; ConvaTec Inc., Skillman, NJ) to the incision site. During dressings change and wound cleansing with normal saline, wound was observed and photographed with a digital camera everyday (Figure 1-1 B). In evaluation for delayed wound healing caused by pressure, I confirmed delayed healing based on the wound area, wound period, macroscopic and histological findings in loadings groups compared with control groups, respectively (n = 5 in each group).

On PWD 7 (just after loading), 8, and 14, animals were sacrificed by administering a lethal dose of pentobarbital sodium intraperitoneally, and tissue samples of the wound area were collected. One dorsal sides of each tissue sample cut in half were then used for histological and immunohistochemistry (IHC) examination containing from granulation to muscle layer. The other lateroabdominal sides containing granulation tissue only were powdered by cryohomogenizing in liquid nitrogen and used for real-time reverse transcription-polymerase chain reaction (RT-PCR), enzyme-linked immunosorbent assay (ELISA) of the substances concentration and fragmented DNA in the tissue, dot blotting, and western blotting, and stored at -80°C until the time of analyses (Figure 1-1 C).

Hematoxylin and eosin staining and IHC

The tissue samples were fixed in 4% paraformaldehyde in phosphate buffer, dehydrated with series of ethanol, cleansed with series of xylene and embedded in paraffin. Longitudinal 5-mm thick sections were deparaffinized and then hematoxylin and eosin (HE) staining and IHC was performed.

CD44, HAS1, and HSP90α immunostaining was performed as follows: the sections were incubated with anti-HCAM rabbit polyclonal antibody (Santa Cruz Biotechnology, Dallas, TX), anti-HAS1 rabbit polyclonal antibody (GenTex INC., Irvine, CA), or anti-HSP90α rabbit polyclonal antibody (Lab Vision Corporation, Fremont, CA) at room temperature for

60 min (each primary antibody was diluted 1:100) after quenching of endogenous peroxidase by incubation in 0.3% hydrogen peroxide diluted with methanol for 30 min and antigen retrieval by autoclaving sections in citrate buffer (pH 6.0). Subsequently, the sections were incubated with biotin-conjugated anti-rabbit IgG antibody (Jackson ImmunoResearch Laboratories, West Grove, PA; diluted 1:1000) for 30 min at room temperature. Immunoreactions were detected using a VectaStain ABC Kit (Vector Laboratories) with 3,3'-diaminobenzidine tetrahydrochloride substrate (Nacalai Tesque, Kyoto, Japan) and counterstained using hematoxylin.

Immunostaining for COX2 and HAS2 was performed by indirect method using anti-COX2 rabbit monoclonal antibody (Cell Signaling Technology, Danvers, MA; diluted 1:100) or anti-HAS2 mouse monoclonal antibody (Santa Cruz Biotechnology; diluted 1:100), and HRP-conjugated secondary antibodies (Jackson ImmunoResearch Laboratories; diluted 1:1000). Any other kind of immunostaining methods was performed as well as methods described above. The specificity of every antibody was confirmed in the positive control samples. The samples were observed using a light microscope (BX41; Olympus, Tokyo, Japan) and an inverted microscope (BIOREVO BZ-9000; Keyence, Osaka, Japan).

RNA extraction and real-time RT-PCR

Total RNA was extracted using the RNeasy Plus Mini Kit (QIAGEN, Hilden, Germany). cDNA synthesis was performed using the TM100™ Thermal Cycler (Bio-Rad, Richmond, CA) and the High Capacity cDNA Reverse Transcription Kit (Life Technologies, Carlsbad, CA). For quantitative RT-PCR, amplification of the target-specific region of cDNA was performed using Power SYBR® Green PCR Master Mix (Life Technologies) in a real-time PCR system (Mx3000P QPCR System; Agilent Technologies, Santa Clara, CA). The PCR protocol was as follows: 40 cycles at 95°C for 30 s and 60°C for 1 min after preheating at

95°C for 10 min. The relative expression level in the pressure loading groups to the control group was calculated by the comparative Ct method using the 18S ribosomal RNA (rRNA) gene as an internal control. The primer sequences of the *Cox2* (GeneBank accession no: NM_017232.3), *Has1* (GeneBank accession no: NM_172323.1), *Has2* (GeneBank accession no: NM_013153.1), *Cd44* (GeneBank accession no: NM_012924.2), *Hsp90aa1* (GeneBank accession no: NM_175761.2) and 18S rRNA were as follows, *Cox2* forward: 5'-CCCACTTCAAGGGAGTCTGG -3' and *Cox2* reverse, 5'-GCAGTCATCAGCCACAGGAG -3'; *Has1* forward, 5'- TTCAAGGCACTGGGTGACTC -3' and Has1 reverse, 5'- CCCAGTATCGAAGGCTGCTC -3'; *Has2* forward, 5'-AGGGGACCTGGTGAGACAGA -3' and *Has2* reverse, 5'-GGGTCAAGCATGGTGTCTGA -3'; *Cd44* forward, 5'- CCGTTACGCAGGTGTATTCC -3' and *Cd44* reverse, 5'- TGTTGAAAGCCTCGCAGAG -3'; *Hsp90aa1* forward, 5'-GTGCGGTTAGTCACGTT -3' and *Hsp90aa1* reverse, 5'- TCGAGTAGAAAGTGTTGATG -3' ; 18S rRNA forward, 5'- TCAAGAACGAAAGTCGGAGG -3' and 18S rRNA reverse, 5'- CCCTTCCGTCAATTCCTTTA -3'.

Quantification of apoptosis and ELISA

The cryohomoginized tissue samples were further homogenized in 1ml of phosphate-buffered saline (PBS) with a handy homogenizer and stored overnight at -20°C. After two freeze-thaw cycles to break the cell membranes, the homogenates were centrifuged for 10 min at 5000 × *g*, at 4°C. The supernatant was diluted 10-fold and assayed. All assayed values were standardized with the concentration of total protein in each sample using Pierce™ BCA Protein Assay Kit (Thermo Fisher Scientific Inc., Waltham, MA).

Quantification of apoptosis was measured using Cell Death Detection ELISA (Roche Applied Science, Mannheim, Germany), in which cytosolic oligonucleosome-bound DNA

was quantitatively measured as DNA fragmentation (Leist et al., 1994). HA concentration was measured using the QnE Hyaluronic Acid ELISA Assay (Biotech Trading Partners, Encinitas, CA). The concentration of HSP90α was measured using the Rat Heat Shock Protein 90α ELISA kit (CUSABIO BIOTECH, Wuhan, China). The concentration of PGE2 was measured using the PGE2 high sensitivity EIA kit (Enzo Life Sciences, Farmingdale, NY). Measurements were performed according to the manufacturer's instructions.

Dot blotting and western blotting

Dot blotting was performed to confirm whether the substances of candidate markers were absorbed to a nitrocellulose membrane. Next, the substance detected by dot blotting was confirmed by western blotting for specificity of the antibody.

In dot blotting experiments, PGE_2 (Biomol GmbH, Hamburg, Germany) was diluted with ethanol to make the concentration of 100 ng/ml as an base concentration and then 10, 1, and 0.1 ng/ml concentrations were made by serial dilution with pure water. HA of the concentrations of 800, 200, and 50 ng/ml from standard collections of the HA ELISA kit described above was prepared. Regarding HSP90α, a granulation tissue sample from a 10-kg loading sample on PWD 8, which was prepared independently of the samples used in the statistical analysis, was used as positive control. The cryohomoginized sample was incubated at 95°C for 10 min after diluting with 1 ml of sodium dodecyl sulfate (SDS) buffer (Sample Buffer, Laemmli 2× Concentrate; Sigma-Aldrich Co., St. Louis, MO; diluted 1:2) and subsequently 5 and 25 times diluted with SDS buffer. Dilution buffers for each substance were used as negative controls. Two-microliter of sample was dropped onto nitrocellulose membranes. After drying the membranes at room temperature for 10 min, the membranes were hydrated with PBS and incubated with Blocking One (Nacalai Tesque, Kyoto, Japan) with shaking at room temperature for 1 h. PGE_2 and HSP90α were detected by an indirect

method using primary antibodies, anti-PGE_2 mouse monoclonal antibody (Cayman Chemical Company, Ann Arbor, MI; diluted 1:10) and anti-HSP90α rabbit polyclonal antibody (Lab Vision Corporation; diluted 1:400), and secondary antibody, HRP-conjugated anti-mouse IgG antibody (Jackson ImmunoResearch Laboratories; diluted 1:1000) and HRP-conjugated anti-rabbit IgG antibody (Jackson ImmunoResearch Laboratories; diluted 1:1000). HA was detected by a VectaStain ABC Kit (Vector Laboratories) and Biotinylated Hyaluronic Acid Binding Protein (SEIKAGAKU CORPORATION, Tokyo, Japan; diluted 1:100). Immunoreactivities with chemiluminescent substrates, Luminata Forte (Merck Millipore, Billerica, MA), were captured by LumiCube (Liponics, Tokyo, Japan)

In western blotting of HSP90α, the sample with SDS buffer in the dot blotting experiment was used. Sample were separated with polyacrylamide gel electrophoresis (200 V, 40 min) and transferred to a nitrocellulose membrane by a semi-dry method. Following incubation (room temperature, 1 h) of the membrane with Blocking One (Nacalai Tesque), HSP90α was detected by the same above-mentioned dot blotting method.

In western blotting of HSP90α, the sample diluted with SDS in the dot blotting experiment was used. Protein components of the sample were separated with acrylamide gel electrophoresis (200 V, 40 min) and transferred to a nitrocellulose membrane by a semi-dry method. Following incubation (room temperature, 1 h) of the membrane with Blocking One (Nacalai Tesque), HSP90α was detected by the same above-mentioned dot blotting method.

Wound blotting

The fresh exudate was collected by attaching a nitrocellulose membrane to the wound surface for 10 sec after cleansing and photographing the wound site. The wound blotting membranes were stored at 4°C until the time of immunostaining.

The collected membranes were hydrated with PBS on PWD 7 before loading, 8, 10, and

14 from animal models. To inactivate endogenous peroxidase and block the membranes, the membranes were incubated with 0.3% hydrogen peroxide in 20% methanol at room temperature for 30 minutes and with Blocking One (Nacalai Tesque) at room temperature for 1 h. HSP90α was detected by immunostaining mentioned above. The images of immunoreactivities with chemiluminescent substrates were flipped horizontally. The mean of staining intensity within the wound area was indicated using ImageJ version 1.42 (NIH) for statistical analyses.

Statistical analysis

The differences among multiple groups were compared by ANOVA, Tukey's, or Dunnett's test. A p value < 0.05 was considered statistically significant (two-sided test). In the verification of delayed healing effect by the skin incisions and the plate insertion, coefficient of variation (CV) was estimated to confirm to reproducibility of wound healing period. The software IBM SPSS Statistics for Windows version 20.0 (IBM, Armonk, NY) was used for all statistical analyses.

RESULTS

Verification of the effects of the skin incisions and plate insertion on delayed healing

The pressure loading that I selected had large invasion to the body by pinching with an indenter applied to the wound and a metal plate inserted into the intraperitoneal through the skin incisions. I therefore prepared 3 groups, which consisted of skin incisions with wound group (the incision group; n = 4), plate insertion through the incisions with wound group (the insertion group; n = 4), and only wound group (the control group; n = 6) to verify delayed healing by these effects. On PWD 7, skin incisions and a metal insertion were performed for 2 h.

Macroscopic findings are shown in Figure 1-2. The wound reduction was strongly large from PWD 8 to 10 in the control group, whereas the wound reductions were relatively small in the incision and insertion groups compared with the control group. Wound area and is shown in Figure 1-3. Regarding the wound areas on PWD 0 and 7, significant difference did not occur in each group. Similarly to macroscopic findings, from PWD 8 to 17, significant difference occurred in the incision and/or insertion groups compared with the control. Between the incision and insertion groups, significant difference was not observed. Healing periods of full-thickness wound were 17.33 ± 1.21 (mean ± SD) days in the control group, 21.25 ± 0.95 days in the incision group, and 20.24 ± 0.95 days in the insertion group and CV was 6.9, 4.7, and 4.5%, respectively. Although wound healing was still delayed by the skin incision and plate insertion, the CV data showed reproducibility of the healing period by this methodology because the values of CV were lower than 10% for each group.

Animal models of delayed wound healing caused by pressure

I prepared these animal models with pressure loadings of 0-, 1-, 5-, and 10-kg/3 cm^2 on the wounds for 2 h on PWD 7 to confirm the wound area, wound period, and macroscopic findings in the loadings groups compared with the control groups, respectively (n = 5 in each group). Regarding the wound areas on PWD 0 and 7 before loading as baseline, significant differences were not observed among the groups (Table 1-1). Macroscopic findings in each group are shown in Figure 1-4. In the 10-kg group, in addition to bleeding, necrotic tissue appeared conspicuously on PWD 8 and 10 and was also present on PWD 14. In the 5-kg group, bleeding represented the main findings, and necrotic tissue was barely visible on PWD 10 and disappeared on PWD 14. In the 1-kg group, bleeding was the main finding, and necrotic tissue was not reliably detectable on PWD 8 and 10. Wound contraction in the 1-kg group happened earlier than in the other loading groups. In the control group, bleeding and

necrotic tissue were not observed at all from PWD 8 to 14. Figure 1-5 shows wound healing periods for each loading intensity. Compared with the control group (20.00 ± 1.00 days [mean ± SD]), the healing period in the 1-, 5-, and 10-kg groups were significantly long (22.60 ± 1.14, $p = 0.042$; 26.20 ± 1.64, $p < 0.001$; and 27.80 ± 1.30 days, $p < 0.001$, respectively). Regarding wound area, relative value to the wound area on PWD 7, during the wound hearing process for each loading intensity, compared with the control on each PWD, a significant difference was observed on PWD 8 in the 1-kg group, from PWD 8 to 19 in the 5-kg group, and from PWD 8 to 20 in the 10-kg group (Figure 1-6). These results met my requirements because delayed healing was dependent on the magnitude of pressure loading.

Histological analysis of the wound in the animal models of delayed wound healing caused by pressure

Tissue damage and inflammatory status were shown by HE staining. Figure 1-7 shows the whole tissue images under low magnification on PWD 7 (just after loading). At 1-kg pressure loading, the thickness of granulation and muscle tissue decreased in the compressed area. At both 5- and 10-kg loading, the muscle and granulation tissue were similarly affected by pressure loading, whereas the degree of collapse at the 10-kg loading was more severe than that at the 5-kg loading.

In figure 1-8, I show the highly magnified images of the granulation tissue at the center of the compressed area (A–D), the blood vessels around the compressed area (E–H), and the deep muscle layer (I–L) on PWD 7 (just after pressure loading). Fibroblasts were the dominant cell type along with a small number of inflammatory cells in the granulation tissue of the control samples (Figure 1-8A). On the other hand, in the loading groups with 1- and 5-kg compression, the layer of granulation tissue and fibroblasts was pressed and thinner, and the granulation tissue at the 10-kg loading was also pressed and thinner, whereas fibroblasts at

the 10-kg loading swelled (Figure 1-8B–D). Around the compressed area, bleeding was visible as leakage of erythrocytes from blood vessels in the loading groups but not in the control group, and a small number of inflammatory cells was observed at 1-, 5-, and 10-kg loading. In the muscle tissue, the loading groups showed tissue degeneration as compared to the control group (Figure 1-8I–L).

On PWD 8, the granulation tissue of the control contained numerous fibroblasts along with a small number of inflammatory cells, just as on PWD 7 (Figure 1-9A). At the 1-kg loading, extreme aggregation of inflammatory cells was observed (Figure 1-9B). On the other hand, there were few cells at the center of the wound bed at both 5- and 10-kg loading although inflammatory cells infiltrated slightly at the 5-kg loading (Figure 1-9C and D). Regarding blood vessels, bleeding was visible in the loading groups on PWD 8 as clearly as on PWD 7. In addition, infiltration of inflammatory cells was frequently identified in the area around the compressed area (Figure 1-9E–H). Infiltration of inflammatory cells and degradation of muscle fibers were more frequently identified in the muscle tissue at 5- and 10-kg loading than at the 1-kg loading (Figure 1-9I–L).

On PWD 14, the granulation tissue of the control contained numerous fibroblasts, just as on other PWDs (Figure 1-10A). Infiltration of fibroblasts was detected at the 1-kg loading but not at 5- or 10-kg loading, and hyalinization of collagen fibers was observed at 5- and 10-kg loading (Figure 1-10B–D). Hyalinization appears glassy and pink after HE staining. Bleeding was not observed in any groups, and infiltration of inflammatory cells was frequently identified around the compressed area in all groups (Figure 1-10E–H). Damage to the muscle tissue progressed in the loading groups; infiltration of inflammatory cells and degradation of muscle fibers increased in a loading-dependent manner (Figure 1-10J–L).

Quantification of apoptosis

Our previous study indicated that the number of apoptotic cells increased with the increase of expression of the candidate markers in the compressed 3D cultures of fibroblasts in a loading-dependent manner (Kanazawa et al., 2014). I therefore assumed that apoptosis is an important factor of delayed healing during pressure loading. Apoptosis was quantified by cytosolic oligonucleosome-bound DNA fragments using ELISA in the compressed wound tissues.

Figure 1-11 shows the results of quantification of apoptosis in each group on PWD 7, 8, and 14. On PWD 7 (just after loading), compared to the controls, the apoptosis level was higher only in the 1-kg group ($p = 0.022$). On PWD 8 and 14, no significant differences among the groups were observed.

Assays of COX2 and PGE2 in animal models

PGE_2 is synthesized from arachidonic acid by COXs and prostaglandin synthases. There are 2 major COX enzymes, COX1 and COX2, and COX1 is largely constitutively expressed, whereas COX2 is induced at sites of inflammation and various types of injury (Majed and Khalil, 2012). I thus assayed the mRNA and protein expression of COX2 and quantified PGE2 synthesis in the granulation tissue of the animal models (n = 5 in each group).

On PWD 7 (just after loading), the mRNA expression of *Cox2* was significantly upregulated in the loading groups as compared to the control group (1-kg group: $p < 0.001$, 5-kg group: $p < 0.001$, and 10-kg group: $p = 0.004$; Figure 1-12A). The expression of *Cox2* was significantly higher in the 5- and 10-kg groups on PWD 8 and in the 1- and 5-kg groups on PWD 14 than in the control groups (on PWD 8: $p < 0.001$ and $p = 0.019$, respectively; on PWD 14: $p < 0.026$ and $p = 0.008$, respectively; Figure 1-12B and C). On PWD 7 (just after loading), 8, and 14, all loading groups showed stronger COX2 staining in granulation tissue as compared to the control groups (Figure 1-13). Although both fibroblasts and neutrophils

were positively stained, majority of the positive cells were fibroblasts.

As for quantification of PGE_2 in granulation tissue, on PWD 7 after lording, the synthesis of PGE_2 was significantly higher in the 1- and 5-kg groups than in the control group (p = 0.043 and p = 0.013, respectively; Figure 1-13A). On PWD 8, significant differences between the loading groups and the controls were not observed (Figure 1-14B). On PWD 14, the synthesis of PGE_2 was significantly higher in the 5- and 10-kg groups than in the control group (p = 0.011 and p = 0.018, respectively; Figure 1-14C). These results suggested that the PGE_2 level was increased by pressure loading.

Assays of HAS1, HAS2, CD44, and HA in animal models

HAS1 and HAS2, which are HA synthases, are expressed in the epidermis and dermis (Sugiyama et al., 1998), and there is a weak correlation between expression levels of HAS and CD44, known as the major HA receptor; the interaction of HA and CD44 contributes to such cellular processes as proliferation and migration (Tammi et al., 2005). We previously showed that the mRNA expression of *Cd44* increases along with the upregulation of *Has2* (Kanazawa et al., 2014). Accordingly, I assayed the mRNA and protein expression of HAS1, HAS2, and CD44 and quantified HA in the granulation tissue of the animal models (n = 5 in each group).

On PWD 7 (just after loading), the mRNA expression of *Has1* was significantly upregulated in the loading groups as compared to the control group (1-kg group: p = 0.038, 5-kg group: $p < 0.001$, and 10-kg group: p = 0.018; Figure 1-15A). On PWD 8, compared to the control, the expression of *Has1* was higher only in the 1-kg group (p = 0.026; Figure 1-15 B). On PWD 14, significant differences in the expression of *Has1* between the loading groups and the controls were not detected (Figure 1-15C). IHC clearly showed that the 1- and 5-kg groups on both PWD 7 (just after loading) and 8 yielded remarkably stronger HAS1 staining

in granulation tissue in comparison with the control groups (Figure 1-16). Although both fibroblasts and vascular endothelial cells were positively stained, majority of the positive cells were fibroblasts.

As for mRNA expression of *Has2*, significant differences between the loading groups and the control were not observed on PWD 7 (just after loading; Figure 1-17A). On the other hand, the expression of *Has2* on PWD 8 was significantly upregulated in the 1- and 5-kg groups as compared to the control group ($p = 0.035$ and $p < 0.001$, respectively; Figure 1-17B). On PWD 14, compared to the control group, the expression of *Has2* was higher only in the 10-kg group ($p < 0.001$; Figure 1-17C). IHC showed that the 1- and 5-kg groups on PWD 8 and the 5- and 10-kg groups on PWD 14 yielded relatively stronger HAS2 staining in the granulation tissue as compared to the control groups (Figure 1-18). Although both fibroblasts and vascular endothelial cells were positively stained, majority of the positive cells were fibroblasts.

Compared to the control group, expression of *Cd44* on PWD 8 was higher only in the 5-kg group ($p = 0.033$), and significant differences between the loading groups and the control group were not detected on PWD 7 (just after loading) and 14 (Figure 1-19A, B, and C). I conducted quantification of CD44 because I wanted to test CD44 as a candidate marker: the extracellular domain of CD44 becomes soluble through cleavage by some matrix metalloproteinases or metalloproteinase domain-containing proteins (Chetty et al., 2012; Kim et al., 2012; Kamarajan et al., 2013). No significant differences in CD44 levels between the loading groups and the control were observed on PWD 7 (just after loading), 8, and 14 (Figure 1-20A, B, and C). IHC revealed that relatively stronger CD44 staining in granulation tissue was not observed in the loading groups compared to the control groups on PWD 7 (just after loading), 8, or PWD 14 (Figure 1-21). Although both fibroblasts and vascular endothelial cells were positively stained, majority of the positive cells were fibroblasts.

Quantification of HA in granulation tissue showed that on PWD 7 (just after loading), the

synthesis of HA was significantly higher in the 5-kg group than in the control group (p = 0.046; Figure 1-22A). On PWD 8, the synthesis of HA was significantly higher in the 1-kg group than in the control group (p = 0.040; Figure 1-22B). On PWD 14, significant differences between the loading groups and the control group were not detected (Figure 1-22C). These results suggested that HA, HAS1, and HAS2 were increased by pressure loading although the CD44 expression was not.

Assays of *Hsp90aa1* and HSP90α in animal models

HSP90α, encoded by the *Hsp90aa1* gene, is the stress-inducible isoform of the molecular chaperone Hsp90 (Zuehlke et al., 2015). I thus assayed the mRNA expression of *Hsp90aa1* and protein expression of HSP90α and quantified HSP90α in the granulation tissue of the animal models (n = 5 in each group).

Compared to the control group, the expression of *Hsp90aa1* on PWD 8 was higher only in the 10-kg group (p = 0.017), and significant differences between the loading groups and the control groups were not detected on PWD 7 (just after loading) and 14 (Figure 1-23A, B, and C). Figure 1-24 shows the result of HSP90α IHC in the granulation tissue of each loading group on PWD 7 (just after loading), 8, and 14. On PWD 7 (just after loading), relatively stronger HSP90α staining in granulation tissue was not observed in the loading groups compared to the control. On the other hand, on PWD 8, the 1-, 5-, and 10-kg groups showed relatively stronger HSP90α staining in granulation tissue as compared to the control group. Notably, the 1-, 5-, and 10-kg groups on PWD 14 showed remarkably stronger HSP90α staining in the granulation tissue. Although both fibroblasts and vascular endothelial cells were positively stained, majority of the positive cells were fibroblasts.

In terms of quantification of HSP90α in the granulation tissue, any significant differences

between the loading groups and the controls were not observed on PWD 7 (just after loading; Figure 1-25A). On PWD 8, the expression of HSP90α was significantly higher in the 5-kg group than in the control group ($p = 0.042$; Figure 1-25B).

On PWD 14, the expression of HSP90α was significantly higher in all loading groups than in the control group (1 kg group: $p = 0.043$, 5 kg group: $p = 0.043$, and 10 kg group: $p = 0.043$; Figure 1-25C). Taken together, these results suggested that the HSP90α level was increased by pressure loading as a function of time.

Analysis of wound exudates

Dot blotting was performed to confirm whether the candidate markers absorbed to a nitrocellulose membrane. Next, the substances detected by dot blotting were confirmed by western blotting for specificity of the antibody. These experiments were conducted for possible clinical application of wound blotting.

PGE_2 and HA were not detected by dot blotting (Figure 1-26A and B), whereas HSP90α was detected in a concentration-dependent manner (Figure 1-26C). Subsequently, in western blotting, HSP90α was observed around 90 kDa (Figure 1-26D). According to these results, I decided to verify HSP90α of the collected membranes including wound exudates of animal models by the wound blotting method.

Figure 1-27A shows the representative immunostaining images of HSP90α on wound blotting membranes. Although the HSP90α signal was not observed in the control group, strong HSP90α signals were detected on PWD 8 in the 5- and 10-kg groups, and on PWD 10 in the 1-, 5-, and 10-kg groups. The immunoreactivity was quantitated in the wound area, which was identified by image processing (Figure 1-27B).

In the quantitative analysis of each PWD, significant differences in HSP90α signals on PWD 7 before loading and 14 were not observed among the loading groups and the control group

(Figure 1-27C). On the other hand, compared with the control groups, significant differences in HSP90α signals were observed in the 10-kg group on PWD 8 and in all loading groups on PWD 10 (10 kg group: $p = 0.002$ on PWD 8; 1 kg group: $p = 0.003$, 5 kg group: $p = 0.002$, and 10 kg group: $p = 0.003$ on PWD 10; Figure 1-27C). Regarding the time course assay, in the 1- and 5-kg groups, HSP90α signals were significantly stronger on PWD 10 than on PWD 7 before loading ($p = 0.042$ and $p = 0.042$, respectively; Figure 1-27D). In the 10-kg groups, the HSP90α signal was significantly stronger on PWD 8 and 10 than on PWD 7 before loading ($p = 0.042$ and $p = 0.042$, respectively; Figure 1-27D). These results suggested that the secretion of HSP90α in wound exudates occurred in response to pressure loading.

DISCUSSION

This is the first study to establish animal models of delayed healing caused by pressure and to identify a marker in wound exudates for detection of delayed healing caused by pressure in an *in vivo* study. In this chapter, upregulation of PGE_2, HA, and HSP90α, the candidate markers from our previous study, was also observed in the loading groups compared to the control groups in the granulation tissue of the rat models. Therefore, I can say that these candidates are possible markers of delayed wound healing caused by pressure. Nevertheless, only HSP90α was found to be applicable to wound blotting for clinical purposes.

Animal models

My results revealed that pressure loading led to delayed healing along with granulation and muscle tissue degradation and bleeding. Indeed, the device used in this study was strongly invasive and lead to delayed healing. These invasive procedures had a strong influence due to skin incisions rather than the plate insertion because in the comparison of the incision group with the insertion group, significant differences were not observed in the healing period and

wound area. Nonetheless, the wound healing in the loading groups was still significantly delayed as compared to the control group with skin incisions and a prate insertion without pressure loading.

In the animal models, delayed healing was dependent on the magnitude of pressure loading according to the macroscopic findings. Necrotic tissue, as observed in the 5- and 10-kg groups, impeded the natural healing process because unviable tissue stimulates ongoing inflammation and leucocyte infiltration, which delay progression to the formation of granulation tissue and reepithelialization and interfere with the mechanism of wound contraction (Hellgren et al., 1986; Miller, 1996; Lewis et al., 2001). In addition, tissue damage and inflammatory status according to the histological analyses revealed that the healing was delayed in a loading-dependent manner.

Hyalinization was observed in the granulation tissue of the animal models on PWD 14. Hyalinization results in glassy and pink appearance after HE staining. Mechanical force such as local pressure within tissue can lead to cellular death and extracellular matrix (ECM) hyalinization (von Böhl and Kuijpers-Jagtman, 2009; Viecilli et al., 2009; Wakasugi et al., 2015). Hence, the findings from the animal models suggest that the surface of granulation tissue was exposed to the external forces such as the compressive and shear forces. Taken together, my data indicate validity of the proposed animal models of delayed wound healing caused by pressure.

Apoptosis

Some studies showed that apoptosis of dermal fibroblasts increases under the influence of mechanical stress including compressive force in *in vitro* experiments (Renò et al., 2003; Yip et al., 2007; Kanazawa et al., 2014) and that apoptosis-related factors may an important role in delayed wound healing (Jiang et al., 2012). Hence, I hypothesized that apoptosis is one of

important factors of delayed healing caused by pressure. However, compared to the control, apoptosis in the 1-kg group significantly increased only on the loading day, and the apoptosis did not increase in a loading-dependent manner. According to these results and my macroscopic findings, it appears that the delayed healing was probably due to necrosis rather than apoptosis because necrotic tissue was observed in the 5- and 10-kg groups but not in the 1-kg group. Some researchers demonstrated that severe prolonged hypoxia and oxidative stress cause necrosis rather than apoptosis (Clutton, 1997; Taimor et al., 1999). During prolonged hypoxia, the combination of a lack of oxygen and nutrients causes energy deprivation, which leads to downregulation of adenosine triphosphate (ATP) and induces cell death by necrosis because the low concentration of ATP disables the apoptotic cascade (Saikumar et al., 1998; McClintock et al., 2002; Greijer and van der Wall, 2004). Thus, it seems that the delayed healing had mechanisms that were different between the 1-kg group and the 5- and 10-kg groups.

Assays of the candidate markers

The expression of COX2 and PGE_2 was increased by pressure loading in the proposed animal models. Aside from our previous study (Kanazawa et al., 2014), there are no studies on compressive loading in dermal fibroblasts, whereas some researchers reported that compressive loading induces COX2 and PGE_2 as a cellular inflammatory response in periodontal ligament cells, synovial fibroblasts, tendon explants, and cartilage explants (Fermor et al., 2002; Kanzaki et al., 2002; Flick et al., 2006; Gosset et al., 2006; Shimomura et al., 2014). Wang and Thampatty (2008) concluded that COX2 is a mechanosensitive enzyme as demonstrated by dynamic compression of cartilage explants. Compressive loading thus is involved in the pathogenesis of tendon overuse injuries, occlusal trauma, and arthritis through accumulation or production of PGE_2 after tissue damage. In addition, induced PGE_2

production performs an important protective or nonprotective function depending on PGE_2 receptors in myocardial and cerebral ischemia (Suzuki et al., 2011; Ikeda-Matsuo, 2013). According to the above reports, the induction of PGE_2 in granulation tissue probably occurs through a mechanosensitive mechanism and/or tissue ischemia under the influence of pressure loading.

HA serves as a structural scaffold in tissues (Mascarenhas et al., 2004) and is reported to alter physical properties of ECM (Kreger et al., 2009), including hydration (Gerdin and Hällgren, 1997), diffusion (Coleman et al., 1998), and viscoelasticity (Xin et al., 2004; Falcone et al., 2006). HA also holds aggregates of proteoglycan (Hardingham and Muir, 1972) and forms huge complexes that perform a load-bearing function in ECM (Hardingham and Fosang, 1992). Because of these multiple functions of HA, accumulation or production of HA indicates that the cells respond to external mechanical stress by synthesizing a matrix that will allow the cells and/or tissue to adapt to the new mechanical environment (Evanko et al., 2007). For this reason, probably, the upregulation of HAS1, HAS2, and HA was observed in the animal models. In addition, HA also accumulates in myocardial ischemia (Waldenström et al., 1991), and COX2-dependent synthesis of PGE_2 stimulates HA synthesis through HAS1 and HAS2 mRNA expression (Sussmann et al., 2004; van den Boom et al., 2006). In light of these facts, HA production in this study was probably mediated by tissue ischemia and PGE_2 production induced by pressure loading.

The *Hsp90aa1* mRNA level increased higher in the loading groups than in the control group on the next day after loading, and its protein, HSP90α, level was also modulated, however, the time course of HSP90α induction was delayed compared with the mRNA induction in my study. This was consistent with the results of immunostaining. A previous study, HSP90α induction caused by heat stimulation as burn wound model, also reported delayed HSP90α induction compared with its mRNA induction (Zhang et al., 2014).

According to these observations, it is possible to propose some mechanisms involved in delayed HSP90α induction. Further studies are required to elucidate the detailed mechanisms of the delayed induction. In any case, HSP90α production induced by pressure loading seems to play an important role in cell repair.

To validate clinical application of these candidate markers to detection of delayed wound healing caused by pressure, I wanted to use wound blotting because this method is a convenient biochemical assay involving noninvasive collection of fresh wound exudates. PGE_2 and HA were unfortunately not detected by dot blotting with a nitrocellulose membrane, whereas HSP90α was detected. The nitrocellulose membrane is widely used for immunoblotting because hydrophobic and electrostatic interactions between the protein and the membrane matrix play a major role in the protein binding (Nakamura et al., 1989). Thus, PGE_2 and HA did not have sufficiently strong interactions with the nitrocellulose membrane for detectable binding. Particularly, the failure of HA binding may be caused by its hydrophilicity. In any case, I can conclude that HSP90α is applicable to wound blotting.

I have demonstrated that HSP90α expression increased in wound exudates of the loading groups in wound blotting experiments on PWD 8 and 10. However, the results of wound exudates on PWD 14 were inconsistent with HSP90α expression results by ELISA and immunostaining on PWD 14. This discrepancy could be owing to the difference between intracellular production and extracellular secretion of HSP90α. Expression and secretion of HSP90α is controlled differently. The intracellular form of HSP90α is one of the molecular chaperones and can maintain cell stability, facilitate correct folding of nascent proteins, redirect misfolded proteins, and cause degradation of a diverse set of client proteins (Schmitt et al., 2007). Various studies showed that hypoxia-triggered production of extracellular HSP90α is mediated by hypoxia-inducible factor 1 (HIF1), and the HSP90α secretion induced by hypoxia acts as the master regulator of initial skin wound healing (Li et al., 2007; Woodley

et al., 2015). Sari et al. (2010) confirmed that HIF1 is induced by pressure loading applied to the skin using the same device as the device used here. For these reasons, in the present study, HSP90α secretion into wound exudates may be mediated by hypoxia induced by pressure loading. On PWD 14, the HSP90α levels of wound exudates were not increased. The possible reason could be an accumulation of the mRNA-translated HSP90α protein in the fibroblasts, since there was a reduced secretion of HSP90α due to a reduction in hypoxia until PWD 14. Nonetheless, I assumed that HSP90α was a suitable marker of delayed healing caused by pressure because HSP90α can be efficiently secreted under the conditions of hypoxia and its production is induced by pressure loading.

In summary, I successfully developed the animal models of delayed wound healing caused by pressure. The increases of PGE_2, HA, and HSP90α were observed in granulation tissue of the loading groups compared with the control groups in animal models. However, besides HSP90α, PGE_2 and HA could not have sufficient interactions with nitrocellulose membrane for binding. In the analysis of wound exudates, HSP90α secretion induced by pressure loading along with delayed healing. Therefore, HSP90α seems to be a promising marker of delayed healing caused by pressure.

CHAPTER 2.

Clinical studies for validation of the markers of delayed wound healing caused by pressure

BACKGROUND

In chapter 1, I identified PGE_2, HA, and HSP90α as markers of delayed wound healing caused by pressure. However, clinical applicability of these markers is still unknown because of the differences among animal species and/or wound types. Therefore, in this chapter, in order to validate these candidate markers of delayed wound healing caused by pressure, I conducted 2 clinical studies as follows.

(1) Validation of PGE_2, HA, and HSP90α as markers in the debridement tissue of a chronic pressure ulcer whose medical history obviously showed the failure of pressure relief in a case study.

(2) Validation of the HSP90α assessment by wound blotting in delayed healing PUs caused by a pressure burden and normal healing PUs due to improvement from exposure to pressure in a case series study.

In addition, to verify involvement of the pressure burden in delayed healing of clinical PUs, further study that applied the HSP90α assessment by wound blotting was conducted in a cross-sectional study.

In the animal models, the analysis of HSP90α level in wound exudates was performed quantitatively using wound blotting method. From these results, HSP90α signal was more or less observed in loading groups, whereas HSP90α signal was almost negative in the control groups. In other words, the wounds with the history of exposure to pressure indicated HSP90α positive, and the wound with the history of nonexposure to pressure indicated HSP90α negative. In view of the clinical application, the ideal marker should be represented by the relationship the two values such as “positive” or “negative”. I considered that HSP90α would be a suitable marker in this point and decided to verify its validity in clinical setting with not quantitative threshold but the judgment of positive or negative in HSP90α signal using wound blotting method.

Thus to achieve the purpose of this chapter, I executed a case study to validate PGE_2, HA, and HSP90α as markers in the debridement tissue of a chronic pressure ulcer whose medical history obviously showed the failure of pressure relief and the case series study to verify the association of HSP90α and delayed wound healing caused by pressure in the case series including cases of PU exposed to pressure and PU improved from exposure to pressure. I then tested whether the cases in clinical PUs with delayed healing were caused by pressure or not using HSP90α as the marker with adjusting the other factors affecting delayed healing in a cross-sectional study.

MATERIALD AND METHODS

Study design

This chapter was composed of three study designs. First, in order to validate PGE_2, HA, and HSP90α as markers to identify pressure-induced delayed wound healing of PUs, a case study conducted. The debridement tissue was immunohistotchemically analysed for three markers in a chronic pressure ulcer whose medical history obviously showed the failure of pressure relief.

Second, in order to validate HSP90α as a marker to reveal pressure burden in non-healing pressure ulcers, the case series study was conducted. The pressure ulcers were investigated in the relationship between HSP90α positive detected by wound blotting and healing progress.

Finally, the cross-sectional study was conducted to statistically analyze the association between HSP90α positive detected by wound blotting and delayed wound healing.

The Ethics Committee of the Graduate School of Medicine, The University of Tokyo, approved the study protocols, which was conducted in accordance with the Helsinki Declaration of 1975.

Settings and participants

Case study

This case study was conducted at a city hospital in an urban area located in Kanagawa. The participant was a patient with delayed healing PU caused by unrelieved pressure. The entire wound and the surrounding skin was debrided under anesthesia for surgical treatment, fixed in 10% neutral buffered formalin, and used for histology and immunohistochemistry for COX2, HAS2, and HSP90α using the methods described in chapter 1.

Case series study

This case series study was conducted at a university hospital in an urban area located in Tokyo, Japan. The participants were patients who were examined for the first time during the routine rounds in an interdisciplinary PU team between July 2014 and August 2015. Inclusion criteria were as follows: (1) patients who had category II, III, IV, or unstageable PUs on the trunk according to the international NPUAP/EPUAP pressure ulcer classification system (NPUAP/EPUAP/PPPIA, 2014), (2) those whose proteins were collected from the wound surface by attaching a nitrocellulose membrane to the wound for at least 2 consecutive weeks. Exclusion criteria were as follows: (1) patients whose PU was suspected infection wound, (2) the examination of the period using the local negative pressure wound therapy. The interdisciplinary PU team, which consists of a plastic surgeon, a dermatologist, a rehabilitation physician, a dietician, a wound ostomy and continence nurse, and nurse scientists, determined and modified, as appropriate, the standardized management protocol based on the guideline of the Japanese Society of PUs once per week.

Cross-sectional study

In this cross-sectional study, the setting, the participants, inclusion criteria, and exclusion criteria were the same as those in the case series study above.

Data collection in the case series and cross-sectional studies

Information on age, sex, height, weight, and nutritional status and systemic condition-related data including calorie intake, albumin, total protein, hemoglobin, C-reactive protein, creatine kinase, lactate dehydrogenase and white blood cell counts was collected from medical charts. Underlying disease of each patient was collected from medical records and described with the ICD-10 classification. The information of fecal or urine contamination to wound region was collected from medical and the PU round records. The body mass index (BMI) was calculated from the collected data on height and weight.

Wound locations and the DESIGN-R® score were collected from the PU round records. The DESIGN-R® tool was developed to evaluate PU severity and to monitor the wound healing process using 7 parameters: depth, exudate, size, inflammation/infection, granulation tissue, necrotic tissue and undermining (Sanada et al., 2011; Matsui et al., 2011).

The photograph of the wound and the membrane of wound blotting were taken after washing and wiping the PU and surrounding skin at the time of the PU team rounds once a week during the follow-up.

Wound blotting procedure

The wound blotting membranes collected from the wound surfaces were stored at 4°C within a week until immunostaining.

After hydration of the collected membranes with PBS, staining and destaining of total protein was performed using the Pierce™ Reversible Protein Stain Kit for Nitrocellulose Membranes (Thermo Fisher Scientific Inc., Waltham, MA) according to the manufacturer's instructions. Endogenous peroxidase was inactivated by 0.3% hydrogen peroxide in 20% methanol because activity of endogenous peroxidase hides the immunoreactivities using the peroxidase-labeled secondary antibody. Then, blocking was performed with the Blocking One

(Nacalai Tesque, Kyoto, Japan). Subsequently, the membranes were incubated with primary antibodies for anti-HSP90α rabbit polyclonal antibody (Lab Vision Corporation, Fremont, CA; dilution 1:400) at room temperature for 30 min and with secondary antibodies, a horseradish peroxidase-conjugated anti-rabbit IgG antibody (Jackson ImmunoResearch Laboratories, West Grove, PA; diluted 1:1000), at room temperature for 10 min. The SNAP i.d.® 2.0 Protein Detection System (Merck Millipore, Billerica, MA) was used all procedures, except for the primary antibody incubation. The chemiluminescence of immunoreactivities was captured by LumiCube (Liponics, Tokyo, Japan) after incubation of the membrane with chemiluminescent substrates, Luminata Forte (Merck Millipore), at room temperature for 2 min.

Image processing was performed with same methods as a previous study (Kitamura et al., 2015). Briefly, all membrane images of luminescence and total protein staining were flipped horizontally, and wound edges on membrane images were identified from the total protein staining images. The sample with luminescent signal within wound area was considered as positive for HSP90α, and the sample without luminescent signal within wound area was considered as negative (Figure 2-1).

Evaluation of delayed healing

The wound area on the digital photograph was measured 3 times by image analysis software (ImageJ version 1.42; NIH), and the mean area was subjected to analysis. The reduction rate of the wound area was calculated by means of the following formula (Jessup, 2006),

$$\text{Reduction rate (\%)} = (A_{t-1} - A_t) / A_t * 100.$$

A_t: Area of wound at the time of assessment

A_{t-1}: Area of wound a week before assessment

In this study, the delayed healing was defined as the less than 10% of reduction rate of wound

area according to the previous reports (Steed et al., 2006; Nakagami et al., 2010).

Evaluation of a PU exposed to pressure

I conducted case series study to validate HSP90α as the marker for delayed healing caused by pressure. I focused on the case series including the case of which PU exposed to pressure due to a patient's activities of daily living (ADL), physical condition, or a specific event that indicated the fact that the PU was hitting on something, or that PU improved from exposure to pressure due to patient's ADL or physical condition described in the PU round record. Regarding these evaluations, I received the supervision of a wound, ostomy, and continence nurse with a PhD degree in medicine without receiving any results of HSP90α by the wound blotting.

Statistical analysis

Descriptive data were presented as mean ± standard deviation or number (%). In the cross-sectional study, generalized estimating equation (GEE) analysis (Zeger and Liang, 1986) with an exchangeable working correlation matrix was used to account for within-patient correlation since we repeatedly examined the same patients with PUs at PU rounds more than three times (weeks). GEE models with a logit link, Binomial working model were fit to determine the association between HSP90α or some variables and delayed healing at the following examination. Estimates of odds ratios (OR) and 95% confidence intervals (CI) for delayed wound healing were reported with covariates unadjusted or adjusted. The candidate variables which might relate to delayed healing including nutritional status, systemic condition-related data, and the information regarding fecal or urine contamination to the wound region were subjected to multivariate analyses when the *p*-value was less than 0.1 in univariate analysis. Pearson's correlation coefficients among the candidates for

multivariate analyses were calculated for continuous variables. When the coefficients more than 0.4 were found between the independent variables, only one of the variables was entered into the model. In addition, adjusted model included age, sex, and DESIGN-R® total score evaluating PU severity as covariates, because these variables were considered as factors related to wound healing (Breslow et al., 1993; van Rijswijk and Polansky, 1994; Kramer and Kearney, 2000; McGinnis et al., 2014; Horn et al., 2015). A p value less than 0.05 was considered as statistically significant (two-sided test). All Statistical analyses were performed using Stata/IC 13.1 (StataCorp, College Station, TX).

RESULTS

Case report

This case study was conducted to validate the candidate markers in a patient with delayed healing PU caused by unrelieved pressure. I thus performed HE staining and immunostaining of a wound sample from the patient.

The patient was a 60-year-old woman who had hemiplegia. She had a full thickness PU that was located in the sacral region and was caused by prolonged pressure due to cerebral hemorrhage-induced unconsciousness for 1 night. After sharp debridement and ointment treatment were administered several times, the PU area covered with necrotic tissue decreased. However, the ulcer remained unhealed caused by pressure resulting from lack of efficient postural change for hemiplegia. In addition, the granulation tissue appeared edematous.

First, I confirmed the microscopic observation by HE staining for the clinical patient with delayed healing in the PU caused by pressure. Fibrinoid degeneration and hyalinization were observed in the surface layer of granulation tissue (Figure 2-2A and B). Subsequently, I examined whether COX2, HAS2, and HSP90α, important proteins of candidate markers, expressed in the clinical sample. I clearly observed the expression of these factors in the

granulation tissue that represented a delayed wound healing caused by unrelieved pressure (Figure 2-2C–E). These results suggested the validity of PGE_2, HA, and HSP90α as markers to detect delayed wound healing caused by pressure.

Participants and wound characteristics

From July 2014 to August 2015, 18 of 35 patients had met the inclusion criteria, which is the patients who have a pressure ulcer of over category or unstageable on the trunk with the data of wound blotting more than 2 consecutive weeks. Of these, 2 patients were excluded due to suspected infection wounds.

The mean age was 66.5 ± 14.5 years among the remaining 16 patients. Ten patients (62.5%) were male, and the mean BMI was 20.6 ± 5.3. In nutritional status-related data, the mean serum albumin level was 2.5 ± 0.5 g/dL, and the mean serum total protein level was 5.7 ± 0.8 g/dL. The most frequent PU sites were the sacrum (n = 9; 56.2%), followed by the coccyx (n=5; 31.3%) and the buttocks and greater trochanter (n=1; 6.3%). The most common PUs (n = 8; 50%) were classified as category II (Table 2-1). All these descriptive data were collected from the first week during the PU rounds. Of 49 examinations in the 16 patients, two examinations were excluded because of including the data of the period using the local negative pressure wound therapy. Consequently, the results of 47 examinations were entered into the analysis (Table 2-2).

Case series study

I executed case series study to verify the association of HSP90α and delayed wound healing in the case series including cases of PU exposed to pressure or PU improved from exposure to pressure. There were 3 case series that met this criterion.

Patient 1 was a 66-year-old male with adrenal cancer and a PU in the sacrum. He was

hospitalized for the purpose of ureteral stent placement. He was using opioid analgesics for cancer pain and was able to walk when cancer pain was calm. His wound was susceptible to pressure because he preferred crossed legs position in the recumbent position. He used an alternating pressure air mattress. However, in 1st week, his wound was exposed to pressure because his sacrum hit the bottom of the mattress. For this reason, weight setting of the mattress was changed to 60-kg from 40-kg as pressure redistribution care. In 2nd week, exposure to pressure in last week caused delayed healing along with HSP90α positive (Figure 2-3A and G), and weight setting was also changed to 70-kg due to hitting the bottom. In 3rd week, exposure to pressure in 2nd week also caused delayed healing along with HSP90α positive (Figure 2-3B and H), and ADL improving increased his mobilization. In 4th week, his mobilization lead to normal healing along with HSP90α negative (Figure 2-3C and I), and his mobilization was continued. In 5th week, his mobilization in 4th week also lead to normal healing along with HSP90α negative (Figure 2-3D and J), on the other hand, his ADL began to be worse and decreased his mobilization. In 6th week, his decreased mobilization in 5th week caused delayed healing along with HSP90α positive (Figure 2-3E and K), and his physical status deteriorated. In 7th week, the deterioration of physical status caused delayed healing, whereas HSP90α was negative (Figure 2-3F and L). The deterioration led to a fluid retention state and weight gain, and he died next week.

Patient 2 was a 78-year-old male patient diagnosed with diabetes and suspected Parkinson‘s disease with a pressure ulcer at the coccyx. He was hospitalized for the purpose of intensive examination and treatment for impaired consciousness, gait disturbance, and lower extremity edema. A suppression band and mittens were used for intense motion by delirium. He was able to be standing and transfer to a wheel chair with light assistance. His wound recovered steadily until 5th week due to his passable ADL and HSP90α was negative for these weeks (Figure 2-4A–D and F–I). However, in 5th week, pressure, which was

measured as 168 mmHg, on the wound by the hard parts of the suppression band caused his pain. In 6th week, the compression by the band in 5th week caused delayed healing along with HSP90α positive (Figure 2-4E and J). Next week, he was transferred to another hospital.

Patient 3 was a 45-year-old male patient diagnosed with schizophrenia with a pressure ulcer at the sacrum. He was hospitalized for the purpose of intensive examination for anemia and malnutrition. A suppression band was used for schizophrenia, and it was difficult to provide pressure redistribution care with due to the suppression band. That is, there was also no effective repositioning care. For these reasons, his wound was exposed pressure, which caused delayed healing in 2nd and 3rd weeks along with HSP90α positive, respectively (Figure 2-5A–D).

Consequently, 1 week after PU was exposed to pressure, the PU showed delayed healing along with HSP90α positive, whereas 1 week after PU improved from exposure to pressure, the PU showed normal healing along with HSP90α negative. Taken together with these case series, HSP90α was able to explain almost the cases of delayed wound healing caused by pressure with its positive signal and the cases of PU improved from exposure to pressure with its negative signal. However, there was an exception in 7th week of patient 1. In this case, deterioration of the physical condition caused delayed healing, whereas HSP90α was negative, even though in the previous week (6th week) delayed healing was observed along with HSP90α positive due to his wound exposed to pressure caused by ADL deterioration continued from the 5th week. The delayed healing of the 7th week may have been caused by deterioration of the physical condition itself rather than by exposure to pressure due to the reduction in his mobility because of his serious condition. Thus, the deterioration of the physical condition led to a fluid retention state and weight gain, and he died next week. Therefore, it appears that HSP90α can explain delayed wound healing caused by pressure. In accordance with this evidence, I then conducted quantitative analysis of repeated

examinations in a cross-sectional study.

Factor analysis of delayed wound healing

Based on the judgment of HSP90α positive or negative, 22 examinations (46.81%) were classified as positive findings of HSP90α, and 25 (53.19%) as negative findings. In delayed healing assessment, 16/22 (72.72%) PUs of examinations in the HSP90α positive group were delayed healing. In contrast, 23/25 (92.00%) PUs of examinations in the HSP90α negative group were normal healing. Eighteen (38.30%) examinations resulted in delayed healing, and 29 (61.70%) did not. The cross tabulation of the examinations in HSP90α positive or negative and delayed healing positive or negative groups is described in Table 2-3.

The GEE model in univariate analysis showed that the odds of detecting delayed healing at the examination compared with the last week examination were higher significantly in HSP90α positive compared with HSP90α negative at the examination (unadjusted OR 32.32, 95% CI 8.42–123.99, $p < 0.001$). Regarding association between other variables and delayed healing, variables including albumin, hemoglobin, and creatin kinase level were found to be possible candidates as the factor of delayed healing for multivariate analysis (Table 2-4). Among these candidate factors, I evaluated the multicollinearity and found a correlation between HSP90α and creatine kinase. As a result, I entered HSP90α in multivariate analysis. The adjusted model demonstrated that HSP90α was significantly associated with delayed healing (adjusted OR 200.58, CI 11.71–3433.19, $p < 0.001$) (Table 2-5). These results suggest that of 18 examinations indicating delayed healing, 16 examinations were suggestive of pressure.

DISCUSSION

In this chapter, I found validity of PGE_2, HA, and HSP90α as markers of delayed wound

healing caused by pressure and a significant association between HSP90α positive and delayed wound healing cased by pressure through clinical study based on the evidence from the case series, namely, that HSP90α was able to explain the cases of delayed wound healing caused by pressure with its positive signal and the cases of PU improved from exposure to pressure with its negative signal. The odds of detecting delayed healing during an examination as compared to the last week's examination were significantly higher for HSP90α positive PUs as compared to HSP90α negative PUs. In addition, measurement of HSP90α concentration in a wound exudate by the wound blotting method is a noninvasive, objective, safe, and harmless approach and is highly useful for wound assessment because there is a scientific and objective rationale behind the analysis of wound exudates for assessment of a wound's condition (Moseley et al., 2004). The results of this chapter seem to be the first report that HSP90α in a wound exudate can indicate delayed wound healing caused by pressure. Furthermore, HSP90α detecting delayed healing caused by pressure with not quantitative threshold but the judgment of positive or negative suggests that this detective method can be performed easily.

In the single case report, HE staining showed hyalinization of dermal collagen in the surface layer of granulation tissue. Hyalinization was also observed in the granulation tissue of the animal models in chapter 1. Hyalinization yields glassy and pink appearance after HE staining. A mechanical force such as local pressure within a tissue can lead to cellular death and ECM hyalinization (von Böhl and Kuijpers-Jagtman, 2009; Viecilli et al., 2009; Wakasugi et al., 2015). Hence, these findings from patients and rat models suggest that the surface of granulation tissue is exposed to external forces such as compressive and shear forces.

In this case, the abundant expression of COX2, HAS2, and HSP90α was observed. These observations suggested that PGE_2, HA, and HSP90α are promising markers for detection of

delayed wound healing caused by pressure. Combined evaluation of these markers might contribute to the more sensitive and/or accurate assessment, although PGE_2 and HA are not appropriate for wound blotting as demonstrated in chapter 1. Further study will be needed to develop effective methods to evaluate them simultaneously in wound exudate.

According to an overview of wound characteristics, 37.5% of all wounds were unstageable PUs in which the base of the ulcer is covered by necrotic tissue in the wound bed (NPUAP/EPUAP/PPPIA, 2014). This proportion is much higher than that in the report of VanGilder et al. (2010): 15%. Cell death in the compressed area yields necrotic tissue (von Böhl and Kuijpers-Jagtman, 2009). In my clinical study, there may have been relatively many PUs exposed to pressure; therefore, there were so many cases of delayed healing caused by pressure along with HSP90α positive.

In addition to pressure, of course, there are other factors associated with delayed healing such as malnutrition, wound infection after contamination with excreta, and the systemic condition due to an underlying disease (Alvarez, 1991; Thomas, 2006). Particularly, with respect to pressure, nutrition, and excreta contamination, these are the subjects of nursing interventions. In the present study, wound infection cases were excluded because I could not differentiate delayed healing caused by exposure to pressure and that caused by wound infection, whereas malnutrition cases were not excluded because almost all patients were malnourished. I thus verified the association between delayed healing and nutritional status, the systemic condition, or excreta contamination in univariate and multivariate analyses. A significant association was not observed in the multivariate analysis. On the other hand, HSP90α showed a significant association with delayed healing in the covariates adjusted model.

The HSP90α release is induced by hypoxia (Li et al., 2007), and Liao et al. (2000) showed that oxidative stress causes a sustained release of HSP90α, which in turn stimulates activation

of the ERK1/2 pathway in rat vascular smooth muscle cells. Generally, compression that is applied to skin tissues causes hypoxia after ischemia through capillary occlusion (Kosiak, 1961). Compressive loading when applied to the skin or dermal fibroblasts induces hypoxia and oxidative stress (Sari et al., 2010; Kanazawa et al., 2014; Sari et al., 2015b). In addition, pressure loading induced HSP90α production in my animal experiments in chapter 1. Thus, HSP90α is secreted into wound exudates through hypoxia and oxidative stress due to exposure of a PU to pressure and thereby can indicate delayed healing in the wound blotting assay. Therefore, I suggest that HSP90α is a suitable marker of delayed healing caused by pressure.

In nursing implementation, the most important issues for PU care are pressure redistribution, nutrition management, and preventing contamination due to incontinence. At present, when wound healing does not proceed, nurses face a dilemma because they do not know what factors caused the delayed healing. HSP90α evaluation by wound blotting as a way to identify pressure-impaired healing should allow for a specific nursing intervention leading to effective and appropriate pressure relief. In addition, results of the cross-sectional study revealed that the pressure burden was a major factor in delayed healing. Therefore, I believe that pressure redistribution for wounds in current care is not being implemented effectively. The biomarker of pressure-induced delayed healing can be an objective indicator in selecting the repositioning frequency and the special support surfaces. Thus, the biomarker enables us to prioritize pressure redistribution care and efficiently allocate medical resources such as nursing time and special support surfaces.

This time, I studied the verification of HSP90α focused on PUs on the trunk. Because it is unusual case that PUs on the limbs are exposed to sustained pressure unless falling down senseless with specific situations such as myocardial infarction and cerebral infarction, I excluded PUs on the limbs. Thus, I am unable to generalize my results to the sites other than

the trunk. To solve this problem, further research with collecting a lot of the cases on other sites is needed. The limited sample size of the case series including cases of PU exposed to pressure or PU improved from exposure to pressure did not allow us to estimate indicator for assessing the diagnostic effectiveness such as the sensitivity, specificity, positive predictive value and negative predictive value. In addition, the participants were recruited from one particular university hospital located in an urban area in Japan. Taking these limitations into consideration, a large-scale prospective study involving a wide variety of settings is needed.

This study revealed that biomarkers are responsible for pressure loading in the granulation tissue. However, their specificities for pressure loading have not been demonstrated. Further studies such as randomized control trials will have to be conducted, to show that pressure redistribution care decreases HSP90α in HSP90α-positive PUs and clarify the specificities for pressure.

In summary, this chapter revealed that delayed wound healing caused by pressure could be detected by HSP90α through clinical study based on the evidence, from the case series, that HSP90α was able to explain the cases of delayed wound healing caused by pressure with its positive signal and the cases of PU improved from exposure to pressure with its negative signal and HSP90α could indicate the significant association with delayed healing in covariates adjusted model. In addition, measuring HSP90α in wound exudate using wound blotting method is noninvasive, objective, safe and harmless and offers the great advantage of wound assessment. These findings indicate that HSP90α is a promising marker of delayed healing caused by pressure.

CONCLUSION

In this thesis, I intended to establish the marker to detect delayed wound healing caused by pressure. In animal experiments, animal models for delayed wound healing caused by pressure could be established. HSP90α secretion induced in wound exudates of animal models by pressure loading along with delayed healing. Based on the results of animal experiments, I verified the usefulness of HSP90α as the marker for delayed wound healing caused by pressure in clinical setting. In case series study, HSP90α could explain the cases of delayed wound healing caused by pressure with its positive signal and the cases of PU improved from exposure to pressure with its negative signal. In the quantitative analysis of repeated examinations, HSP90α could indicate significant association with delayed healing in covariates adjusted model. These results indicate HSP90α is a suitable marker to detect delayed healing caused by pressure.

ACKNOWLEDGMENTS

My final task is to acknowledge all contributors to the work described in this thesis. This is difficult; a lot of people helped to design, implement, sponsor, and critically review the work. I will try to acknowledge all those who have helped, but if you find your name missing, please accept that I am as grateful to you as to those listed below.

First, Professor Hiromi Sanada (The University of Tokyo, Department of Gerontological Nursing/Wound care management) gifted me with an excellent opportunity to investigate a challenging research theme. Her advice was always precise and elegant and much encouraged me. Her philosophy profoundly affected my research philosophy. It would be my pressure if a reader could find her spirit of scientific research in this thesis.

Dr. Gojiro Nakagami who is a basic and clinical research scientist (The University of Tokyo, Department of Gerontological Nursing/Wound care management) provided me with accurate academic advice and suggestions on basic and clinical research. He generously provided the protocol related to pressure loading experiment. In addition, without his extensive advice of statistical analysis in clinical research, this thesis would not have been possible. I learnt many things from him on how to be a better researcher.

Dr. Takeo Minematsu who is a basic research scientist (The University of Tokyo, Department of Gerontological Nursing/Wound care management) provided me with extensive assistance and guidance. Without his extensive advice in executing animal experiments, fundamental techniques in histological analysis, and excellent suggestions from a molecular biology perspective, this thesis would not have been possible.

Professor Junko Sugama (Kanazawa University, Department of Clinical Nursing) lectured me about fundamental techniques to pressure loading experiments, particularly management of anesthesia. She generously provided me the equipment for creating animal models in this thesis. This pressure loading experiments is based on her 15 years of work on pressure ulcer

modeling.

Dr. Shinichi Ikeda who is a basic research scientist (The University of Tokyo, Department of Gerontological Nursing/Wound care management) provided me with many techniques related to basic research, particularly the analysis of protein expression. His excellent advice allowed me to push on with my research in animal experiments.

Professor Taketoshi Mori who is an engineering scientist (The university of Tokyo, Department of Life Support Technology) critically reviewed my thesis and advised me on the composition of my research theme. I was very pleased to receive revision.

I would like to express my gratitude to members of the Department of Gerontological Nursing/Wound care management and Life Support Technology at The University of Tokyo. I am also grateful for the support given to me by my many friends. Last but not least, I would like to say thanks to my father and my mother for their support and encouraging me.

This study was supported by a grant-in-aid for scientific research from the Japanese Society of Pressure Ulcers (Principle investigator; Toshiki Kanazawa) and a grant-in-aid for research activities from the Graduate Program for social ICT Global Creative Leaders of The University of Tokyo.

10th, December 2015

REFERENCE

Alvarez OM. Pressure ulcers: critical considerations in prevention and management. Clin Mater. 1991;8:209-22.

Asada M, Nakagami G, Minematsu T, Nagase T, Akase T, Huang L, Yoshimura K, Sanada H. Novel biomarkers for the detection of wound infection by wound fluid RT-PCR in rats. Exp Dermatol. 2012;21(2):118-22.

Bennett G, Dealey C, Posnett J. The cost of pressure ulcers in the UK. Age Ageing. 2004 May;33:230-5.

Berlowitz DR. Thomas DR and Compton GA (eds.), Pressure Ulcers in the Aging Population: A Guide for Clinicians, chapter 2, Incidence and Prevalence of Pressure Ulcers Pressure Ulcers in the Aging Population; A Guide for Clinicians, Springer Science+Business Media New York 2014

Berlowitz DR, Brienza DM. Are all pressure ulcers the result of deep tissue injury? A review of the literature. Ostomy Wound Manage. 2007;53:34-8.

Breslow RA, Hallfrisch J, Guy DG, Crawley B, Goldberg AP. The importance of dietary protein in healing pressure ulcers. J Am Geriatr Soc. 1993;41:357-62.

Buchner J. Hsp90 & Co. - a holding for folding. Trends Biochem Sci. 1999;24:136-41.

Chen G, Cao P, Goeddel DV. TNF-induced recruitment and activation of the IKK complex require Cdc37 and Hsp90. Mol Cell. 2002;9:401-10.

Chetty C, Vanamala SK, Gondi CS, Dinh DH, Gujrati M, Rao JS. MMP-9 induces CD44 cleavage and CD44 mediated cell migration in glioblastoma xenograft cells. Cell Signal. 2012;24:549-59.

Clutton S. The importance of oxidative stress in apoptosis. Br Med Bull. 1997;53:662-8.

Coleman PJ, Scott D, Abiona A, Ashhurst DE, Mason RM, Levick JR. Effect of depletion of interstitial hyaluronan on hydraulic conductance in rabbit knee synovium. J Physiol. 1998;509:695-710.

Croce MA, Dyne K, Boraldi F, Quaglino D Jr, Cetta G, Tiozzo R, Pasquali Ronchetti I. Hyaluronan affects protein and collagen synthesis by in vitro human skin fibroblasts. Tissue Cell. 2001;33:326-31.

David-Raoudi M, Tranchepain F, Deschrevel B, Vincent JC, Bogdanowicz P, Boumediene K, Pujol JP. Differential effects of hyaluronan and its fragments on fibroblasts: relation to wound healing. Wound Repair Regen. 2008;16:274-87.

Dealey C, Posnett J, Walker A. The cost of pressure ulcers in the United Kingdom. J Wound Care. 2012;21:261-2, 264, 266.

Defloor T, De Bacquer D, Grypdonck MH. The effect of various combinations of turning and pressure reducing devices on the incidence of pressure ulcers. Int J Nurs Stud. 2005;42:37-46.

Demiot C, Sarrazy V, Javellaud J, Gourloi L, Botelle L, Oudart N, Achard JM. Erythropoietin restores C-fiber function and prevents pressure ulcer formation in diabetic mice. J Invest Dermatol. 2011;131:2316-22.

Dowsett C, Newton H. Wound Bed Preparation: TIME in practice. Wounds UK. 2005;1:48-70.

Evanko SP, Tammi MI, Tammi RH, Wight TN. Hyaluronan-dependent pericellular matrix. Adv Drug Deliv Rev. 2007;59:1351-65.

Falcone SJ, Palmeri DM, Berg RA. Rheological and cohesive properties of hyaluronic acid. J Biomed Mater Res A. 2006;76:721-8.

Fermor B, Weinberg JB, Pisetsky DS, Misukonis MA, Fink C, Guilak F. Induction of cyclooxygenase-2 by mechanical stress through a nitric oxide-regulated pathway. Osteoarthritis Cartilage. 2002;10:792-8.

Fiorucci S, Meli R, Bucci M, Cirino G. Dual inhibitors of cyclooxygenase and 5-lipoxygenase. A new avenue in anti-inflammatory therapy? Biochem Pharmacol. 2001;62:1433-8.

Flick J, Devkota A, Tsuzaki M, Almekinders L, Weinhold P. Cyclic loading alters biomechanical properties and secretion of PGE2 and NO from tendon explants. Clin Biomech. 2006;21:99-106.

Galea-Lauri J, Richardson AJ, Latchman DS, Katz DR. Increased heat shock protein 90 (hsp90) expression leads to increased apoptosis in the monoblastoid cell line U937 following induction with TNF-alpha and cycloheximide: a possible role in immunopathology. J Immunol. 1996;157:4109-18.

Gallagher P, Barry P, Hartigan I, McCluskey P, O'Connor K, O'Connor M. Prevalence of pressure ulcers in three university teaching hospitals in Ireland. J Tissue Viability. 2008;17:103-9.

Gerdin B, Hällgren R. Dynamic role of hyaluronan (HYA) in connective tissue activation and inflammation. J Intern Med. 1997;242:49-55.

Gosset M, Berenbaum F, Levy A, Pigenet A, Thirion S, Saffar JL, Jacques C. Prostaglandin E2 synthesis in cartilage explants under compression: mPGES-1 is a mechanosensitive gene. Arthritis Res Ther. 2006;8:R135.

Greijer AE, van der Wall E. The role of hypoxia inducible factor 1 (HIF-1) in hypoxia induced apoptosis. J Clin Pathol. 2004;57:1009-14.

Hardingham TE, Fosang AJ. Proteoglycans: many forms and many functions. FASEB J. 1992;6:861-70.

Hardingham TE, Muir H. The specific interaction of hyaluronic acid with cartillage proteoglycans. Biochim Biophys Acta. 1972;279:401-5.

Hellgren L, Mohr V, Vincent J. Proteases of Antarctic krill-a new system for effective enzymatic debridement of necrotic ulcerations. Experientia. 1986;42:403-4.

Hendrichova I, Castelli M, Mastroianni C, Piredda M, Mirabella F, Surdo L, De Marinis MG, Heath T, Casale G. Pressure ulcers in cancer palliative care patients. Palliat Med. 2010;24:669-73.

Horn SD, Barrett RS, Fife CE, Thomson B. A Predictive Model for Pressure Ulcer Outcome: The Wound Healing Index. Adv Skin Wound Care. 2015;28:560-72.

Houwing R, Overgoor M, Kon M, Jansen G, van Asbeck BS, Haalboom JR. Pressure-induced skin lesions in pigs: reperfusion injury and the effects of vitamin E. J Wound Care. 2000;9:36-40.

Huang SP, Huang CH, Shyu JF, Lee HS, Chen SG, Chan JY, Huang SM. Promotion of wound healing using adipose-derived stem cells in radiation ulcer of a rat model. J Biomed Sci. 2013;20:51.

Iizaka S, Sanada H, Minematsu T, Oba M, Nakagami G, Koyanagi H, Nagase T, Konya C, Sugama J. Do nutritional markers in wound fluid reflect pressure ulcer status? Wound Repair Regen. 2010;18:31-7.

Iizaka S, Sugama J, Nakagami G, Kaitani T, Naito A, Koyanagi H, Matsuo J, Kadono T, Konya C, Sanada H. Concurrent validation and reliability of digital image analysis of granulation tissue color for clinical pressure ulcers. Wound Repair Regen. 2011;19:455-63.

Ikeda-Matsuo Y. The role of prostaglandin E2 in stroke-reperfusion injury. Yakugaku Zasshi. 2013;133:947-54. In Japanese.

Inoue H, Murakami T, Ajiki T, Hara M, Hoshino Y, Kobayashi E. Bioimaging assessment and effect of skin wound healing using bone-marrow-derived mesenchymal stromal cells with the artificial dermis in diabetic rats. J Biomed Opt. 2008;13:064036.

Itano N, Kimata K. Molecular cloning of human hyaluronan synthase. Biochem Biophys Res Commun. 1996;222:816-20

Itano N, Sawai T, Yoshida M, Lenas P, Yamada Y, Imagawa M, Shinomura T, Hamaguchi M, Yoshida Y, Ohnuki Y, Miyauchi S, Spicer AP, McDonald JA, Kimata K. Three isoforms of mammalian hyaluronan synthases have distinct enzymatic properties. J Biol Chem. 1999;274:25085-92.

Jessup RL. What is the best method for assessing the rate of wound healing? A comparison of 3 mathematical formulas. Adv Skin Wound Care. 2006;19:138-47.

Jiang L, Zhang E, Yang Y, Zhang C, Fu X, Xiao J. Effectiveness of apoptotic factors expressed on the wounds of patients with stage III pressure ulcers. J Wound Ostomy Continence Nurs. 2012;39:391-6.

Kamarajan P, Shin JM, Qian X, Matte B, Zhu JY, Kapila YL. ADAM17-mediated CD44 cleavage promotes orasphere formation or stemness and tumorigenesis in HNSCC. Cancer Med. 2013;2:793-802.

Kanazawa T, Nakagami G, Minematsu T, Yamane T, Huang L, Mugita Y, Noguchi H, Mori T, Sanada H. Biological responses of three-dimensional cultured fibroblasts by sustained compressive loading include apoptosis and survival activity. PLoS One. 2014;9:e104676.

Kanzaki H, Chiba M, Shimizu Y, Mitani H. Periodontal ligament cells under mechanical stress induce osteoclastogenesis by receptor activator of nuclear factor kappaB ligand up-regulation via prostaglandin E2 synthesis. J Bone Miner Res. 2002;17:210-20.

Kim YH, Jung JC. Suppression of tunicamycin-induced CD44v6 ectodomain shedding and apoptosis is correlated with temporal expression patterns of active ADAM10, MMP-9 and MMP-13 proteins in Caki-2 renal carcinoma cells. Oncol Rep. 2012;28:1869-74.

Kitamura A, Yoshida M, Minematsu T, Nakagami G, Iizaka S, Fujita H, Naito A, Takahashi K, Mori T, Sanada H. Prediction of healing progress of pressure ulcers by distribution analysis of protein markers on necrotic tissue: A retrospective cohort study. Wound Repair Regen. 2015;23:772-7.

Koivukangas V, Annala AP, Salmela PI, Oikarinen A. Delayed restoration of epidermal barrier function after suction blister injury in patients with diabetes mellitus. Diabet Med. 1999;16:563-7.

Kosiak M. Etiology of decubitus ulcers. Arch Phys Med Rehabil. 1961;42:19-29.

Kramer JD, Kearney M. Patient, wound, and treatment characteristics associated with healing in pressure ulcers. Adv Skin Wound Care. 2000;13:17-24.

Kreger ST, Voytik-Harbin SL. Hyaluronan concentration within a 3D collagen matrix modulates matrix viscoelasticity, but not fibroblast response. Matrix Biol. 2009;28:336-46.

Krouskop TA, Reddy NP, Spencer WA, Secor JW. Mechanisms of decubitus ulcer formation—an hypothesis. Med Hypotheses. 1978;4:37-9.

Krouskop TA. A synthesis of the factors that contribute to pressure sore formation. Med Hypotheses. 1983;11:255-67.

Leist M, Gantner F, Bohlinger I, Germann PG, Tiegs G, Wendel A. Murine hepatocyte apoptosis induced in vitro and in vivo by TNF-alpha requires transcriptional arrest. J Immunol. 1994;153:1778-88.

Lewis R, Whiting P, ter Riet G, O'Meara S, Glanville J. A rapid and systematic review of the clinical effectiveness and cost-effectiveness of debriding agents in treating surgical wounds healing by secondary intention. Health Technol Assess. 2001;5:1-131.

Li W, Li Y, Guan S, Fan J, Cheng CF, Bright AM, Chinn C, Chen M, Woodley DT. Extracellular heat shock protein-90alpha: linking hypoxia to skin cell motility and wound healing. EMBO J. 2007;26:1221-33.

Liao DF, Jin ZG, Baas AS, Daum G, Gygi SP, Aebersold R, Berk BC. Purification and identification of secreted oxidative stress-induced factors from vascular smooth muscle cells. J Biol Chem. 2000;275:189-96.

Majed BH, Khalil RA. Molecular mechanisms regulating the vascular prostacyclin pathways and their adaptation during pregnancy and in the newborn. Pharmacol Rev. 2012;64:540-82.

Maroski J, Vorderwülbecke BJ, Fiedorowicz K, Da Silva-Azevedo L, Siegel G, Marki A, Pries AR, Zakrzewicz A. Shear stress increases endothelial hyaluronan synthase 2 and hyaluronan synthesis especially in regard to an atheroprotective flow profile. Exp Physiol. 2011;96:977-86.

Mascarenhas MM, Day RM, Ochoa CD, Choi WI, Yu L, Ouyang B, Garg HG, Hales CA, Quinn DA. Low molecular weight hyaluronan from stretched lung enhances interleukin-8 expression. Am J Respir Cell Mol Biol. 2004;30:51-60.

Matsui Y, Furue M, Sanada H, Tachibana T, Nakayama T, Sugama J, Furuta K, Tachi M, Tokunaga K, Miyachi Y. Development of the DESIGN-R with an observational study: an absolute evaluation tool for monitoring pressure ulcer wound healing. Wound Repair Regen 2011;19:309-15.

McClintock DS, Santore MT, Lee VY, Brunelle J, Budinger GR, Zong WX, Thompson CB, Hay N, Chandel NS. Bcl-2 family members and functional electron transport chain regulate oxygen deprivation-induced cell death. Mol Cell Biol. 2002;22:94-104.

McGinnis E, Greenwood DC, Nelson EA, Nixon J. A prospective cohort study of prognostic factors for the healing of heel pressure ulcers. Age Ageing. 2014;43:267-71.

McInnes E, Dumville JC, Jammali-Blasi A, Bell-Syer SE. Support surfaces for treating pressure ulcers. Cochrane Database Syst Rev. 2011;7:CD009490.

Miller M. Wound care. The role of debridement in wound healing. Community Nurs 1996;2:52, 54-5.

Minematsu T, Nakagami G, Yamamoto Y, Kanazawa T, Huang L, Koyanagi H, Sasaki S, Uchida G, Fujita H, Haga N, Yoshimura K, Nagase T, Sanada H. Wound blotting: a convenient biochemical assessment tool for protein components in exudate of chronic wounds. Wound Repair Regen. 2013;21:329-34

Mitsuhashi M, Yamaguchi M, Kojima T, Nakajima R, Kasai K. Effects of HSP70 on the compression force-induced TNF-α and RANKL expression in human periodontal ligament cells. Inflamm Res. 2011;60:187-94.

Moore ZE, Cowman S, Conroy RM. A randomised controlled clinical trial of repositioning, using the 30° tilt, for the prevention of pressure ulcers. J Clin Nurs. 2011;20:2633-44.

Moore ZE, Cowman S. Repositioning for treating pressure ulcers. Cochrane Database Syst Rev. 2012;9:CD006898.

Moseley R, Stewart JE, Stephens P, Waddington RJ, Thomas DW. Extracellular matrix metabolites as potential biomarkers of disease activity in wound fluid: lessons learned from other inflammatory diseases? Br J Dermatol. 2004;150:401-13.

Nakagami G, Sanada H, Iizaka S, Kadono T, Higashino T, Koyanagi H, Haga N. Predicting delayed pressure ulcer healing using thermography: a prospective cohort study. J Wound Care. 2010;19:465-6, 468, 470.

Nakagami G, Sanada H, Sugama J, Morohoshi T, Ikeda T, Ohta Y. Detection of Pseudomonas aeruginosa quorum sensing signals in an infected ischemic wound: an experimental study in rats. Wound Repair Regen. 2008;16:30-6.

Nakamura K, Tanaka T, Takeo K. Characterization of protein binding to a nitrocellulose membrane. SEIBUTSU BUTSURI KAGAKU. 1989;33:293-303.

Narumiya S, Sugimoto Y, Ushikubi F. Prostanoid receptors: structures, properties, and functions. Physiol Rev. 1999;79:1193-226.

National Pressure Ulcer Advisory Panel, European Pressure Ulcer Advisory Panel and Pan Pacific Pressure Injury Alliance. Prevention and Treatment of Pressure Ulcers: Quick Reference Guide. Haesler, E. (ed). Cambridge Media, 2014.

O'Loughlin A, Kulkarni M, Creane M, Vaughan EE, Mooney E, Shaw G, Murphy M, Dockery P, Pandit A, O'Brien T. Topical administration of allogeneic mesenchymal stromal cells seeded in a collagen scaffold augments wound healing and increases angiogenesis in the diabetic rabbit ulcer. Diabetes. 2013;62:2588-94.

Okuwa M, Sugama J, Sanada H, Konya C, Kitagawa A. Measuring the pressure applied to the skin surrounding pressure ulcers while patients are nursed in the 30 degree position. J Tissue Viability. 2005;15:3-8.

Parish LC, Lowthian P, Witkowski JA. The decubitus ulcer: many questions but few definitive answers. Clin Dermatol. 2007;25:101-8.

Park JY, Pillinger MH, Abramson SB. Prostaglandin E2 synthesis and secretion: the role of PGE2 synthases. Clin Immunol. 2006;119:229-40.

Pearl LH, Prodromou C. Structure and in vivo function of Hsp90. Curr Opin Struct Biol. 2000;10:46-51.

Pratt WB, Toft DO. Regulation of signaling protein function and trafficking by the hsp90/hsp70-based chaperone machinery. Exp Biol Med. 2003;228:111-33.

Renò F, Sabbatini M, Lombardi F, Stella M, Pezzuto C, Magliacani G, Cannas M. In vitro mechanical compression induces apoptosis and regulates cytokines release in hypertrophic scars. Wound Repair Regen. 2003;11:331-6.

Sae-Sia W, Wipke-Tevis DD, Williams DA. The effect of clinically relevant pressure duration on sacral skin blood flow and temperature in patients after acute spinal cord injury. Arch Phys Med Rehabil. 2007;88:1673-80.

Saikumar P, Dong Z, Patel Y, Hall K, Hopfer U, Weinberg JM, Venkatachalam MA. Role of hypoxia-induced Bax translocation and cytochrome c release in reoxygenation injury. Oncogene. 1998;17:3401-15.

Salcido R, Donofrio JC, Fisher SB, LeGrand EK, Dickey K, Carney JM, Schosser R, Liang R. Histopathology of pressure ulcers as a result of sequential computer-controlled pressure sessions in a fuzzy rat model. Adv Wound Care. 1994;7:23-4, 26, 28 passim.

Salcido R, Popescu A, Ahn C. Animal models in pressure ulcer research. J Spinal Cord Med. 2007;30:107-16.

Sanada H, Iizaka S, Matsui Y, Furue M, Tachibana T, Nakayama T, Sugama J, Furuta K, Tachi M, Tokunaga K, Miyachi Y; Scientific Education Committee of the Japanese Society of Pressure Ulcers. Clinical wound assessment using DESIGN-R total score can predict pressure ulcer healing: pooled analysis from two multicenter cohort studies. Wound Repair Regen 2011;19:559-67.

Sanada H, Miyachi Y, Ohura T, Moriguchi T, Tokunaga K, Shido K, Nakagami G. The Japanese pressure ulcer surveillance study: a retrospective cohort study to determine prevalence of pressure ulcers in Japanese hospitals. Wounds. 2008;20:176-82.

Sandulache VC, Parekh A, Li-Korotky H, Dohar JE, Hebda PA. Prostaglandin E2 inhibition of keloid fibroblast migration, contraction, and transforming growth factor (TGF)-beta1-induced collagen synthesis. Wound Repair Regen. 2007;15:122-33.

Sari Y, Nagase T, Minematsu T, Akase T, Nakagami G, Sanada H, Sugama J. Hypoxia is involved in deep tissue injury formation in a rat model. Wounds. 2010;22:45-51.

Sari Y, Minematsu T, Huang L, Noguchi H, Mori T, Nakagami G, Nagase T, Oe M, Sugama J, Yoshimura K, Sanada H. Establishment of a novel rat model for deep tissue injury deterioration. Int Wound J. 2015a;12:202-9.

Sari Y, Sanada H, Minematsu T, Nakagami G, Nagase T, Huang L, Noguchi H, Mori T, Yoshimura K, Sugama J. Vibration inhibits deterioration in rat deep-tissue injury through HIF1-MMP axis. Wound Repair Regen. 2015b;23:386-93.

Schmitt E, Gehrmann M, Brunet M, Multhoff G, Garrido C. Intracellular and extracellular functions of heat shock proteins: repercussions in cancer therapy. J Leukoc Biol. 2007;81:15-27.

Sehgal R, Kumar VL. Calotropis procera latex-induced inflammatory hyperalgesia--effect of antiinflammatory drugs. Mediators Inflamm. 2005;2005:216-20.

Shimomura K, Kanamoto T, Kita K, Akamine Y, Nakamura N, Mae T, Yoshikawa H, Nakata K. Cyclic compressive loading on 3D tissue of human synovial fibroblasts upregulates prostaglandin E2 via COX-2 production without IL-1β and TNF-α. Bone Joint Res. 2014;3:280-8.

Siu PM, Tam EW, Teng BT, Pei XM, Ng JW, Benzie IF, Mak AF. Muscle apoptosis is induced in pressure-induced deep tissue injury. J Appl Physiol. 2009;107:1266-75.

Spicer AP, Augustine ML, McDonald JA. Molecular cloning and characterization of a putative mouse hyaluronan synthase. J Biol Chem. 1996;271:23400-6.

Spicer AP, Olson JS, McDonald JA. Molecular cloning and characterization of a cDNA encoding the third putative mammalian hyaluronan synthase. J Biol Chem. 1997;272:8957-61.

Sreedhar AS, Csermely P. Heat shock proteins in the regulation of apoptosis: new strategies in tumor therapy: a comprehensive review. Pharmacol Ther. 2004;101:227-57.

Steed DL, Attinger C, Colaizzi T, Crossland M, Franz M, Harkless L, Johnson A, Moosa H, Robson M, Serena T, Sheehan P, Veves A, Wiersma-Bryant L. Guidelines for the treatment of diabetic ulcers. Wound Repair Regen. 2006;14:680-92.

Stekelenburg A, Oomens CW, Strijkers GJ, Nicolay K, Bader DL. Compression-induced deep tissue injury examined with magnetic resonance imaging and histology. J Appl Physiol. 2006;100:1946-54.

Su WH, Cheng MH, Lee WL, Tsou TS, Chang WH, Chen CS, Wang PH. Nonsteroidal anti-inflammatory drugs for wounds: pain relief or excessive scar formation? Mediators Inflamm. 2010;2010:413238.

Sugama J, Sanada H, Nakatani T, Nagakawa T, Inagaki M. Pressure-induced ischemic wound healing with bacterial inoculation in the rat. Wounds. 2005;17:157-68.

Sugama J, Sanada H, Takahashi M. Reliability and validity of a multi-pad pressure evaluator for pressure ulcer management. J Tissue Viability. 2002;12:148-53.

Sugiyama Y, Shimada A, Sayo T, Sakai S, Inoue S. Putative hyaluronan synthase mRNA are expressed in mouse skin and TGF-beta upregulates their expression in cultured human skin cells. J Invest Dermatol. 1998;110:116-21.

Sussmann M, Sarbia M, Meyer-Kirchrath J, Nüsing RM, Schrör K, Fischer JW. Induction of hyaluronic acid synthase 2 (HAS2) in human vascular smooth muscle cells by vasodilatory prostaglandins. Circ Res. 2004;94:592-600.

Suzuki J, Ogawa M, Watanabe R, Takayama K, Hirata Y, Nagai R, Isobe M. Roles of prostaglandin E2 in cardiovascular diseases. Int Heart J. 2011;52:266-9.

Taimor G, Lorenz H, Hofstaetter B, Schlüter KD, Piper HM. Induction of necrosis but not apoptosis after anoxia and reoxygenation in isolated adult cardiomyocytes of rat. Cardiovasc Res. 1999;41:147-56.

Tammi R, Pasonen-Seppänen S, Kolehmainen E, Tammi M. Hyaluronan synthase induction and hyaluronan accumulation in mouse epidermis following skin injury. J Invest Dermatol. 2005;124:898-905.

Tariq G, George B, Cruz S, Mosende V. Pressure ulcer prevalence and prevention in Sheikh Khalifa Medical City, Abu Dhabi. Wounds Middle East. 2014;1:1-7

Terasawa K, Minami M, Minami Y. Constantly updated knowledge of Hsp90. J Biochem. 2005;137:443-7.

Thomas DR. Prevention and treatment of pressure ulcers. J Am Med Dir Assoc. 2006;7:46-59.

Toivola DM, Strnad P, Habtezion A, Omary MB. Intermediate filaments take the heat as stress proteins. Trends Cell Biol. 2010;20:79-91.

Tong M, Tuk B, Hekking IM, Pleumeekers MM, Boldewijn MB, Hovius SE, van Neck JW. Heparan sulfate glycosaminoglycan mimetic improves pressure ulcer healing in a rat model of cutaneous ischemia-reperfusion injury. Wound Repair Regen. 2011;19:505-14.

Tsuji S, Ichioka S, Sekiya N, Nakatsuka T. Analysis of ischemia-reperfusion injury in a microcirculatory model of pressure ulcers. Wound Repair Regen. 2005;13:209-15.

Tsumano T, Kawai K, Ishise H, Nishimoto S, Fukuda K, Fujiwara T, Kakibuchi M. A new mouse model of impaired wound healing after irradiation. J Plast Surg Hand Surg. 2013;47:83-8.

van den Boom M, Sarbia M, von Wnuck Lipinski K, Mann P, Meyer-Kirchrath J, Rauch BH, Grabitz K, Levkau B, Schrör K, Fischer JW. Differential regulation of hyaluronic acid synthase isoforms in human saphenous vein smooth muscle cells: possible implications for vein graft stenosis. Circ Res. 2006;98:36-44.

van Rijswijk L, Polansky M. Predictors of time to healing deep pressure ulcers. Ostomy Wound Manage. 1994;40:40-2, 44, 46-8 passim.

Vanden Berghe T, Kalai M, van Loo G, Declercq W, Vandenabeele P. Disruption of HSP90 function reverts tumor necrosis factor-induced necrosis to apoptosis. J Biol Chem. 2003;278:5622-9.

Vanderwee K, Clark M, Dealey C, Gunningberg L, Defloor T. Pressure ulcer prevalence in Europe: a pilot study. J Eval Clin Pract. 2007;13:227-35.

VanGilder C, Amlung S, Harrison P, Meyer S. Results of the 2008-2009 International Pressure Ulcer Prevalence Survey and a 3-year, acute care, unit-specific analysis. Ostomy Wound Manage. 2009;55:39-45.

VanGilder C, MacFarlane GD, Harrison P, Lachenbruch C, Meyer S. The demographics of suspected deep tissue injury in the United States: an analysis of the International Pressure Ulcer Prevalence Survey 2006-2009. Adv Skin Wound Care. 2010 Jun;23:254-61.

Verzijl N, DeGroot J, Thorpe SR, Bank RA, Shaw JN, Lyons TJ, Bijlsma JW, Lafeber FP, Baynes JW, TeKoppele JM. Effect of collagen turnover on the accumulation of advanced glycation end products. J Biol Chem. 2000;275:39027-31.

Victorian Quality Council. VQC State-wide PUPPS 3 Pressure ulcer point prevalence survey. Department of Human Services 2006.

Viecilli RF, Katona TR, Chen J, Hartsfield JK Jr, Roberts WE. Orthodontic mechanotransduction and the role of the P2X7 receptor. Am J Orthod Dentofacial Orthop. 2009;135:e1-16;discussion 694-5.

von Böhl M, Kuijpers-Jagtman AM. Hyalinization during orthodontic tooth movement: a systematic review on tissue reactions. Eur J Orthod. 2009;31:30-6.

Wakasugi M, Ueshima S, Tei M, Tori M, Yoshida K, Tsujimoto M, Akamatsu H. Multiple hepatic sclerosing hemangioma mimicking metastatic liver tumor successfully treated by laparoscopic surgery: Report of a case. Int J Surg Case Rep. 2015;8C:137-40.

Waldenström A, Martinussen HJ, Gerdin B, Hällgren R. Accumulation of hyaluronan and tissue edema in experimental myocardial infarction. J Clin Invest. 1991;88:1622-8.

Wang JH, Thampatty BP. Mechanobiology of adult and stem cells. Int Rev Cell Mol Biol. 2008;271:301-46.

Wild T, Rahbarnia A, Kellner M, Sobotka L, Eberlein T. Basics in nutrition and wound healing. Nutrition. 2010;26:862-6.

Woodley DT, Wysong A, DeClerck B, Chen M, Li W. Keratinocyte Migration and a Hypothetical New Role for Extracellular Heat Shock Protein 90 Alpha in Orchestrating Skin Wound Healing. Adv Wound Care. 2015;4:203-12.

Xin X, Borzacchiello A, Netti PA, Ambrosio L, Nicolais L. Hyaluronic-acid-based semi-interpenetrating materials. J Biomater Sci Polym Ed. 2004;15:1223-36.

Yip CP, Walker D, Fernlund G, Pinder K. Role of dermal fibroblasts in rat skin tissue biomechanics. Biomed Mater Eng. 2007;17:109-17.

Young JC, Moarefi I, Hartl FU. Hsp90: a specialized but essential protein-folding tool. J Cell Biol. 2001;154:267-73.

Zeger SL, Liang KY. Longitudinal data analysis for discrete and continuous outcomes. Biometrics. 1986;42:121-30.

Zhang Y, Bai X, Wang Y, Li N, Li X, Han F, Su L, Hu D. Role for heat shock protein 90α in the proliferation and migration of HaCaT cells and in the deep second-degree burn wound healing in mice. PLoS One. 2014;9:e103723.

Zuehlke AD, Beebe K, Neckers L, Prince T. Regulation and function of the human HSP90AA1 gene. Gene. 2015;570:8-16.

Tables

Table 1-1 Comparison of initial wound area (PWD 0) and just before pressure loading (PWD 7) in 0-, 1-, 5- and 10-kg loading groups (n = 5 each).

Date	0 kg	1 kg	5 kg	10 kg	*p*-value
PWD 0	2.154 ± 0.287	2.050 ± 0.101	2.007 ± 0.073	2.045 ± 0.084	0.595
PWD 7	1.115 ± 0.394	0.996 ± 0.121	1.095 ± 0.128	1.141 ± 0.068	0.709

Mean ± SD (cm^2). Multiple comparison was performed by ANOVA. PWD = post wounding day.

Table 2-1 Demographic characteristics, nutritional status, and underlying disease of participants, and characteristics of pressure ulcers.

Variable	Female	Male	Total
Age, mean ± SD	64.7 ± 6.7	67.6 ± 17.9	66.5 ± 14.5
Sex, n	6	10	16
Height, cm, mean ± SD	158.7 ± 3.2	167.3 ± 5.4	164.8 ± 6.2
Weight, kg, mean ± SD	57.3 ± 19.2	55.4 ± 11.7	55.6 ± 14.3
Body mass index, kg/m^2, mean ± SD	22.5 ± 8.2	19.8 ± 4.1	20.6 ± 5.3
Calorie intake, kcal, mean ± SD	925.0 ± 307.5	989.8 ± 749.1	969.8 ± 631.4
Serum albumin level, g/dL, mean ± SD	2.5 ± 0.5	2.5 ± 0.4	2.5 ± 0.5
Serum total protein level, g/dL, mean ± SD	5.8 ± 1.2	5.6 ± 0.5	5.7 ± 0.8
Serum C-reactive protein level, mg/dL, mean ± SD	5.4 ± 9.2	4.8 ± 4.2	5.0 ± 6.2
Serum creatin kinase level, IU/L, mean ± SD	131.4 ± 206.5	175.5 ± 172.0	158.5 ± 178.8
Serum lactate dehydrogenase level, IU/L, mean ± SD	372.5 ± 162.2	260.4 ± 43.1	308.4 ± 120.1
Hemoglobin level, g/dL, mean ± SD	11.0 ± 1.9	9.6 ± 1.4	10.1 ± 1.7
Whie blood cell level, number/mL, mean ± SD	10.4 ± 3.0	8.1 ± 4.3	9.0 ± 3.9
Underlying disease[a]			3
Malignant neoplasms, digestive organs			2
Diabetes mellitus			2
Malignant neoplasms, lip, oral cavity and pharynx			1
Arthropathies			1
Cerebrovascular diseases			1
Certain disorders involving the immune mechanism			1
Chronic lower respiratory diseases			1
Extrapyramidal and movement disorders			1
Injury, hip and thigh			1
Malignant neoplasms, endocrine glands and related structures			1
Renal tubulo-interstitial diseases			1
Schizophrenia, schizotypal and delusional disorders			1
Location, n			
Sacrum			9
Coccyx			5
Buttocks			1
Greater trochanter			1
Depth, n			
Category II			8
Category III			2
Unstageable			6
Wound variable, mean ± SD			
DESIGN-R® total score (range 0–66)			12.2 ± 5.74
Wound area, cm^2			9.6 ± 12.3

SD = standard deviation.
[a] ICD-10 classfication

Table 2-2 Wound characteristics and nutritional status in repeated examinations.

No.	ID	Time[a]	Age	Sex	Location	HSP90α	Delayed healing[b]	Wound area	Last week area	Size reduction[c]	Height	Weight	Calorie[d]	Alb	TP	CRP	CK	LDH	Hb	WBC	Contamination[e]	DESIGN-R®
1	1	1	66	Male	Sacrum	Positive	Positive	1.945	2.135	0.089	170.0	63.1	1320	1.8	5.4	6.36		372	7.5	15.1	Negative	15
2	1	2				Positive	Positive	1.881	1.945	0.033		−	1890	2.7	5.9	7.86	66	392	9.4	21.6	Negative	15
3	1	3				Negative	Negative	1.579	1.881	0.161		−	2190	2.2	5.7	8.47	37	297	9.5	21.1	Negative	16
4	1	4				Negative	Negative	0.809	1.579	0.488		66.0	2000	1.9	5.3	15.52	19	352	8.8	17.5	Negative	16
5	1	5				Positive	Positive	1.896	0.809	−1.344		−	1960	1.8	5.2	6.98	20	296	8.9	9.6	Negative	16
6	1	6				Negative	Positive	2.156	1.896	−0.137		67.9	980	1.5	5.1	21.53	30	306	8.4	14.4	Negative	16
7	2	1	71	Female	Sacrum	Negative	Negative	0.456	0.556	0.180	−	−	700	2.2	5.3	3.27	24	302	13.6	18.0	Positive	14
8	2	2				Negative	Negative	0.243	0.456	0.467	−	−	420	1.7	4.5	26.61	14	248	13.5	24.4	Positive	10
9	3	1	57	Female	Sacrum	Negative	Negative	0.116	0.757	0.847	156.2	47.2	1000			1.12	41	610	11.3	13.4	Negative	4
10	3	2				Positive	Negative	0.070	0.116	0.397		−	840	2.8	5.9	1.80		420	10.4	8.1	Negative	4
11	4	1	78	Male	Coccyx	Negative	Negative	1.475	6.157	0.760	158.9	48.5	1010	3.2		0.21		294	8.8	6.4	Positive	7
12	4	2				Negative	Negative	0.919	1.475	0.377		−	1261	3.4	5.7	0.23		288	10.1	6.6	Negative	7
13	4	3				Negative	Negative	0.424	0.919	0.539		48.5	1465	3.5	5.9	0.07		194	10.7	7.4	Negative	7
14	4	4				Negative	Negative	0.361	0.424	0.149		−	1485	3.1	5.3	0.52			9.7	8.1	Negative	7
15	4	5				Positive	Positive	0.626	0.361	−0.734		−	1625	3.1	5.3	4.02	24		10.0	13.2	Negative	7
16	5	1	82	Male	Sacrum	Positive	Positive	17.826	17.986	0.009	170.0	80.0	400	2.4	5.4	4.93		461	10.4	8.9	Positive	14
17	5	2				Positive	Positive	19.025	17.826	−0.067		−	1759	2.3	5.6	8.38		381	10.1	15.4	Negative	19
18	5	3				Negative	Negative	13.407	19.025	0.295		−	1759	2.4	5.1	2.19		282	12.3	8.8	Negative	19
19	5	4				Negative	Negative	9.842	13.407	0.266		55.2	1759	3.1	6.7	0.16		203	13.3	10.3	Negative	19
20	5	5				Negative	Positive	10.057	9.842	−0.022		55.0	1880	2.8	5.7	0.97		220	12.6	8.2	Negative	19
21	5	6				Negative	Negative	6.727	8.588	0.217		−	1880							7.6	Negative	17
22	6	1	45	Male	Sacrum	Positive	Positive	17.861	18.588	0.039	178.0	53.6	420	2.7	6.3	0.69			10.2	7.8	Positive	20
23	6	2				Positive	Positive	17.380	17.861	0.027		−	1400	2.7	5.6	1.57	115	138	9.5	4.1	Positive	20
24	7	1	57	Female	Sacrum	Negative	Negative	2.596	3.327	0.220	156.0	30.2	1200	3.0	5.6	0.02	27	383	9.2	10.5	Negative	7
25	7	2				Negative	Negative	1.642	2.596	0.367		29.6	1000	3.1	5.5	0.02	22	344	9.0	9.1	Negative	4
26	7	3				Negative	Negative	1.320	1.642	0.196		28.8	1100	3.0	5.3	1.37	14	246	10.3	9.7	Negative	4
27	7	4				Positive	Negative	1.107	1.320	0.161		30.7	1100	3.5	5.7	0.04	15	241	10.3	6.5	Negative	4
28	8	1	60	Male	Sacrum	Negative	Negative	1.148	2.043	0.438	166.5	37.7	820	2.2	4.3	0.10	40	265	7.9	8.0	Negative	9
29	8	2				Positive	Positive	1.429	1.148	−0.245		38.9	1200	2.1	3.9	0.54	39	255	7.4	4.8	Negative	7
30	8	3				Positive	Positive	1.425	1.429	0.003		39.0	800	2.2	4.4	0.46	26	364	7.3	5.2	Negative	7
31	8	4				Negative	Negative	0.986	1.318	0.252		36.8	1200	2.1		1.54	15	241	9.2	4.3	Positive	9
32	8	5				Positive	Positive	0.936	0.986	0.051		37.1	1640	2.0		0.04	12	227	8.7	4.6	Negative	9
33	8	6				Negative	Negative	0.298	0.936	0.682		37.3	1160	2.3		0.03	12	221	8.9	7.1	Negative	7
34	8	7				Negative	Negative	0.230	0.298	0.228		38.8	1400	2.3		0.21	11	252	8.1	3.7	Negative	7
35	9	1	78	Male	Sacrum	Negative	Negative	32.800	41.900	0.217	169.0	54.1	210	2.6	5.5	2.54	35	173	12.5	10.0	Negative	11
36	10	1	73	Female	Coccyx	Positive	Positive	9.211	9.328	0.013	−	−	1134	2.7	7.2	2.87	42	206	11.8	6.7	Negative	20
37	10	2				Positive	Negative	5.370	9.211	0.417	−	58.4	1125	2.1		4.50			10.1		Negative	10
38	11	1	65	Female	Coccyx	Positive	Positive	8.004	6.239	−0.283	162.6	66.2	1000	1.4	4.2	0.91		567	7.9	5.1	Negative	11
39	12	1	78	Male	Coccyx	Positive	Negative	2.770	3.490	0.206	167.0	43.7	1500	2.0	5.5	2.12	53	241	8.2	4.4	Negative	12
40	13	1	86	Male	Buttocks	Positive	Positive	3.891	3.979	0.022	163.0	48.3	540	2.2		2.91		170	8.7	7.7	Negative	15
41	13	2				Negative	Negative	3.415	3.891	0.122		−	1120	2.2		1.94		155	11.3	4.2	Negative	14
42	13	3				Positive	Positive	3.344	3.415	0.021		−	1600	2.5		3.98		178	8.8	5.3	Negative	14
43	13	4				Positive	Negative	2.661	3.344	0.204		−	1300	2.6		0.66		174	8.3	5.1	Negative	7
44	14	1	65	Female	GT	Negative	Negative	23.714	32.981	0.281	160.0	82.7	1292	2.5		4.24		319	11.6	7.6	Positive	28
45	15	1	73	Male	Sacrum	Positive	Positive	2.620	1.250	−1.096	161.1	62.9	600	3.4	7.3	0.48	57	361	10.6	7.4	Negative	7
46	15	2				Positive	Negative	1.900	2.620	0.275		−	1430	2.5	6.8	5.82	40	209	11.7	9.9	Negative	7
47	16	1	30	Male	Coccyx	Negative	Negative	2.396	2.840	0.156	169.0	61.0	1800	2.5	6.6	9.63			10.6	10.8	Negative	9

[a] Time = the number of observations in the same patient (ID).

[b] Delayed healing = the wound area reduction less than 10% compared with that of last week.

[c] Size reduction = 1−(Wound area)/(Lastweek area).

[d] Calorie = calorie intake.

[e] Contamination = fecal or urine contamination to the wound region.

GT = Greater trochanter, Alb = Albumin, TP = Total protein, Hb = Hemoglobin, CRP = C-reactive protein

All of the units are the same in Table 2-1

Table 2-3 Cross tabulation of the examinations in HSP90α positive or negative and delayed healing positive or negative groups.

	Delayed healing		
HSP90α	Positive No. (%)	Negative No. (%)	Total (%)
Positive	16(30.04)	6 (12.77)	22 (46.81)
Negative	2(4.26)	23 (48.94)	25 (53.19)
Total (%)	18 (38.30)	29(61.70)	47 (100.00)

Table 2-4 Univariate analysis of association to delayed healing of pressure ulcers.

Variables	Unadjusted		
	n	OR (95% CI)	*p*-value
HSP90α positive	*47*	32.32 (8.42-123.99)	< 0.001
Calorie intake	*47*	0.99 (0.99-1.00)	0.844
Albumin level	*45*	0.33 (0.12-0.99)	0.048
Total protein level	*34*	0.85 (0.34-2.11)	0.728
Hemoglobin level	*46*	0.63 (0.40-1.00)	0.051
CRP level	*46*	1.03 (0.93-1.14)	0.54
Creatine kinase level	*26*	1.04 (0.99-1.10)	0.099
LDH level	*41*	1.00(0.99-1.00)	0.381
WBC level	*46*	0.98 (0.86-1.11)	0.755
Fecal or urine contamination	47	0.95 (0.19-1.18)	0.955

OR = odds ratio, CI = confidence interval, CRP = C-reactive protein,
LDH = lactate dehydrogenase, WBC = white blood cell.
This model accounts for within-patient correlation by generalized estimating equation using an exchangeable structure for the working correlation matrix.

Table 2-5 Multivariable analysis of association to delayed healing of pressure ulcers.

Variables	Adjusted		
	n	OR (95% CI)	*p*-value
HSP90α positive	*45*	200.58 (11.71-3433.19)	< 0.001
Albumin level	*45*	0.97 (0.05-17.26)	0.986
Hemoglobin level	*45*	0.81 (0.36-1.81)	0.621

OR = odds ratio, CI = confidence

This model accounts for within-patient correlation by generalized estimating equation using an exchangeable structure for the working correlation matrix.

Adjusted odds ratios for HSP90α, albumin level, hemoglobin level age, sex, DESIGN-R® total score as covariates.

Figures

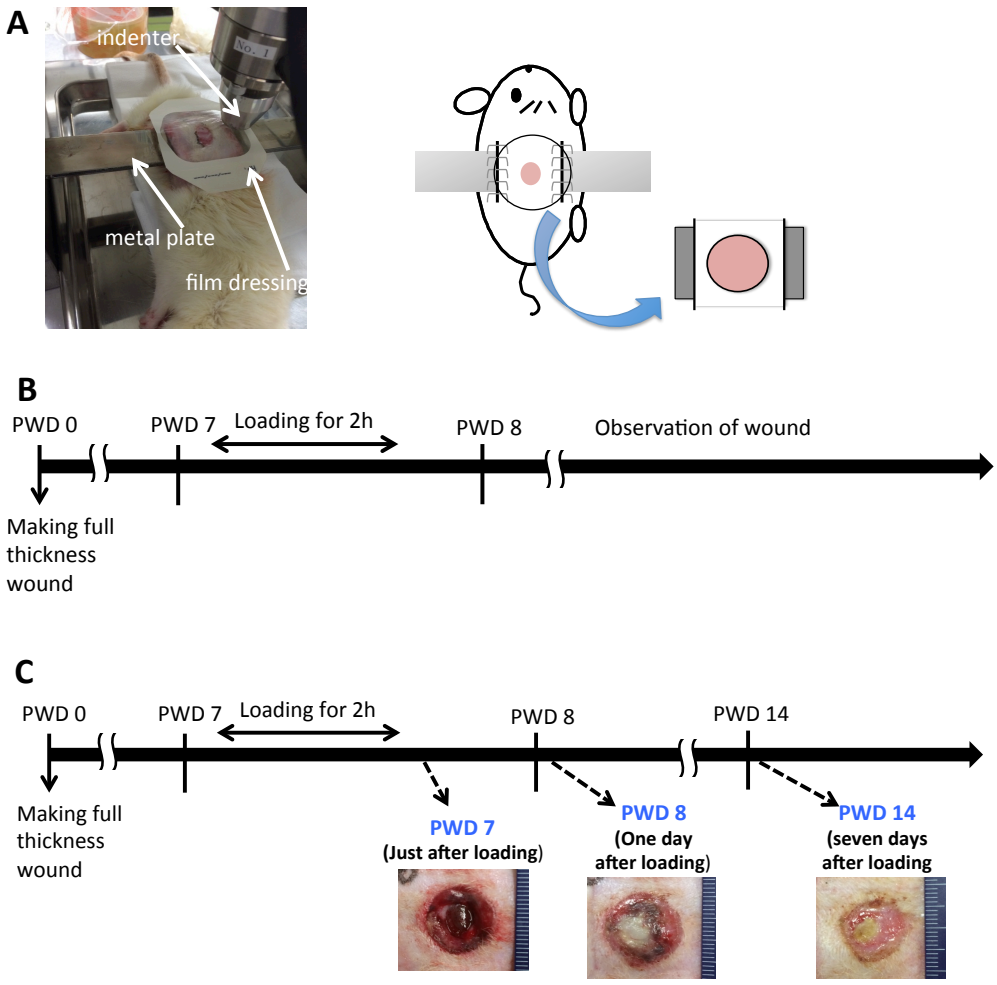

Figure 1-1 Pressure loading procedure and Experimental schedule. A: Pressure loading device. On PWD 7, pressure loading were applied to each wound using pressure loading device for PU model developed by Sugama et al., 2005. Skin incisions were created in lateroabdominal and dorsal region using sterile scissors then a metal plate was inserted under the wound. In this study, the indenter was modified by attaching rounded prominence to the tip to press the center of the wound. Pressure loadings of 0-, 1-, 5-, and 10-kg/3 cm^2 were applied to the wounds for 2 h. The 0-kg loading group meant the control group, and thus into this group a plate was inserted only without pressure loading. During pressure loading, all wounds were covered with the film dressing. After 2 h loading, the metal plate was removed and skin incisions were sutured. The form dressing was applied to the wound and hydrocolloid dressing to the incision site. B: Experimental schedule. In all wounds of all PWDs, dressings change, wound cleansing with normal saline, wound observation, and photographing with a digital camera were performed everyday. C: Timing of sampling for analyses. On PWD 7 (just after loading), 8, and 14, animals were sacrificed by administering a lethal dose of pentobarbital sodium intraperitoneally, and tissue samples of the wound area were collected. PWD, post-wounding day.

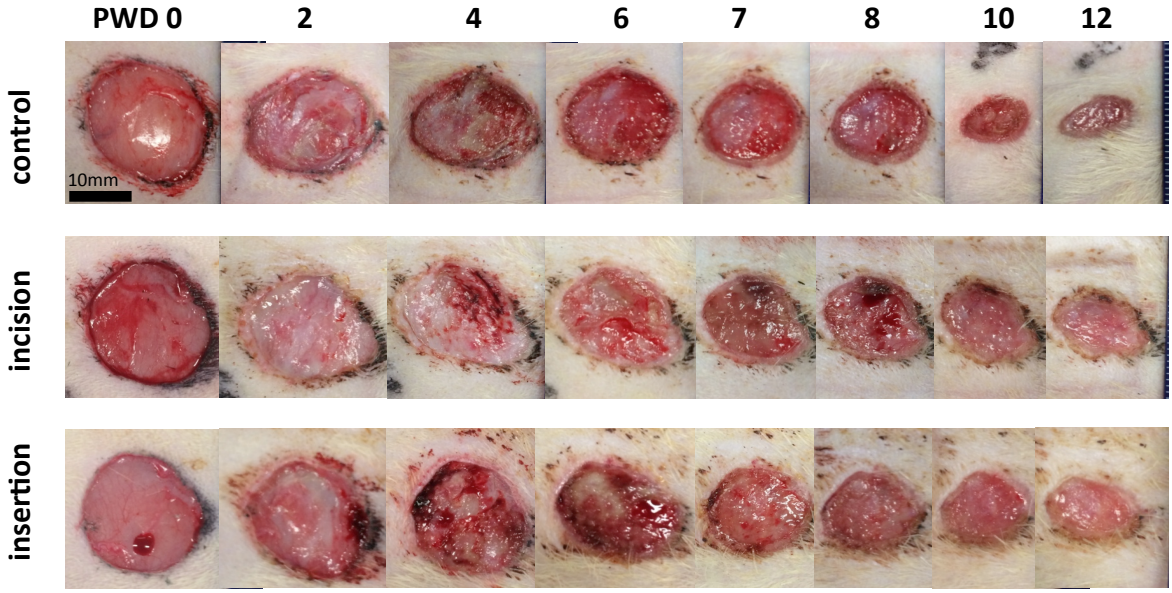

Figure 1-2 Macroscopic findings effected by the skin incision and the plate insertion. Three groups were prepared, which consisted of skin incisions with wound group (the incision group), plate insertion through the incisions with wound group (the insertion group), and only wound group (the control group) to verify delayed healing by these effects. On PWD 7, skin incisions and a metal insertion were performed for 2 h. PWD, post-wounding day-wounding.

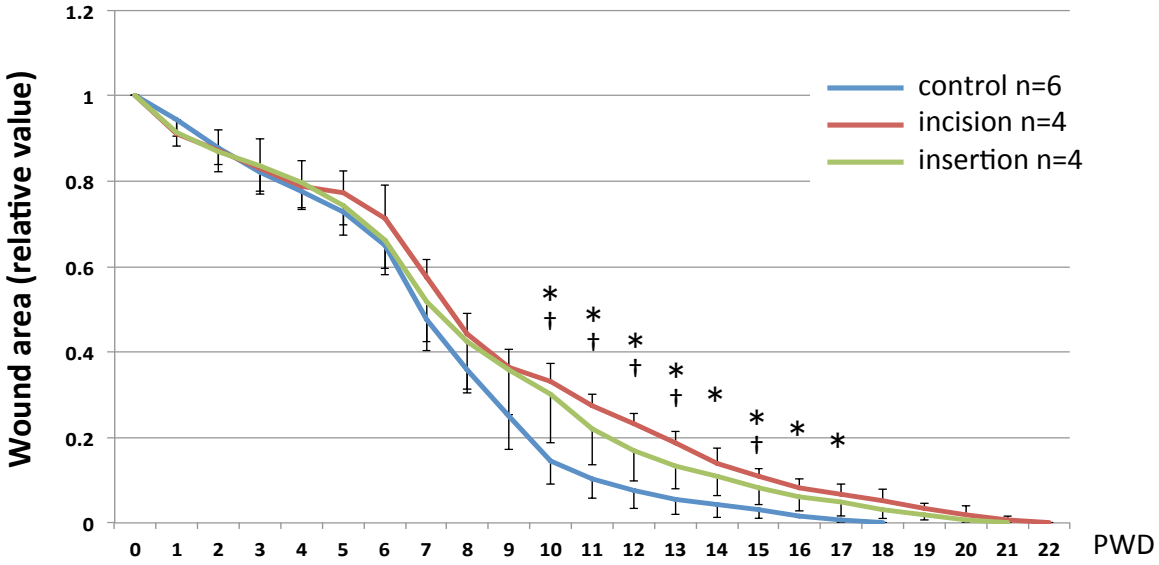

Figure 1-3 Wound area under the influence of the skin incision and plate insertion (mean ± SD). Three gropes were prepared, which consisted of skin incisions with wound group (the incision group), plate insertion through the incisions with wound group (the insertion group), and only wound group (the control group) to verify delayed healing by these effects. On PWD 7, skin incisions and a metal insertion were performed for 2 h. Wound area was measured from photographs of wounds by version 1.42. Multiple comparisons were performed by Tukey's test. *; control vs. incision $p < 0.05$, †; control vs. insertion $p < 0.05$. PWD, post-wounding day.

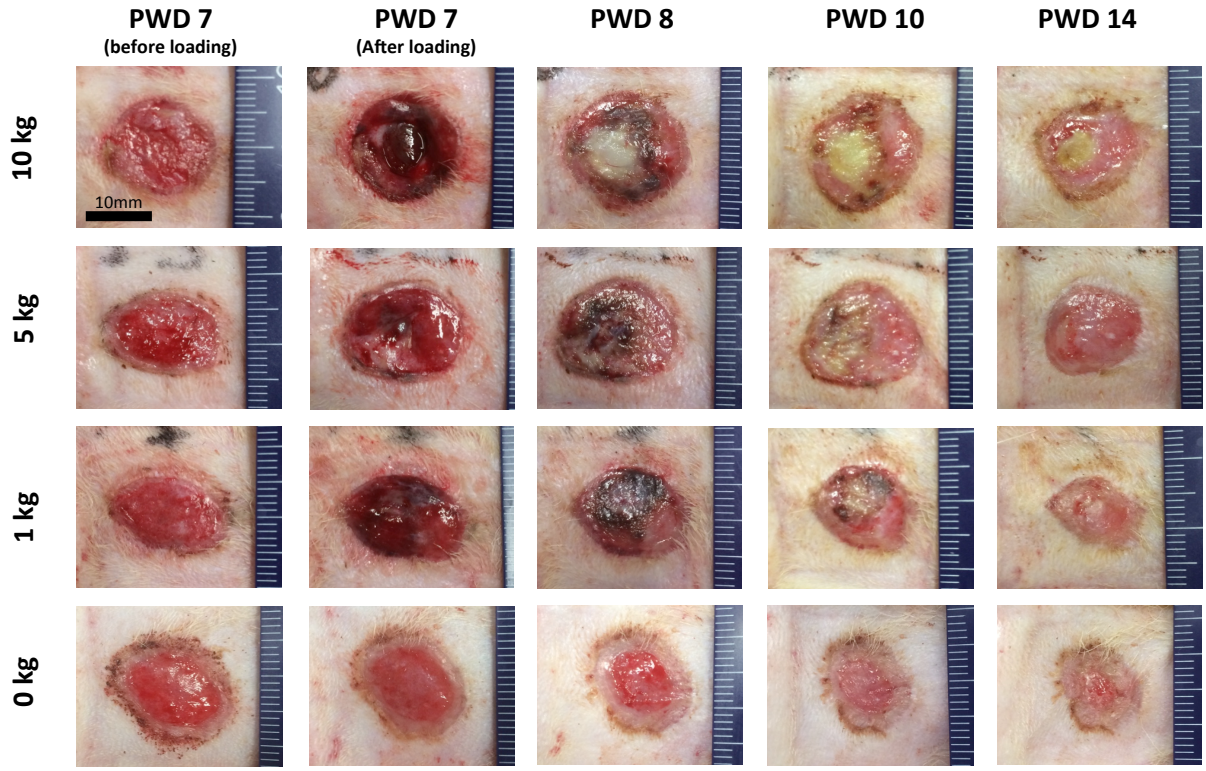

Figure 1-4 Macroscopic findings of wound after loading of 0-, 1-, 5- and 10-kg loading. Animal models that pressure loadings of 0-, 1-, 5-, and 10-kg/3 cm^2 were applied to the wounds for 2 h on PWD 7 were prepared. Each wound was covered with hydrocellular form dressing overlaid with polyurethane film dressing. In the 0-kg, pressure was not applied for wounds after plate insertion as the control. During pressure loading, all wounds were covered with the film dressing. In all wounds of all PWDs, dressings change, wound cleansing with normal saline, wound observation, and photographing with a digital camera were performed everyday. PWD, post-wounding day.

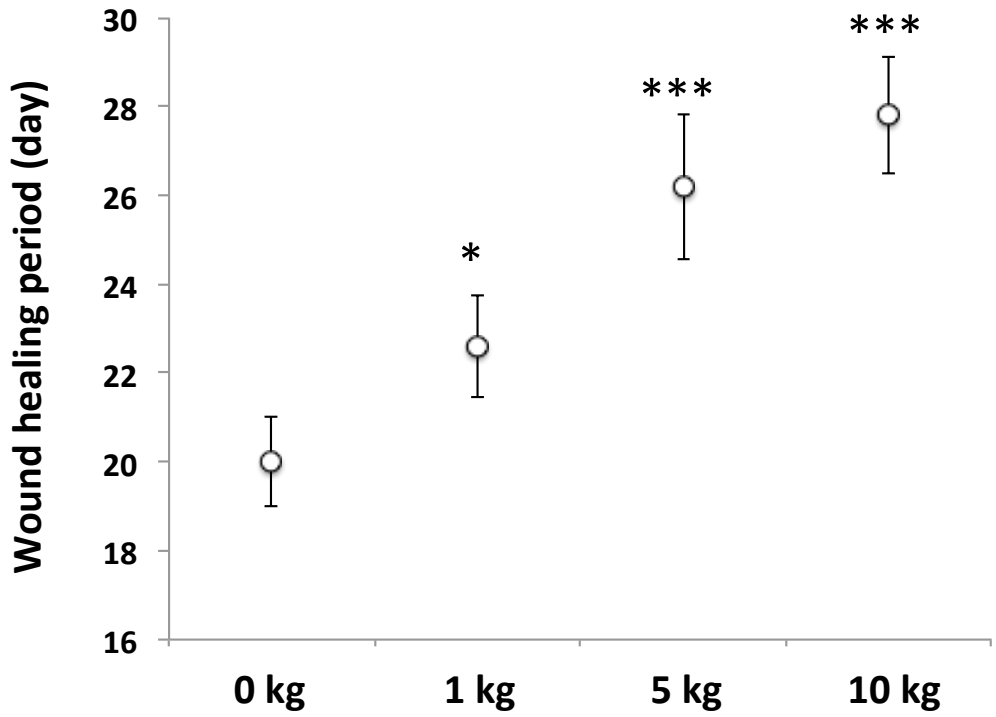

Figure 1-5 Wound healing period in 0-, 1-, 5- and 10-kg groups. Animal models that pressure loadings of 0-, 1-, 5-, and 10-kg/3 cm^2 were applied to the wounds for 2 h on PWD 7 were prepared. Each wound was covered with hydrocellular form dressing with film dressing as a secondary dressing to keep the form dressing attached to the wound. The 0-kg group meant the control group, and thus into this group, a plate was inserted only without pressure loading. During pressure loading, all wounds were covered with the film dressing. In all wounds of all PWDs, dressings change, wound cleansing with normal saline, wound observation, and photographing with a digital camera were performed everyday. Wound healing date means the date of the epithelialization completion. Multiple comparisons were performed by Dunnett's test compared with the control group. n = 5 (mean ± SD). *; < 0.05, **; < 0.01, ***; < 0.001. PWD, post-wounding day.

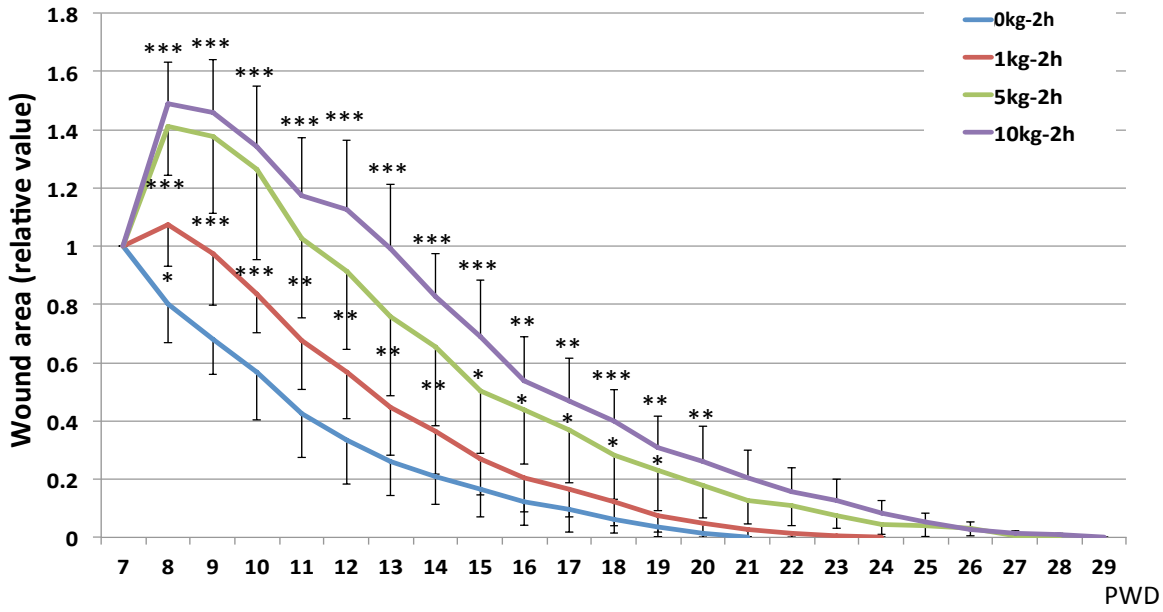

Figure 1-6 Wound area during hearing process in 0-, 1-, 5- and 10-kg loading groups. Animal models that pressure loadings of 0-, 1-, 5-, and 10-kg/3 cm^2 were applied to the wounds for 2 h on PWD 7 were prepared. Each wound was covered with hydrocellular form dressing with film dressing as a secondary dressing to keep the form dressing attached to the wound. The wound area was measured every day after wounding using ImageJ version 1.42. The 0-kg group meant the control group, and thus into this group, a plate was inserted only without pressure loading. During pressure loading, all wounds were covered with the film dressing. In all wounds of all PWDs, dressings change, wound cleansing with normal saline, wound observation, and photographing with a digital camera were performed everyday. Multiple comparisons were performed by Dunnett's test compared with the control group. n = 5 (mean ± SD). *; < 0.05, **; < 0.01, ***; < 0.001. PWD, post-wounding day.

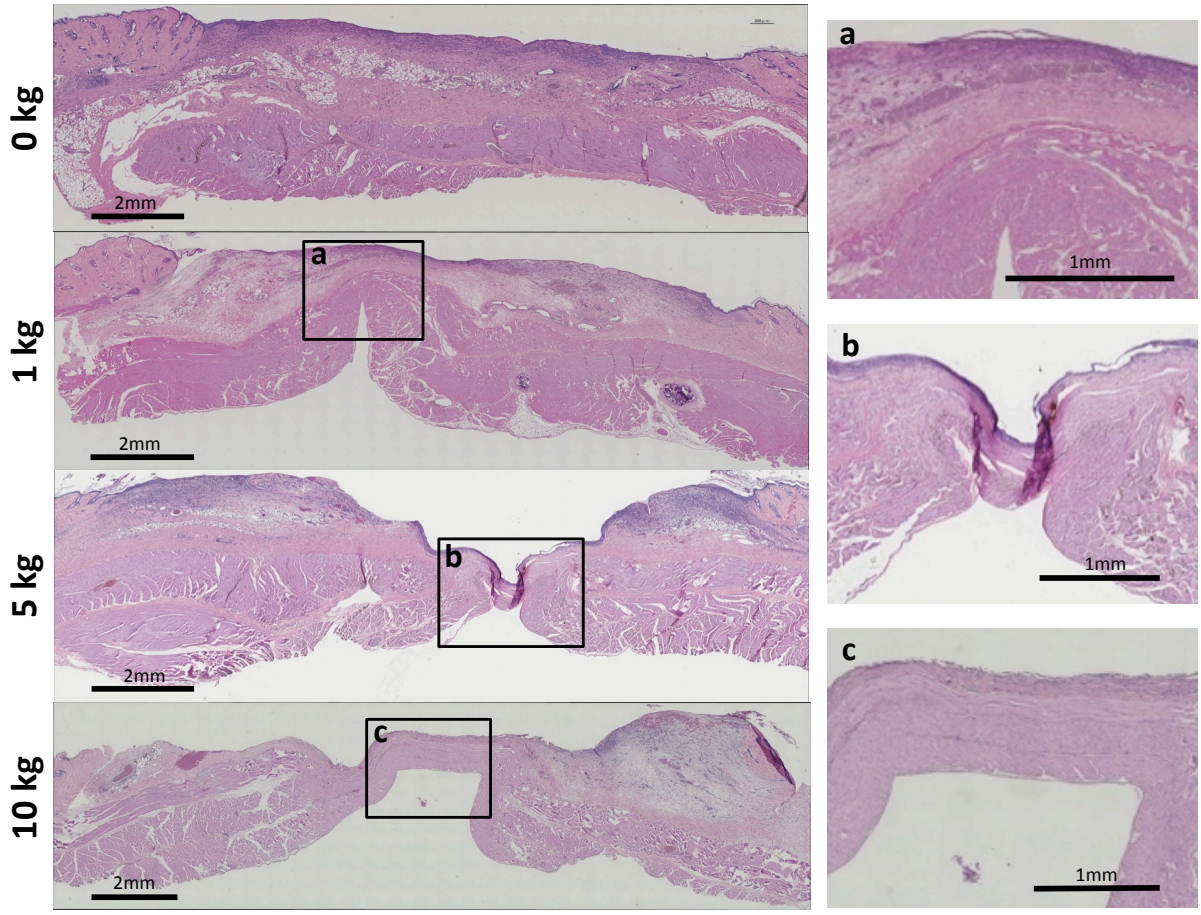

Figure 1-7 Whole section images of full-thickness wounds on PWD 7 (just after loading). The 0-. 1-, 5-, and 10-kg loadings were applied for the center of full-thickness wound created on the flank of rats. Tissue of wound site and surrounding skin was harvested and histologically analyzed just after pressure loading. In the 1-kg loading, the muscle tissue was affected by pressure loading than the granulation tissue. In both the 5- and 10-kg loading, the muscle and granulation tissue, to the same degree, were affected by pressure loading, and the degree of collapse in the 10-kg was larger than the 5-kg. PWD, post-wounding day.

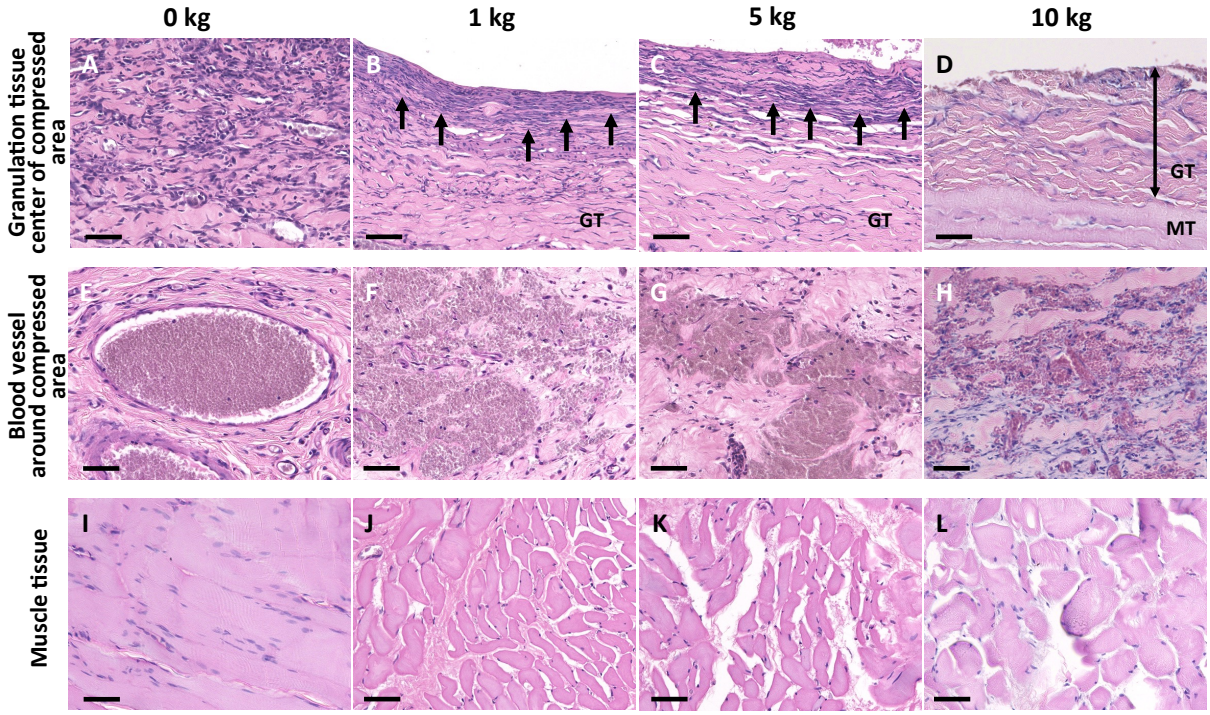

Figure 1-8 Histology of granulation tissue and subcutaneous muscle tissue in magnified images on PWD 7 (just after loading). The 0-. 1-, 5-, and 10-kg loadings were applied for the center of full-thickness wound created on the flank of rats. Tissue of wound site and surrounding skin was harvested and histologically analyzed just after pressure loading. Fibroblasts were dominant cells along with slight inflammatory cells in the granulation tissue of the control tissue (A). On the other hand, in the loading groups applied the 1- and 5-kg compression, the layer of granulation tissue and fibroblasts were pressed and thinner, and granulation tissue of the 10-kg loading was also pressed and thinner, whereas fibroblasts of the 10-kg loading swelled (B–D). Arrows indicates the area of pressed fibroblasts (B and C). Two-headed arrow indicates the layer of granulation tissue. Regarding around the compressed area, bleeding was shown as the leakage of erythrocytes from blood vessels in the loading groups but not in the control group, and slight inflammatory cells were observed in the 1-, 5-, and 10-kg loading. In the muscle tissue, the loading groups showed tissue degeneration compared with the control group (I–L). Scale bar: 50μm. GT, Granulation tissue. MT, Muscle tissue. PWD, post-wounding day.

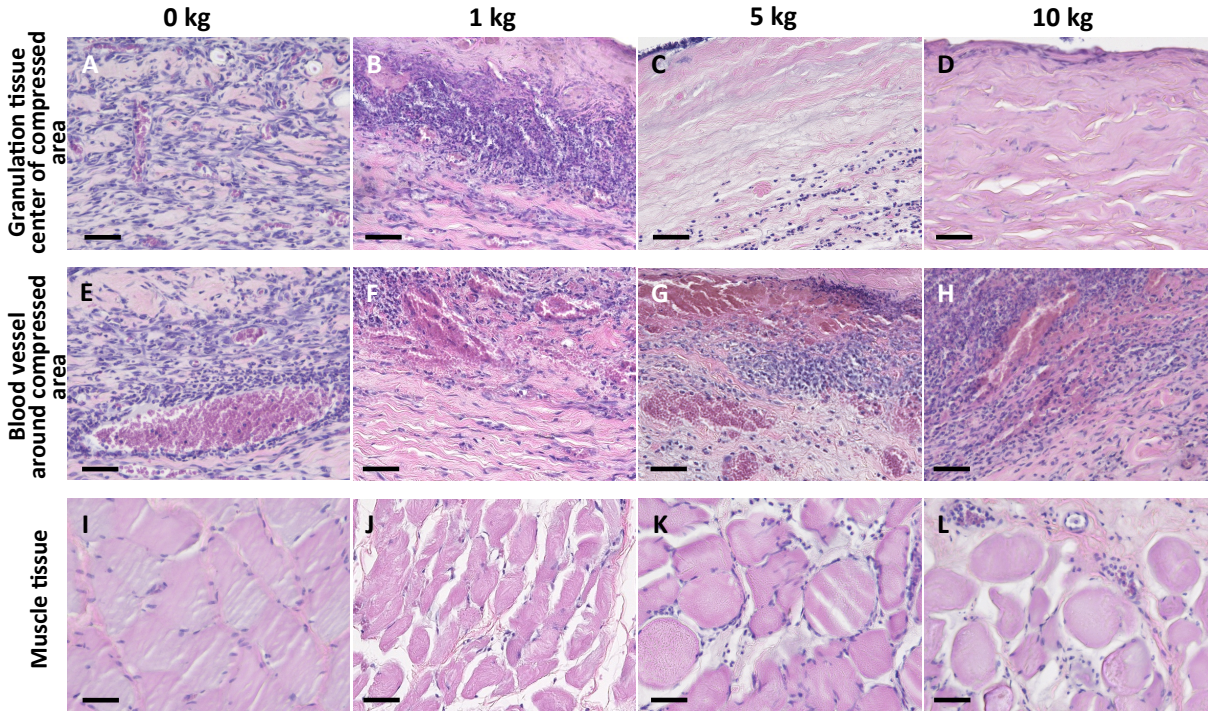

Figure 1-9 Histology of granulation tissue and subcutaneous muscle tissue in magnified images. The 0-. 1-, 5-, and 10-kg loadings were applied for the center of full-thickness wound created on the flank of rats. Tissue of wound site and surrounding skin was harvested and histologically analyzed just after pressure loading. On PWD 8, the granulation tissue of the control contained fibroblast abundantly along with some inflammatory cells, similarly to PWD 7(A). In the 1-kg, extreme aggregation of inflammatory cells was observed (Figure 1-9 B). On the other hand, although inflammatory cells slightly infiltrated the center area of wound bed in the 5-kg, there were little cells in both the 5- and 10-kg (C and D). Regarding blood vessels, bleeding along with leakage of erythrocytes was observed in the loading group as well as PWD 7. In addition, infiltration of inflammatory cells was frequently identified in the area around wound bed (F–H). Infiltration of inflammatory and degradation of muscle tissue were more frequently identified in the 5- and 10-kg than the 1-kg (J–L). Scale bar: 50μm. PWD, post-wounding day.

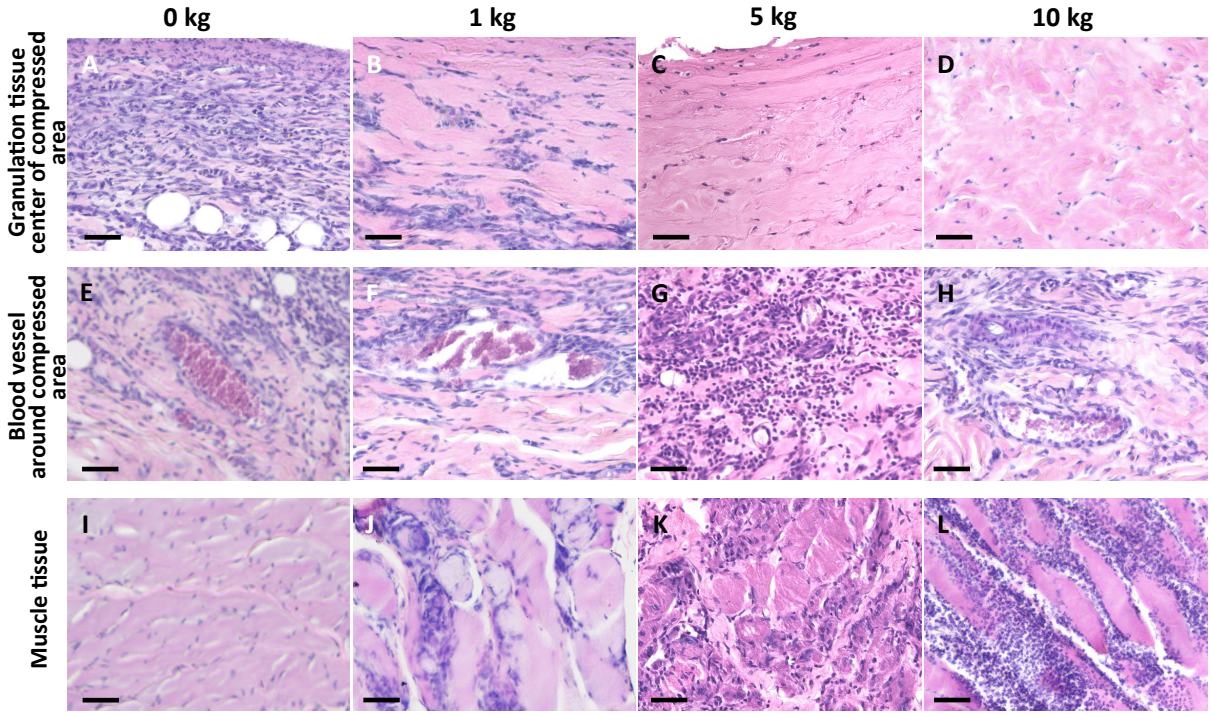

Figure 1-10 Histology of granulation tissue and subcutaneous muscle tissue in magnified images on PWD 14. The 0-. 1-, 5-, and 10-kg loadings were applied for the center of full-thickness wound created on the flank of rats. Tissue of wound site and surrounding skin was harvested and histologically analyzed just after pressure loading. On PWD 14, the granulation tissue of the control contained fibroblast abundantly, similarly to other PWDs (A). Infiltration of fibroblasts was proceeding in the 1-kg but not in the 5- and 10-kg, and hyalinization of collagen fiber was observed in the 5- and 10-kg (B–D). Bleeding was not observed in the loading group as well as the control, and infiltration of inflammatory cells was frequently identified (E–H). Damages of the muscle tissue were progressed in the loading group; infiltration of inflammatory and degradation of tissue were observed in loading dependent manner (J–L). Scale bar: 50μm. PWD, post-wounding day.

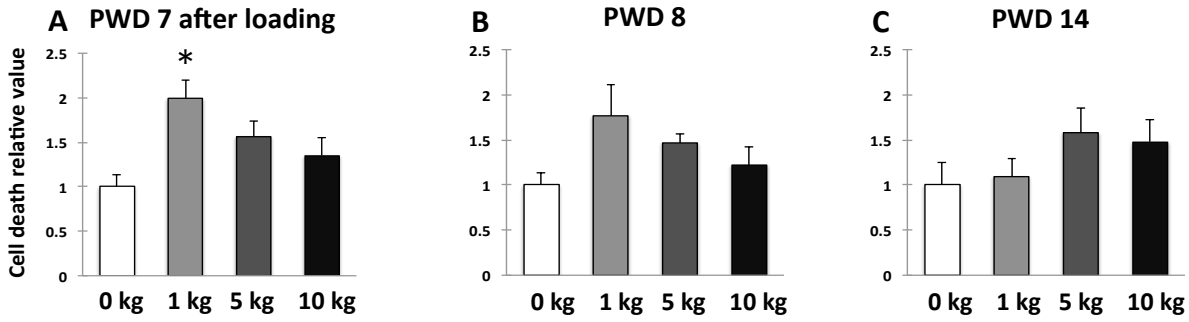

Figure 1-11 Quantification of apoptosis in granulation tissue of each group on PWD 7 (just after loading), 8, and 14. The 0-. 1-, 5-, and 10-kg loadings were applied for the center of full-thickness wound created on the flank of rats. Tissue of wound site was harvested and analyzed on PWD 7 (just after loading), PWD 8, and PWD14.These showed the result of quantification of apoptosis in each group on PWD 7, 8, and 14. On PWD 7 (just after loading), apoptosis level was higher in the 1-kg group only than in the control ($p = 0.022$). On PWD 8 and 14, any significant differences between the loading groups and the control were not found. Multiple comparisons were performed by Dunnett's test compared with the control group. $n = 5$ (mean ± SE). *; < 0.05, **; < 0.01, ***; < 0.001. PWD, post-wounding day.

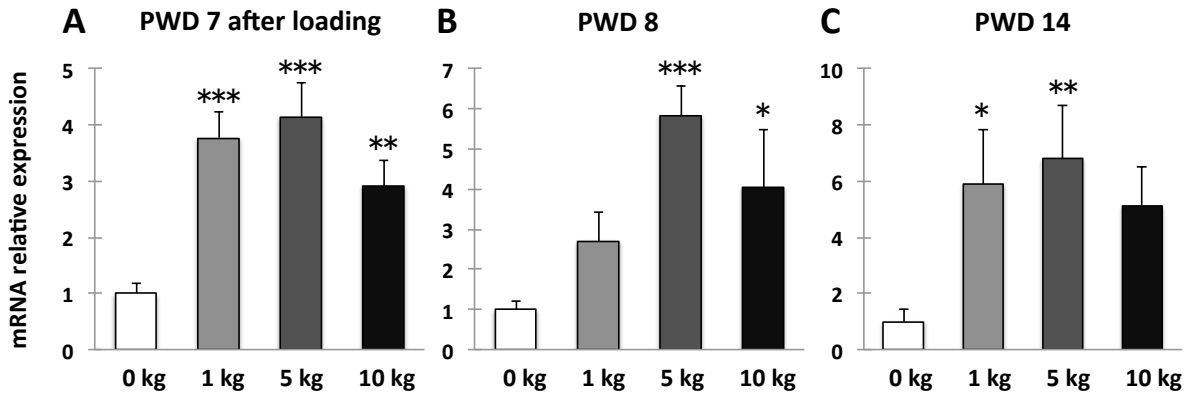

Figure 1-12 *Cox2* mRNA expression in granulation tissue of each loading group on PWD 7 (just after loading), 8, and 14. The 0-. 1-, 5-, and 10-kg loadings were applied for the center of full-thickness wound created on the flank of rats. Tissue of wound site was harvested and analyzed on PWD 7 (just after loading), PWD 8, and PWD14. On PWD 7 (just after loading), the mRNA expression of Cox1 was significantly upregulated in the loading groups than in the control group (the 1-kg; $p < 0.001$, the 5-kg; $p < 0.001$, and the 10-kg; $p = 0.004$) (A). The expression of Cox2 was significantly higher in the 5- and 10-kg groups on PWD 8 and in the 1- and 5-kg groups on PWD 14 than the control groups, respectively (on PWD 8; $p < 0.001$ and $p = 0.019$, respectively: on PWD 14; $p < 0.026$ and $p = 0.008$, respectively) (B and C). Multiple comparisons were performed by Dunnett's test compared with the control group. n = 5 (mean ± SE). *; < 0.05, **; < 0.01, ***; < 0.001. PWD, post-wounding day.

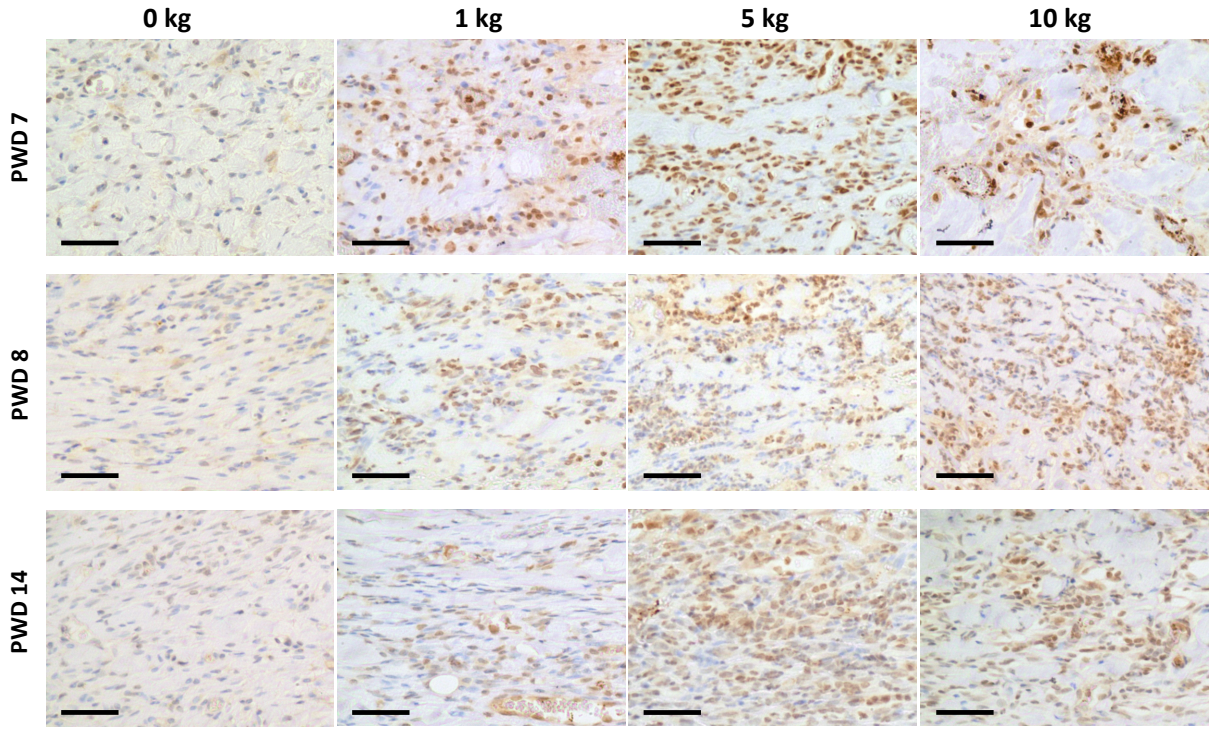

Figure 1-13 Immunohistochemistry for COX2 in granulation tissue of each loading group on PWD 7 (just after loading), 8, and 14. The 0-. 1-, 5-, and 10-kg loadings were applied for the center of full-thickness wound created on the flank of rats. Tissue of wound site was harvested and analyzed on PWD 7 (just after loading), PWD 8, and PWD14. On PWD 7 (just after loading), 8, and 14, all loading groups showed stronger COX2 staining in the granulation tissue compared with the control groups, respectively Scale bar: 50μm. Scale bar: 50μm. PWD, post-wounding day.

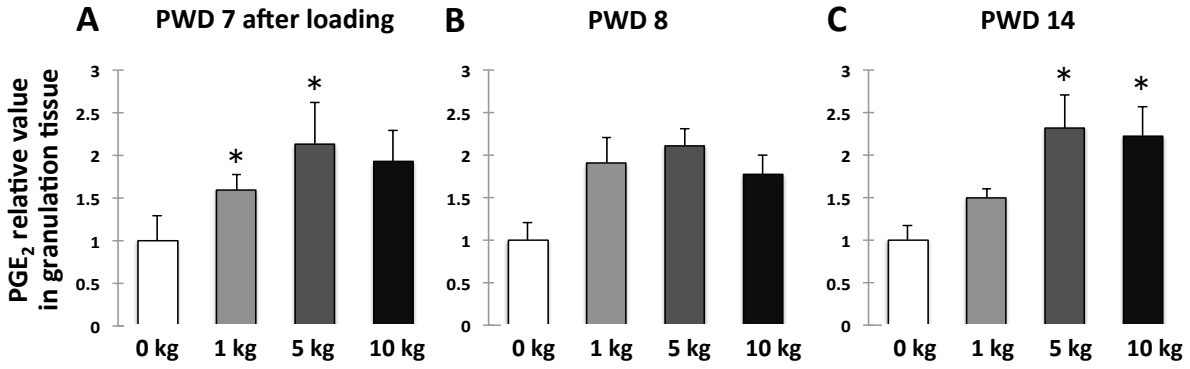

Figure 1-14 Quantification of PGE_2 in granulation tissue of each loading group on PWD 7 (just after loading), 8, and 14. The 0-. 1-, 5-, and 10-kg loadings were applied for the center of full-thickness wound created on the flank of rats. Tissue of wound site was harvested and analyzed on PWD 7 (just after loading), PWD 8, and PWD14. On PWD 7 after lording, the expression of PGE2 was significantly higher in the 1- and 5-kg groups than in the control group ($p = 0.043$, $p = 0.013$, respectively) (A). On PWD 8, any significant differences between the loading groups and the control were not found (B). On PWD 14, the expression of PGE2 was significantly higher in the 5- and 10-kg groups than in the control group ($p = 0.011$, $p = 0.018$, respectively) (C). These results suggested that the PGE2 level and inflammation were increased by pressure loading. Multiple comparisons were performed by Dunnett's test compared with the control group. n = 5 (mean ± SE). *; < 0.05, **; < 0.01, ***; < 0.001. PWD, post-wounding day.

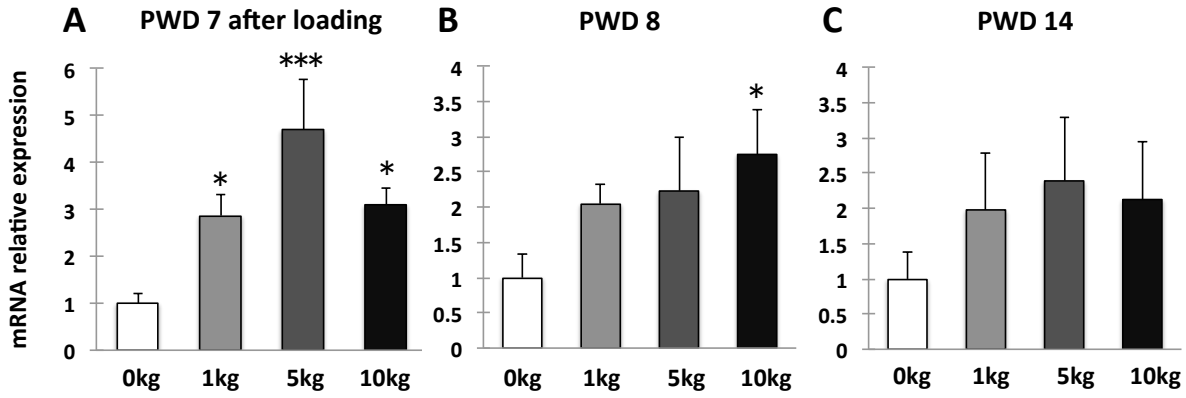

Figure 1-15 *Has1* mRNA expression in granulation tissue of each loading group on PWD 7 (just after loading), 8, and 14. The 0-. 1-, 5-, and 10-kg loadings were applied for the center of full-thickness wound created on the flank of rats. Tissue of wound site was harvested and analyzed on PWD 7 (just after loading), PWD 8, and PWD14. On PWD 7 (just after loading), the mRNA expression of Has1 was significantly upregulated in the loading groups than in the control group (the 1-kg; $p = 0.038$, the 5-kg; $p < 0.001$, and the 10-kg; $p = 0.018$) (A). On PWD 8, the expression of Has1 was higher in the 1-kg group only than in the control ($p = 0.026$) (B). On PWD 14, any significant differences in the expression of Has1 between the loading groups and the control were not found (C). Multiple comparisons were performed by Dunnett's test compared with the control group. $n = 5$ (mean ± SE). *; < 0.05, **; < 0.01, ***; < 0.001. PWD, post-wounding day.

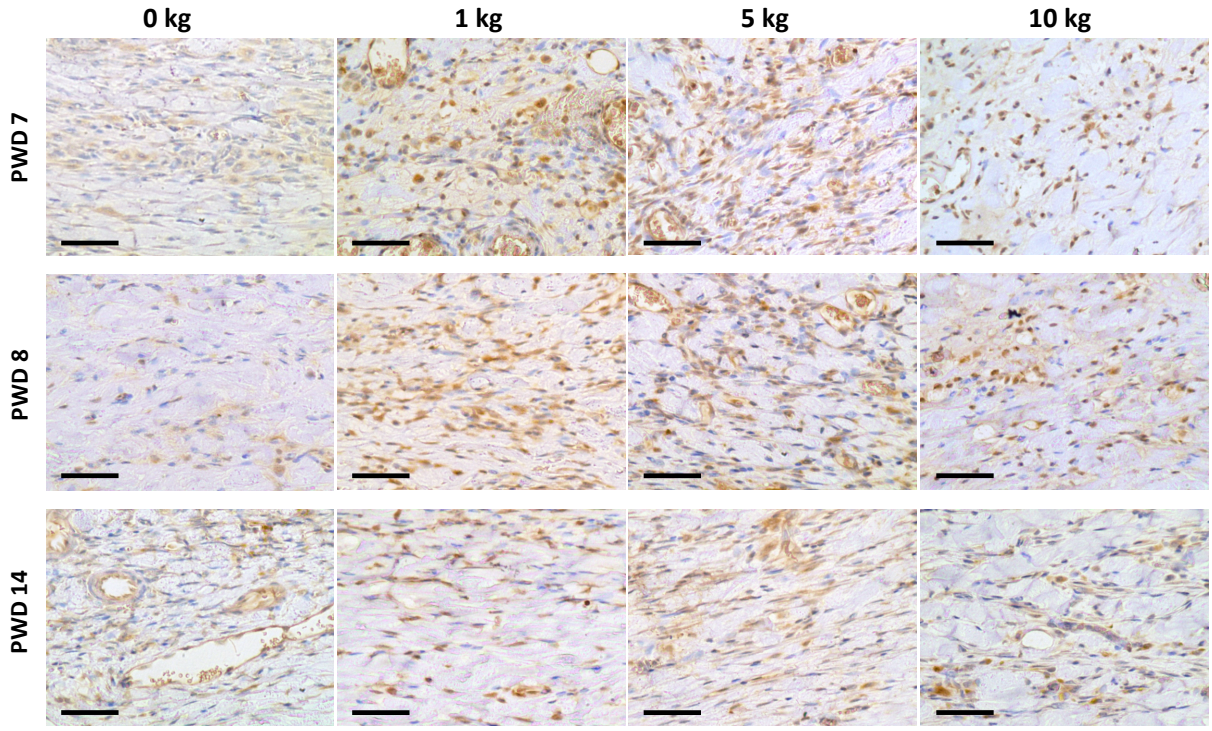

Figure 1-16 Immunohistochemistry for HAS1 in granulation tissue of each loading group on PWD 7 (just after loading), 8, and 14. The 0-. 1-, 5-, and 10-kg loadings were applied for the center of full-thickness wound created on the flank of rats. Tissue of wound site was harvested and analyzed on PWD 7 (just after loading), PWD 8, and PWD14. Notably, the 1- and 5-kg groups on both PWD 7 (just after loading) and 8 showed remarkably stronger HAS1 staining in the granulation tissue compared with the control groups, respectively. Scale bar: 50μm. PWD, post-wounding day.

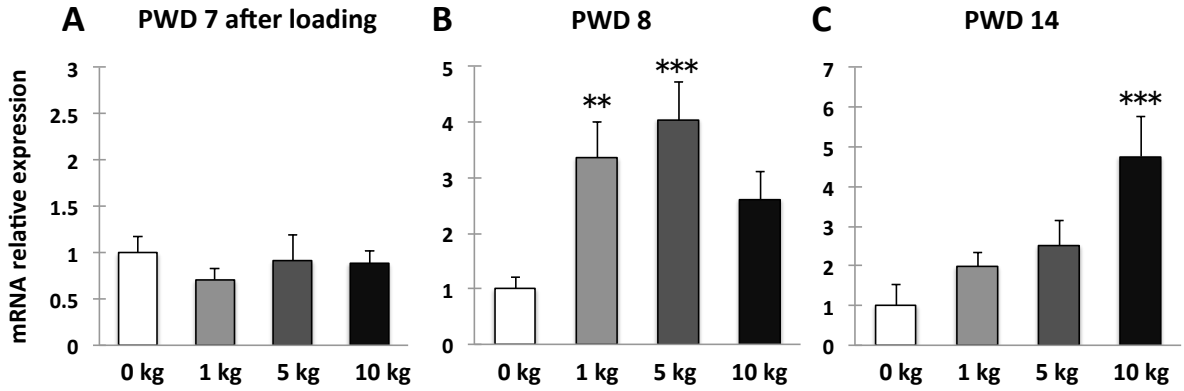

Figure 1-17 *Has2* mRNA expression in granulation tissue of each loading group on PWD 7 (just after loading), 8, and 14. The 0-. 1-, 5-, and 10-kg loadings were applied for the center of full-thickness wound created on the flank of rats. Tissue of wound site was harvested and analyzed on PWD 7 (just after loading), PWD 8, and PWD14. In the mRNA expression of Has2, any significant differences between the loading groups and the control were not found on PWD 7 (just after loading) (A). On the other hand, the expression of Has2 on PWD 8 was significantly upregulated in the 1- and 5-kg groups than in the control group ($p = 0.035$ and $p < 0.001$, respectively) (B). On PWD 14, the expression of Has2 was higher in the 10-kg group only than in the control group ($p < 0.001$) (C). Multiple comparisons were performed by Dunnett's test compared with the control group. n = 5 (mean ± SE). *; < 0.05, **; < 0.01, ***; < 0.001. PWD, post-wounding day.

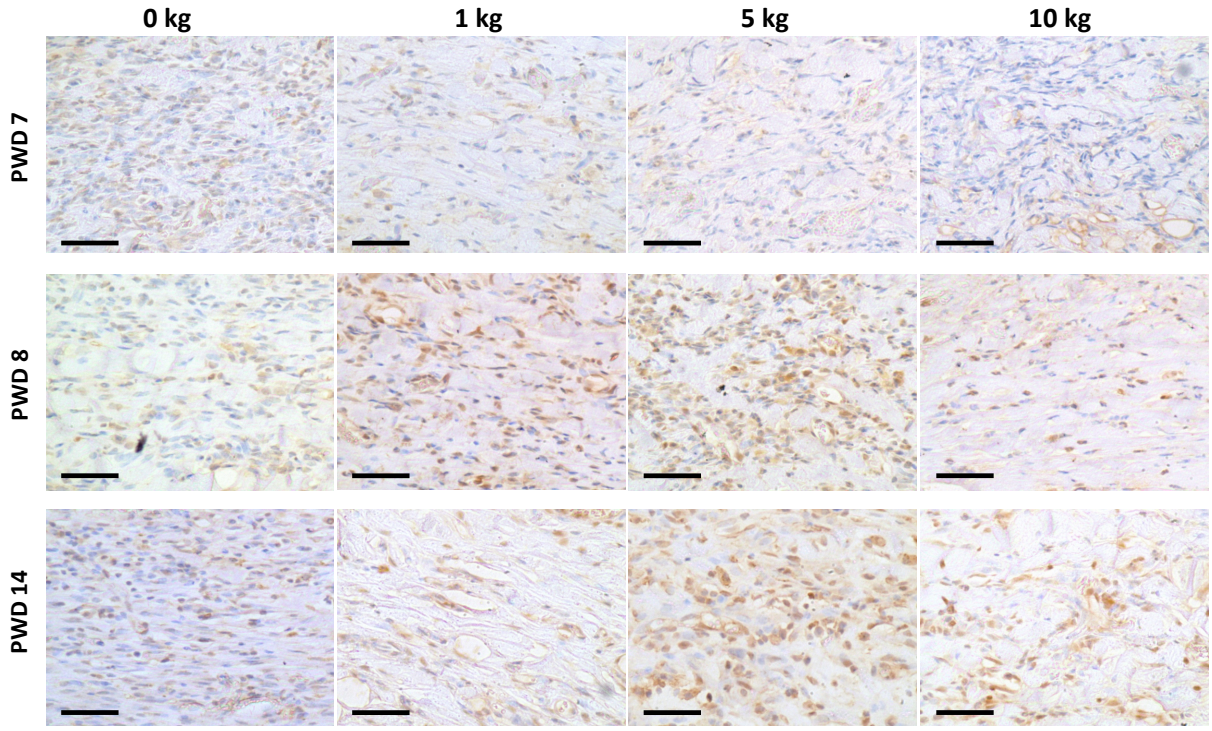

Figure 1-18 Immunohistochemistry for HAS2 in granulation tissue of each loading group on PWD 7 (just after loading), 8, and 14. The 0-. 1-, 5-, and 10-kg loadings were applied for the center of full-thickness wound created on the flank of rats. Tissue of wound site was harvested and analyzed on PWD 7 (just after loading), PWD 8, and PWD14. The 1- and 5-kg groups on both PWD 8 and the 5- and 10-kg groups on PWD 14 showed relatively stronger HAS2 staining in the granulation tissue compared with the control groups, respectively. Scale bar: 50μm. PWD, post-wounding day.

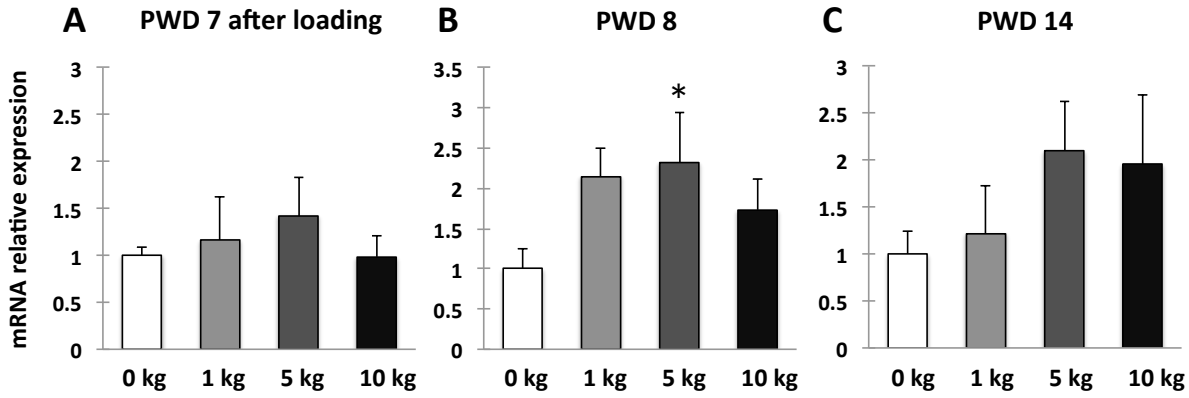

Figure 1-19 *Cd44* mRNA expression in granulation tissue of each loading group on PWD 7 (just after loading), 8, and 14. The 0-. 1-, 5-, and 10-kg loadings were applied for the center of full-thickness wound created on the flank of rats. Tissue of wound site was harvested and analyzed on PWD 7 (just after loading), PWD 8, and PWD14. The expression of Cd44 on PWD 8 was higher in the 5-kg group only than in the control group ($p = 0.033$), and any significant differences between the loading groups and the control were not found on PWD 7 (just after loading) and 14 (A, B, and C). Multiple comparisons were performed by Dunnett's test compared with the control group. n = 5 (mean ± SE). *; < 0.05, **; < 0.01, ***; < 0.001. PWD, post-wounding day.

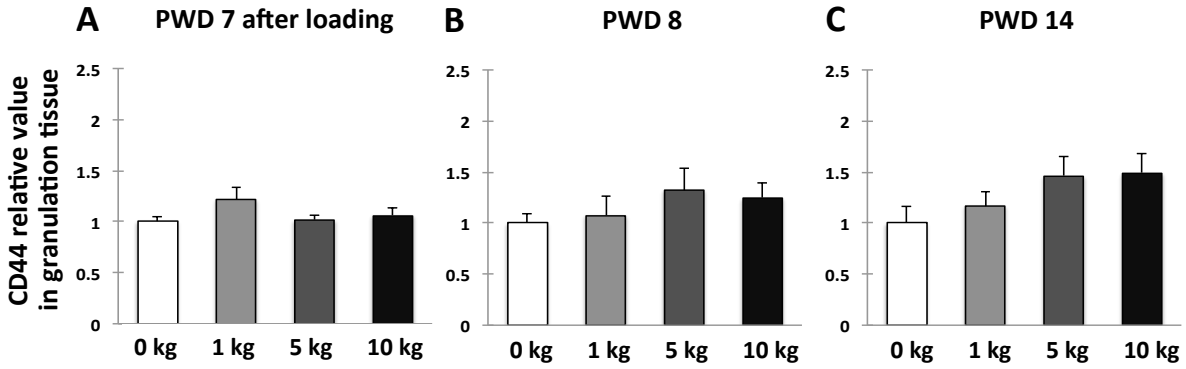

Figure 1-20 Quantification of CD44 in granulation tissue of each loading group on PWD 7 (just after loading), 8, and 14. The 0-. 1-, 5-, and 10-kg loadings were applied for the center of full-thickness wound created on the flank of rats. Tissue of wound site was harvested and analyzed on PWD 7 (just after loading), PWD 8, and PWD14. Any significant differences in CD44 level between the loading groups and the control were not found on PWD 7 (just after loading), 8, and 14 (A, B, and C). Multiple comparisons were performed by Dunnett's test compared with the control group. n = 5 (mean ± SE). *; < 0.05, **; < 0.01, ***; < 0.001. PWD, post-wounding day.

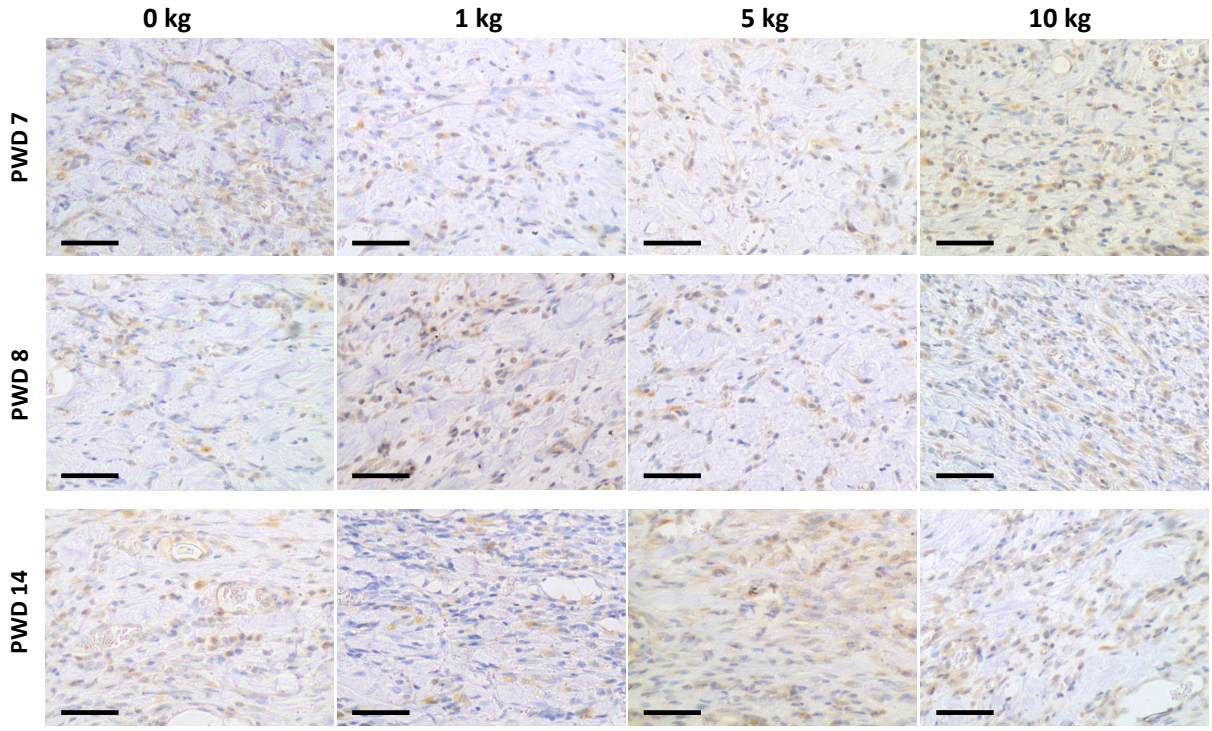

Figure 1-21 Immunohistochemistry for CD44 in granulation tissue of granulation tissue of each loading group on PWD 7 (just after loading), 8, and 14. The 0-. 1-, 5-, and 10-kg loadings were applied for the center of full-thickness wound created on the flank of rats. Tissue of wound site was harvested and analyzed on PWD 7 (just after loading), PWD 8, and PWD14. Relatively stronger CD44 staining in the granulation tissue were not also found between the loading groups and the control on PWD 7 (just after loading), 8, and 14. Scale bar: 50μm. PWD, post-wounding day.

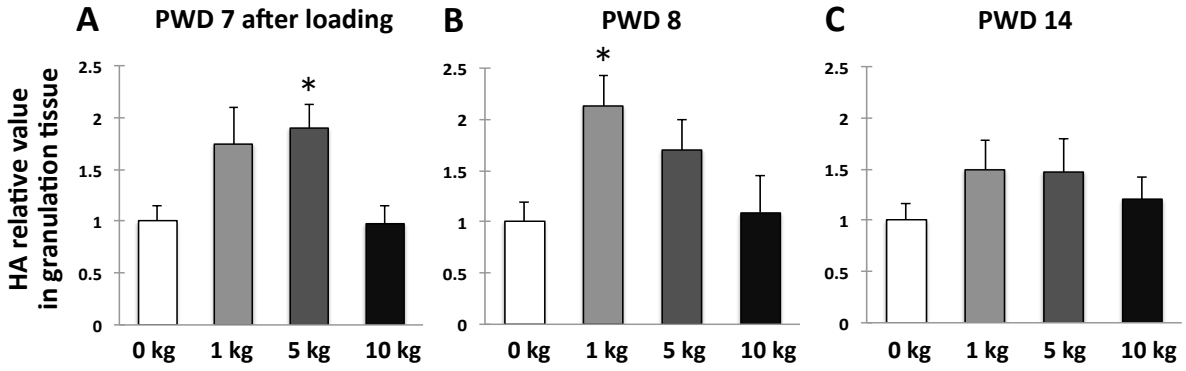

Figure 1-22 Quantification of HA in granulation tissue of each loading group on PWD 7 after loading, 8, and 14. The 0-. 1-, 5-, and 10-kg loadings were applied for the center of full-thickness wound created on the flank of rats. Tissue of wound site was harvested and analyzed on PWD 7 (just after loading), PWD 8, and PWD14. On PWD 7 after lording, the expression of HA was significantly higher in the 5-kg group than in the control group ($p = 0.046$) (A). On PWD 8, the expression of HA was significantly higher in the 1-kg group than in the control group ($p = 0.040$) (B). On PWD 14, any significant differences between the loading groups and the control were not found (C). These results suggested that the HA level was increased by pressure loading, though CD44 level did not increase along with the increases of HAS1, HAS2, and HA. Multiple comparisons were performed by Dunnett's test compared with the control group. n = 5 (mean ± SE). *; < 0.05, **; < 0.01, ***; < 0.001. PWD, post-wounding day.

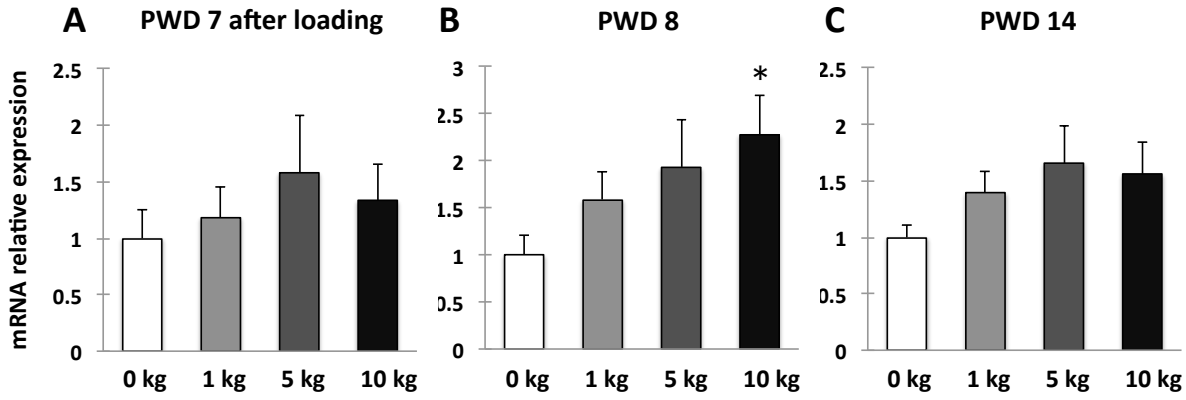

Figure 1-23 *Hsp90aa1* mRNA expression in granulation tissue of each loading group on PWD 7 (just after loading), 8, and 14. The 0-. 1-, 5-, and 10-kg loadings were applied for the center of full-thickness wound created on the flank of rats. Tissue of wound site was harvested and analyzed on PWD 7 (just after loading), PWD 8, and PWD14. The expression of Hsp90aa1 on PWD 8 was higher in the 10-kg group only than in the control group ($p = 0.017$), and any significant differences between the loading groups and the control were not found on PWD 7 (just after loading) and 14 (A, B, and C). Multiple comparisons were performed by Dunnett's test compared with the control group. n = 5 (mean ± SE). *; < 0.05, **; < 0.01, ***; < 0.001. PWD, post-wounding day.

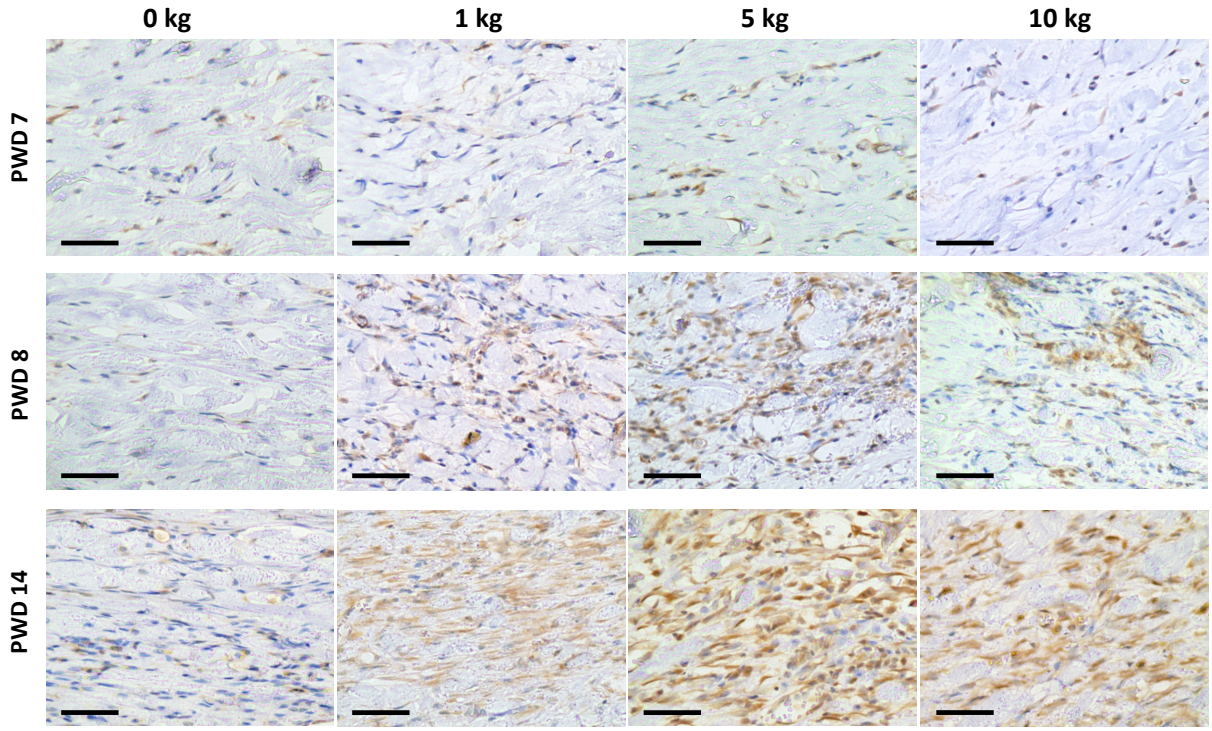

Figure 1-24 Immunohistochemistry for HSP90α in granulation tissue of each loading group on PWD 7 (just after loading), 8, and 14. The 0-. 1-, 5-, and 10-kg loadings were applied for the center of full-thickness wound created on the flank of rats. Tissue of wound site was harvested and analyzed on PWD 7 (just after loading), PWD 8, and PWD14. On PWD 7 (just after loading), relatively stronger HSP90α staining in the granulation tissue were not also found between the loading groups and the control. On the other hand, on PWD 8, the 1-, 5-, and 10-kg groups showed relatively stronger HSP90α staining in the granulation tissue compared with the control group. Notably, the 1-, 5-, and 10-kg groups on PWD 14 showed remarkably stronger HSP90α staining in the granulation tissue compared with the control group. Scale bar: 50μm. PWD, post-wounding day.

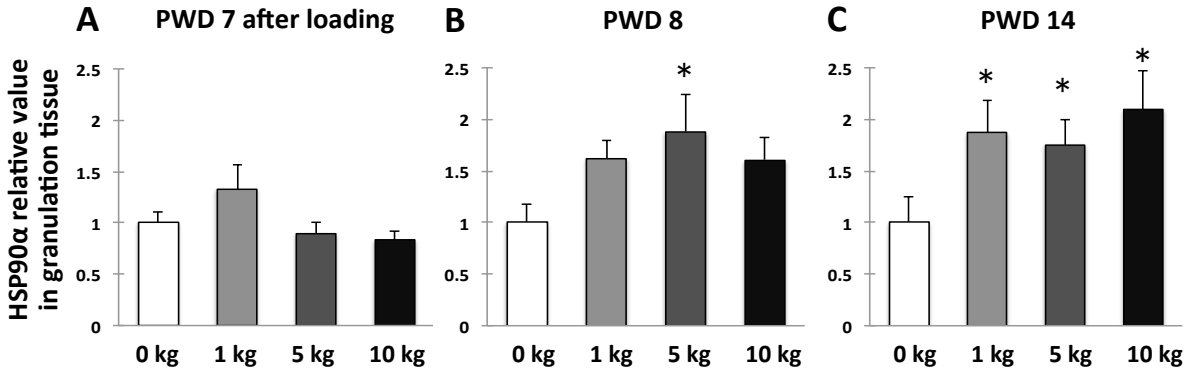

Figure 1-25 Quantification of HSP90α in granulation tissue of each loading group on PWD 7, 8, and 14. The 0-. 1-, 5-, and 10-kg loadings were applied for the center of full-thickness wound created on the flank of rats. Tissue of wound site was harvested and analyzed on PWD 7 (just after loading), PWD 8, and PWD14. Any significant differences between the loading groups and the control were not found on PWD 7 (A). On PWD 8, the expression of HA was significantly higher in the 5-kg group than in the control group ($p = 0.042$) (B). Interestingly, on PWD 14 the expression of HSP90α was significantly higher in all loading groups than in the control group (the 1-kg; $p = 0.043$, the 5-kg; $p = 0.043$, and the 10-kg; $p = 0.043$) (C). Taken together, these results suggested that the HSP90α level was increased by pressure loading in elapsed time dependent manner. Multiple comparisons were performed by Dunnett's test compared with the control group. $n = 5$ (mean ± SE). *; < 0.05, **; < 0.01, ***; < 0.001. PWD, post-wounding day.

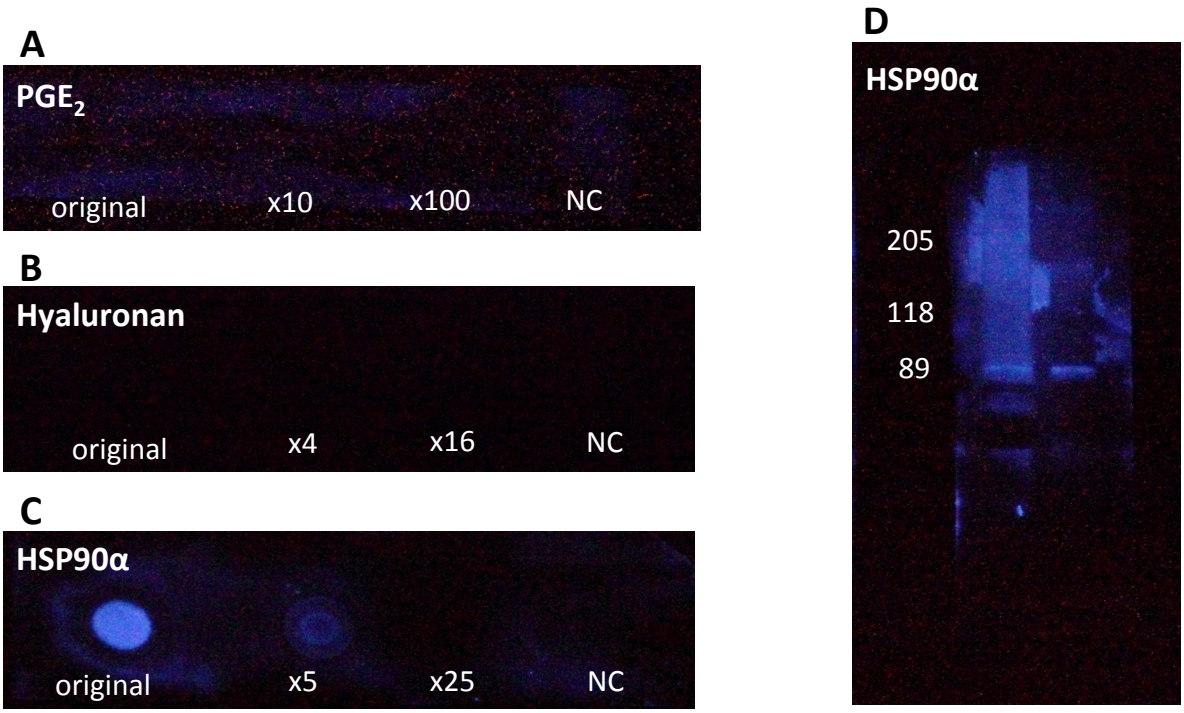

Figure 1-26 Detection of PGE2, HA, and HSP90α in dot blotting and HSP90α western blotting. PGE2 and HA were not detected by dot blotting (A and B), whereas HSP90α was detected in concentration dependent manner (C). In western blotting HSP90α was observed around 90 kDa (D). From these results, we decided to verify HSP90α of the collected membranes including wound exudates of animal models by wound blotting method.

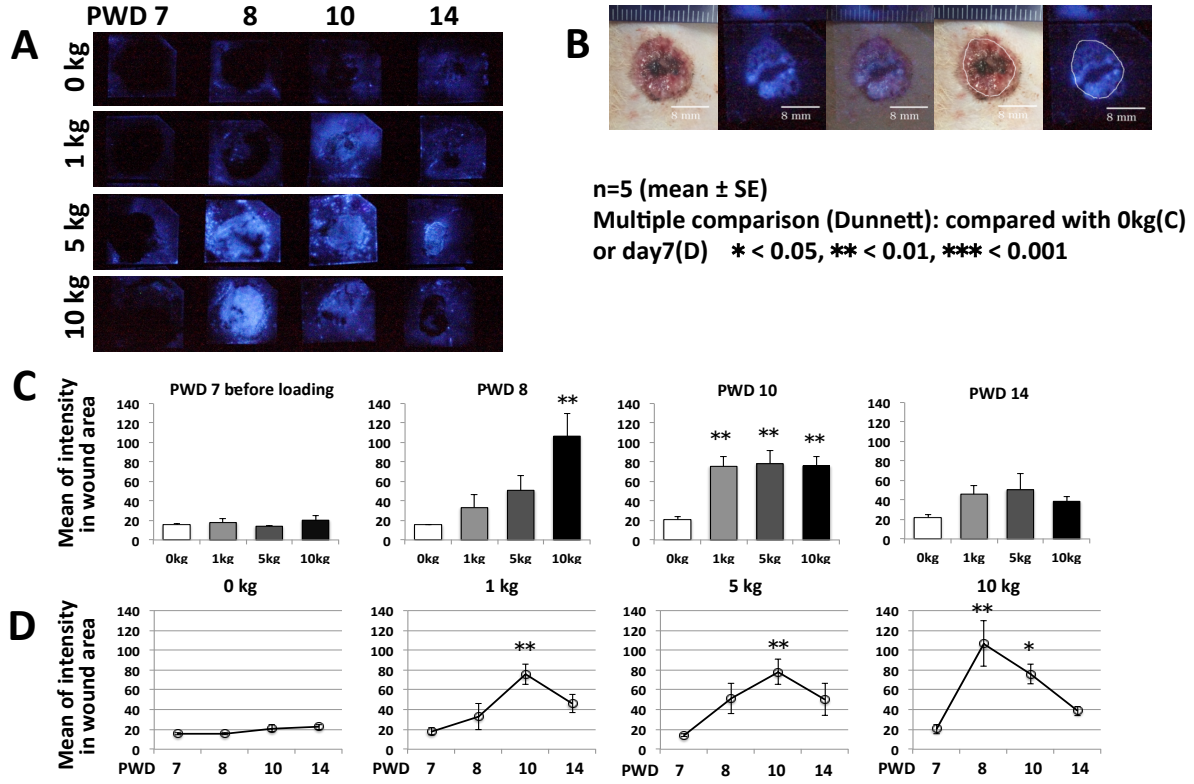

Figure 1-27 Evaluation of exudate HSP90α in 0-, 1-, 5- and 10-kg loading groups by wound blotting. (A) showed the representative immunostaining images of HSP90α. The HSP90α signal on all PWDs of the control and on PWD 7 before loading of the loading group was almost negative, and the strong HSP90α signal on PWD 8 of the 5- and 10-kg and on PWD 10 of the 1-, 5-, and 10-kg was detected. The images of immunoreactivities with chemiluminescent substrates were flipped horizontally. The mean of staining intensity within the wound area was indicated using ImageJ version 1.42 for statistical analyses (B). Any significant differences of HSP90α signal on PWD 7 before loading and 14 were not found the loading groups and the control, respectively (C). On the other hand, significant differences of HSP90α signal in the 10-kg group on PWD 8 and in all loading groups on PWD 10 were observed compared with the control groups, respectively (the 10-kg; $p = 0.002$ on PWD 8: the 1-kg; $p = 0.003$, the 5-kg; $p = 0.002$, and the 10-kg; $p = 0.003$ on PWD 10) (C). Regarding time course assay, in the 1- and 5-kg groups, HSP90α signal was significantly higher on PWD 10 than on PWD 7 before loading, respectively ($p = 0.042$ and $p = 0.042$, respectively) (D). In the 10-kg groups, HSP90α signal was significantly higher on PWD 8 and 10 than on PWD 7 before loading, respectively ($p = 0.042$ and $p = 0.042$, respectively) (D). These results suggested that the increase of HSP90α in wound exudates occurred in response to pressure loading. Multiple comparisons were performed by Dunnett's test compared with the control group (C) or the PWD 7group (D). n = 5 (mean ± SE). *; < 0.05, **; < 0.01, ***; < 0.001. PWD, post-wounding day.

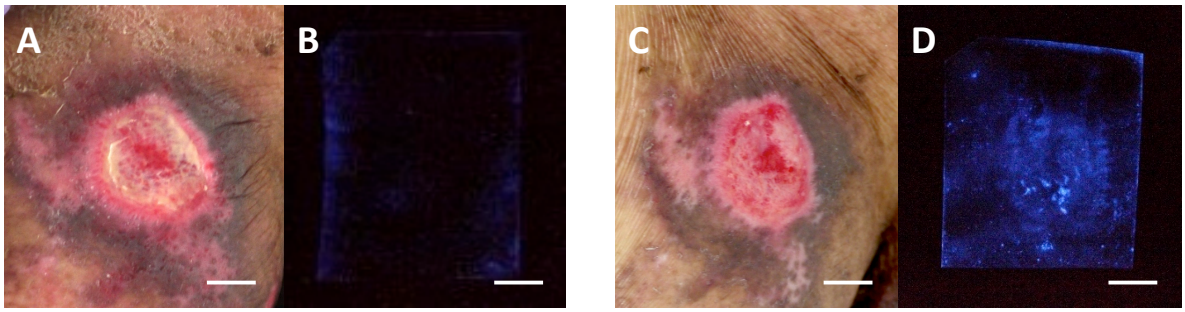

Figure 2-1 Typical negative and positive patterns of HSP90α in pressure ulcers by clinical wound blotting. Gross appearance (A: 3rd week and C: 4th week) and immunostaining images of wound blotting (B: 3rd week and D: 4th week) in a pressure ulcer at the buttocks of an 86-year-old male patient. The sample with luminescent signal within wound area was considered as positive for HSP90α (D), and the sample without luminescent signal within wound area was considered as negative (B). Scale bar: 1cm.

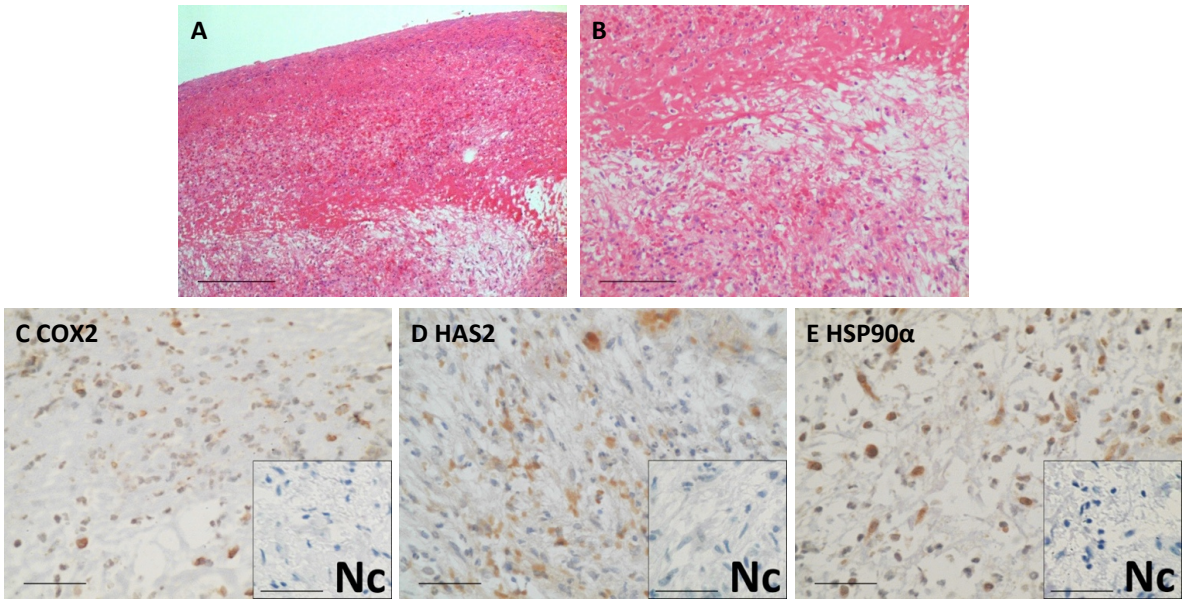

Figure 2-2 Histological and immunohistological analysis of a pressure ulcer representing delayed healing caused by pressure. Representative sections of granulation tissue in unhealed wound due to pressure (HE staining, A: scale bar = 200 μm, B: scale bar = 100 μm). C, D, and E: immunostaining for COX2 (C), HAS2 (D), and HSP90α (E). All images were present in the region of (A). In all Nc images, immunostaining was performed without primary antibodies. Scale bars = 40 μm for all images excluding (A) and (B). The patient was a 60-year-old woman suffering from hemiplegia and hospitalized. She had a full-thickness PU in the sacral region that was caused by prolonged pressure due to cerebral hemorrhage-induced unconsciousness for one night. Although a sharp debridement and ointment treatment were administered several times, the ulcer remained unhealed due to pressure resulting from lack of efficient post-wounding day-wounding dayural change for hemiplegia.

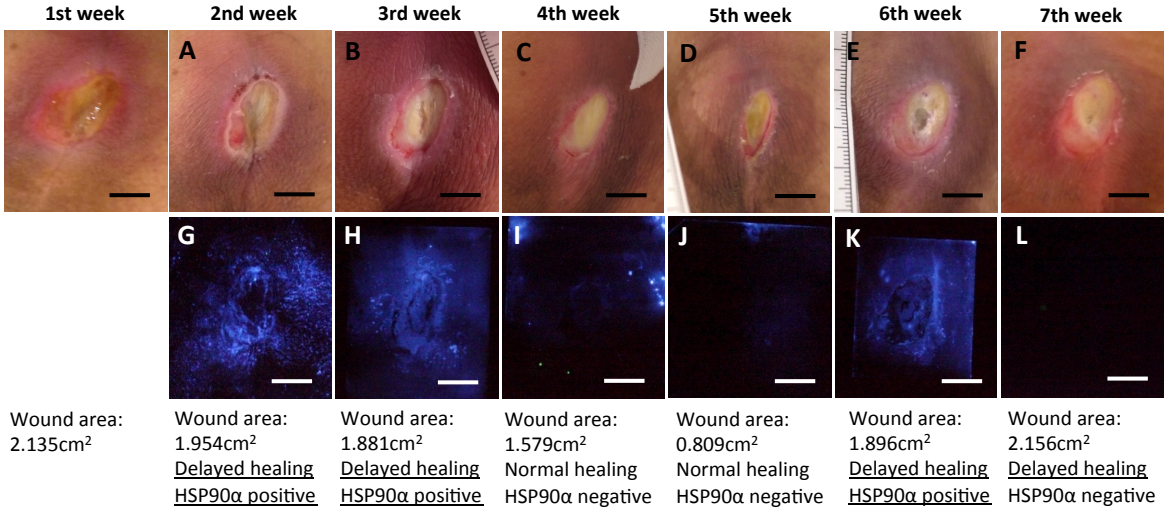

Figure 2-3 Longitudinal observations of wound appearances and HSP90α signals in subject ID 1. A 66-year-old male patient diagnosed with adrenal cancer with a pressure ulcer at the sacrum. He was hospitalized for the purpose of ureteral stent placement. He was using opioid analgesics for cancer pain and was able to walk when cancer pain was calm. His wound was susceptible to pressure loading because he preferred crossed legs position in the recumbent position. He used an alternating pressure air mattress. However, in 1st week, his wound was exposed to pressure because his sacrum hit the bottom of the mattress. For this reason, weight setting of the mattress was changed to 60-kg from 40-kg as pressure redistribution care. In 2nd week, exposure to pressure in last week caused delayed healing along with HSP90α positive (A and G), and weight setting was also changed to 70-kg due to hitting the bottom. In 3rd week, exposure to pressure in 2nd week also caused delayed healing along with HSP90α positive (B and H), and ADL improving increased his mobilization. In 4th week, his mobilization lead to normal healing along with HSP90α negative (C and I), and his mobilization was continued. In 5th week, his mobilization in 4th week also lead to normal healing along with HSP90α negative (D and J), on the other hand, his ADL began to be worse and decreased his mobilization. In 6th week, his decreased mobilization in 5th week caused delayed healing along with HSP90α positive (E and K), and his physical status deteriorated. In 7th week, the deterioration of physical status caused delayed healing, whereas HSP90α was negative (F and L). His status deterioration lead to fluid retention state and weight gain, and he died next week. Delayed healing represents the wound area reduction less than 10% compared with that of the last week. Scale bar: 1cm.

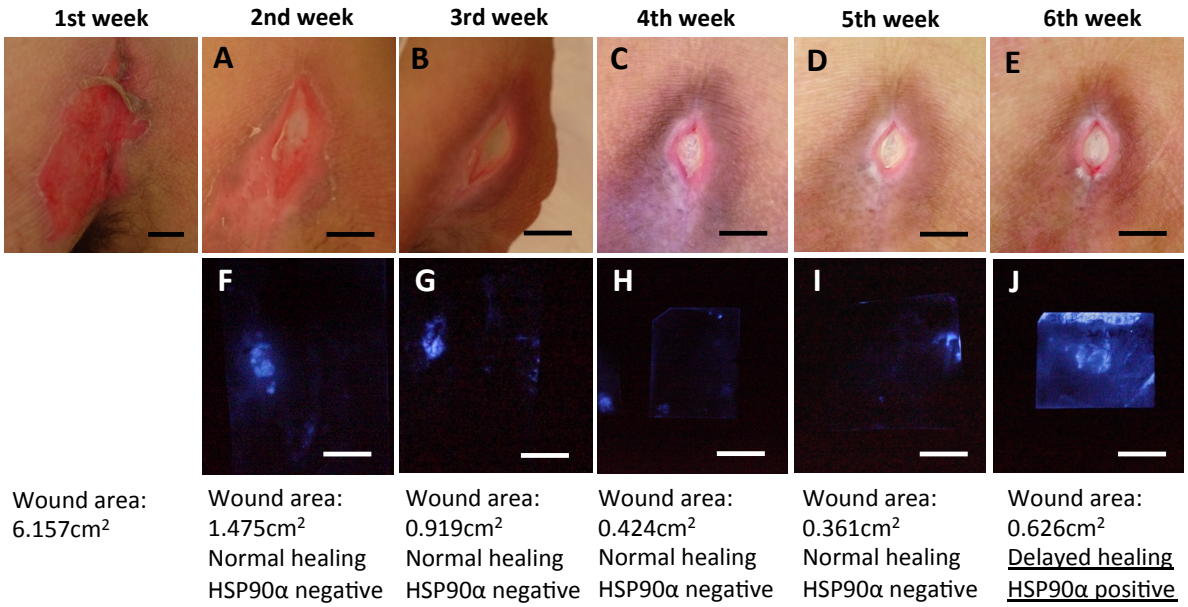

Figure 2-4 Longitudinal observations of wound appearances and HSP90α signals in subject ID 4. A 78-year-old male patient diagnosed with diabetes and suspected Parkinson's disease with a pressure ulcer at the coccyx. He was hospitalized for the purpose of intensive examination and treatment for impaired consciousness, gait disturbance, and lower extremity edema. A suppression band and mittens were used for intense motion by delirium. He was able to be standing and transfer to a wheel chair with light assistance. His wound recovered steadily until 5th week due to his passable ADL and HSP90α was negative for these weeks (Figure 2-2 A–D and F–I). However, in 5th week, pressure, which was measured as 168 mmHg, on the wound by the hard parts of the suppression band caused his pain. In 6th week, the compression by the band in 5th week caused delayed healing along with HSP90α positive. Next week, he was transferred to other hospital. Delayed healing represents the wound area reduction less than 10% compared with that of the last week. Scale bar: 1cm.

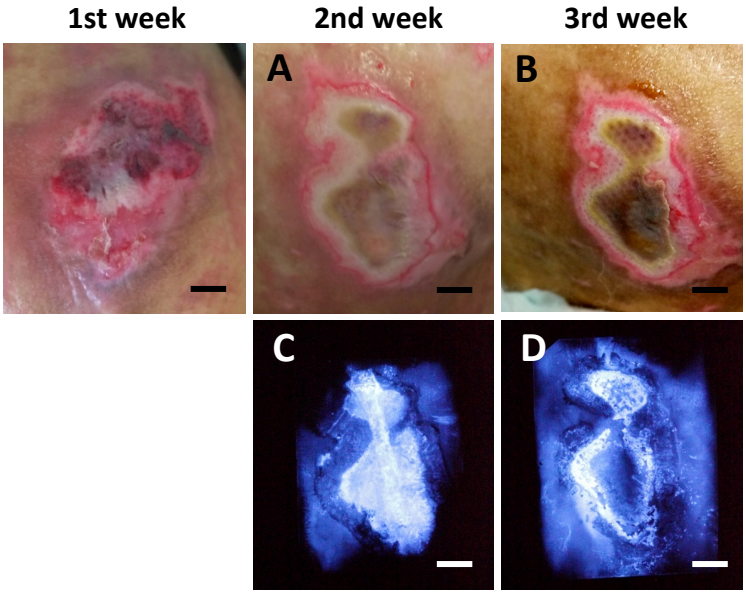

Figure 2-5 Longitudinal observations of wound appearances and HSP90α signals in subject ID 6. A 45-year-old male patient diagnosed with schizophrenia with a pressure ulcer at the sacrum. He was hospitalized for the purpose of intensive examination for anemia and malnutrition. A suppression band was used for schizophrenia, and it was difficult to provide pressure redistribution care with due to the suppression band. That is, there was also no effective repositioning care. For these reasons, his wound was exposed pressure, which caused delayed healing in 2nd and 3rd weeks along with HSP90α positive, respectively (A and C; B and D, respectively). Delayed healing represents the wound area reduction less than 10% compared with that of last week. Scale bar: 1cm.